

Supplementary Material

The hydroxyquinoline analog YUM70 inhibits GRP78 to induce ER stress-mediated apoptosis in pancreatic cancer

Soma Samanta¹, Suhui Yang¹, Bikash Debnath¹, Ding Xue¹, Yuting Kuang^{1,2}, Kavya Ramkumar^{1,2}, Amy S. Lee³, Mats Ljungman⁴, and Nouri Neamati^{1*}

¹Department of Medicinal Chemistry, College of Pharmacy, Rogel Cancer Center, University of Michigan, Ann Arbor, MI, 48109, USA. ²Department of Pharmacology and Pharmaceutical Sciences, School of Pharmacy, University of Southern California, Los Angeles, CA, USA. ³Department of Biochemistry and Molecular Medicine, University of Southern California, Keck School of Medicine, USC Norris Comprehensive Cancer Center, Los Angeles 90089, CA, USA, ⁴Department of Radiation Oncology, Rogel Cancer Center, Center for RNA Biomedicine, University of Michigan Medical School, and Department of Environmental Health Sciences, School of Public Health, University of Michigan, Ann Arbor, Michigan 48109, USA.

*Corresponding Author: Nouri Neamati, Ph.D. Department of Medicinal Chemistry, College of Pharmacy, Rogel Cancer Center, University of Michigan, North Campus Research Complex, 1600 Huron Parkway, Bldg 520, Room 1363, Ann Arbor, MI 48109, Phone: 734-647-2732, Email: neamati@umich.edu

Chemistry

The synthesis of YUM70 and its analogs was generally accomplished by employing the Betti reaction as a modified type of Mannich reaction (Scheme 1) (1). Also, *O*-methylation of two hydroxyquinoline compounds (**4**, **8** and **10**) was carried out by using methyl iodide in the presence of base to yield the analogs **15-17** (Scheme 1). Some of 7-substituted-8-hydroxyquinolines, especially containing aniline in place of amide at C-9, were reported to undergo a retro-Mannich fragmentation (2). Although a poor leaving group, the aniline was somehow displaced to result in the formation of a reactive quinone methide, which in turn is readily attacked by a nucleophile. The similar trends had been found in deamination of phenolic Mannich bases, and the deamination reaction involves elimination of a primary or secondary amine from a Mannich base to afford the vinyl derivative of the original substrates (3,4). In order to test whether our synthetic compounds are likely to undergo a retro-Mannich reaction, we examined the stability of compounds in the presence of different nucleophiles such as aniline, morpholine, piperidine, sodium hydroxide, or sodium acetate under acidic or basic condition (Table I). Interestingly, no reaction occurred either at room temperature for 36 – 63 hours or at 50 °C for 7 – 16 hours, indicating that the retro-Mannich pathway is much less favorable for the amide-containing series of compounds. It is probably because the amide nitrogen at C-9 is less basic than the corresponding aniline nitrogen. In agreement with this finding, the similar 8-hydroxyquinoline compounds have been reported to show good ADME properties, but such analogs containing aniline moiety at C-9 were unstable in the assay (5,6).

Table I. Stability test of 7-substituted amides of 8-hydroxyquinoline analogs

Compound	Reaction condition				Result
	Acid/Base	Nucleophile	Temperature (°C)	Time (hr)	
YUM70 (4)	NaOH (10 eq.)	Aniline (5 eq.)	room temperature	63	No change
			50°C	63	No change
	NaOH (10 eq.)	Piperidine (3 eq.)	room temperature	63	No change
			50°C	63	No change
	NaOH (5 eq.)	NaOH (5 eq.)	room temperature	63	No change
			50°C	63	No change
	HCl (10 eq.)	EtOH (5 mL)	room temperature	63	No change
			50°C	63	No change
	HCl (10 eq.)	NaOAc (5 eq.)	room temperature	63	No change
			50°C	63	No change
YUM94 (13)	NaOH (10 eq.)	Aniline (3 eq.)	room temperature	36	No change
			50°C	7	No change
	NaOH (10 eq.)	Morpholine (3 eq.)	room temperature	36	No change
			50°C	7	No change
	NaOH (5 eq.)	NaOH (5 eq.)	room temperature	36	No change
			50°C	7	No change

General chemical methods:

All commercial chemicals and solvents were reagent grade and were used without further purification unless otherwise specified. Analytical thin layer chromatography was performed on Merck precoated plates (silica gel 60 F₂₅₄) to follow the course of the reactions. ¹H and ¹³C NMR spectra were recorded on a Bruker Ultrashield 300 MHz, a Bruker Ascend 400 MHz, or 500 MHz Varian NMR spectrometer. Chemical shifts (δ) of NMR are reported in parts per million (ppm) units relative to the residual undeuterated solvent. The following abbreviations were used to describe peak splitting patterns when appropriate: s (singlet), d (doublet), t (triplet), q (quartet), m (multiplet), bs (broad singlet), dd (doublet of doublets), td (triplet of doublets). Coupling constants (J) are expressed in hertz unit (Hz). Mass spectra were obtained on a Shimadzu LCMS-2020 liquid chromatography mass spectrometer or on a Thermo-Scientific LCQ Fleet mass spectrometer. The purity of compounds was determined by UPLC or HPLC analysis. The Waters Acquity H class analytical UPLC was used for UV detection at 230 and 254 nm wavelengths. The reverse phase column was used in the Acquity UPLC BEH (C18-1.7 μ m, 2.1 mm \times 50 mm). The analytical HPLC Shimadzu HPLC Test Kit C18 column (3 μ m, 4.6 \times 50 mm) was used under the following gradient elution condition: mobile phase A of acetonitrile/water (10-95%) or mobile phase B of methanol/water (10-95%). The purity was established by integration of the areas of major peaks detected at 254 nm. All tested compounds had \geq 95% purity unless mentioned. For some compounds, flash chromatography was performed using a Biotage Isolera One flash purification system.

Detailed synthetic procedures and characterization

***N*-(benzo[d][1,3]dioxol-5-yl(5-chloro-8-hydroxyquinolin-7-yl)methyl)butyramide (YUM70, 4).** A mixture of 5-chloro-8-hydroxyquinoline (486 mg, 2.57 mmol), piperonal (1.06 g, 7.02 mmol), and butyramide (200 mg, 2.34 mmol) were stirred neat at 130-150 °C for 6-12 hrs. Upon heating, the reaction mixture melted and solid was formed after completion of the reaction. The solid was isolated by multiple trituration with ethyl acetate and diethyl ether, and the crude product was purified by recrystallization from ethanol to yield **YUM70** as a tan solid (302 mg, 32%). **¹H NMR** (500 MHz, DMSO-*d*₆) δ: 10.30 (bs, 1H), 8.94 (dd, *J* = 4.1, 1.5 Hz, 1H), 8.66 (d, *J* = 8.8 Hz, 1H), 8.46 (dd, *J* = 8.5, 1.5 Hz, 1H), 7.72-7.69 (m, 1H), 7.70 (s, 1H), 6.84-6.80 (m, 2H), 6.70 (d, *J* = 8.1 Hz, 1H), 6.60 (d, *J* = 8.7 Hz, 1H), 5.95 (s, 2H), 2.18 (t, *J* = 7.2 Hz, 2H), 1.51 (sextet, *J* = 7.2 Hz, 2H), 0.84 (t, *J* = 7.3 Hz, 3H). **¹³C NMR** (101 MHz, DMSO-*d*₆) δ: 171.85, 149.64, 149.52, 147.78, 146.58, 139.14, 136.40, 132.96, 126.53, 126.18, 125.26, 123.38, 120.57, 119.05, 108.51, 107.84, 101.43, 49.72, 37.71, 19.25, 14.08. **MS** (ESI) *m/z* = 399 (M+H)⁺. **UPLC** (mobile phase A): purity 97.4%.

***N*-((5-chloro-8-hydroxyquinolin-7-yl)(phenyl)methyl)butyramide (YUM72, 5).** The same procedure for the synthesis of **YUM70** was followed using 5-chloro-8-hydroxyquinoline (103 mg, 0.55 mmol), benzaldehyde (162 mg, 1.5 mmol), and butyramide (44 mg, 0.50 mmol) as reactants to yield **YUM72** as a shiny brown solid (106 mg, 60%). **¹H NMR** (500 MHz, DMSO-*d*₆) δ: 10.32 (bs, 1H), 8.95 (dd, *J* = 4.2, 1.5 Hz, 1H), 8.74 (d, *J* = 8.8 Hz, 1H), 8.47 (dd, *J* = 8.5, 1.5 Hz, 1H), 7.72-7.69 (m, 1H), 7.69 (s, 1H), 7.32-7.29 (m, 2H), 7.25-7.20 (m, 3H), 6.70 (d, *J* = 8.7 Hz, 1H), 2.19 (t, *J* = 7.2 Hz, 2H), 1.53 (sextet, *J* = 7.4 Hz, 2H), 0.85 (t, *J* = 7.4 Hz, 3H). **¹³C NMR** (101 MHz, DMSO-*d*₆) δ: 171.93, 149.69, 149.66, 142.43, 139.14, 132.98, 128.85, 127.42, 127.38,

126.75, 125.98, 125.29, 123.41, 119.03, 49.93, 37.71, 19.26, 14.09. **MS** (ESI) $m/z = 355$ (M+H)⁺.

UPLC (mobile phase A): purity 98.8%.

***N*-(1-(5-chloro-8-hydroxyquinolin-7-yl)butyl)butyramide (YUM75, 6)**. The same procedure for the synthesis of **YUM70** was followed using 5-chloro-8-hydroxyquinoline (100 mg, 0.53 mmol), butyraldehyde (177 mg, 2.4 mmol), and butyramide (43 mg, 0.48 mmol) as reactants. The product obtained from recrystallization was further purified by column chromatography (*n*-hexane:EtOAc=5:1, EtOAc) to yield **YUM75** as a beige solid (25 mg, 16%). **¹H NMR** (500 MHz, DMSO-*d*6) δ : 10.09 (bs, 1H), 8.93 (dd, $J = 4.2, 1.5$ Hz, 1H), 8.44 (dd, $J = 8.7, 1.5$ Hz, 1H), 8.24 (d, $J = 8.5$ Hz, 1H), 7.68 (dd, $J = 8.5, 4.1$ Hz, 1H), 7.63 (s, 1H), 5.40-5.36 (m, 1H), 2.11 (td, $J = 7.2, 3.2$ Hz, 2H), 1.63 (q, $J = 7.6$ Hz, 2H), 1.50 (sextet, $J = 7.4$ Hz, 2H), 1.39-1.33 (m, 1H), 1.28-1.23 (m, 1H), 0.87 (t, $J = 7.4$ Hz, 3H), 0.83 (t, $J = 7.4$ Hz, 3H). **¹³C NMR** (101 MHz, DMSO-*d*6) δ : 172.02, 149.46, 149.12, 139.02, 132.88, 127.90, 126.01, 124.91, 123.06, 118.88, 46.63, 37.85, 37.69, 19.68, 19.29, 14.07, 14.00. **MS** (ESI) $m/z = 343$ (M+Na)⁺. **UPLC** (mobile phase A): purity 97.9%.

2-Chloro-*N*-((5-chloro-8-hydroxyquinolin-7-yl)(phenyl)methyl)acetamide (YUM79, 7). The same procedure for the synthesis of **YUM70** was followed using 5-chloro-8-hydroxyquinoline (100 mg, 0.53 mmol), benzaldehyde (156 mg, 1.4 mmol), and 2-chloroacetamide (46 mg, 0.48 mmol) as reactants to yield **YUM79** as a brown solid (59 mg, 34%). **¹H NMR** (500 MHz, DMSO-*d*6) δ : 10.43 (bs, 1H), 9.17 (d, $J = 8.5$ Hz, 1H), 8.95 (dd, $J = 4.4, 1.5$ Hz, 1H), 8.49-8.46 (m, 1H), 7.72 (dd, $J = 8.5, 4.2$ Hz, 1H), 7.67 (s, 1H), 7.34-7.31 (m, 2H), 7.27-7.22 (m, 3H), 6.65 (d, $J = 8.4$ Hz, 1H), 4.19 (d, $J = 2.6$ Hz, 2H). **¹³C NMR** (101 MHz, DMSO-*d*6) δ : 165.89, 149.89, 149.76, 141.58, 139.16, 133.02, 128.97, 127.65, 127.40, 126.63, 125.45, 125.05, 123.56, 119.16, 50.79, 43.19. **MS** (ESI) $m/z = 383$ (M+Na)⁺. **UPLC** (mobile phase A): purity 94.3%.

2-Chloro-*N*-((5-chloro-8-hydroxyquinolin-7-yl)(3-methoxyphenyl)methyl)acetamide

(**YUM82, 8**). The same procedure for the synthesis of **YUM70** was followed using 5-chloro-8-hydroxyquinoline (196 mg, 1.04 mmol), 3-methoxybenzaldehyde (392 mg, 2.82 mmol), and 2-chloroacetamide (90 mg, 0.94 mmol) as reactants to yield **YUM82** as an ivory solid (52 mg, 14%). ¹H NMR (400 MHz, DMSO-*d*₆) δ: 10.43 (bs, 1H), 9.16 (d, *J* = 8.4 Hz, 1H), 8.97 (dd, *J* = 4.4, 1.6 Hz, 1H), 8.49 (dd, *J* = 8.4, 1.6 Hz, 1H), 7.74 (dd, *J* = 8.4, 4.4 Hz, 1H), 7.66 (s, 1H), 7.25 (t, *J* = 8.0 Hz, 1H), 6.85-6.82 (m, 3H), 6.64 (d, *J* = 8.8 Hz, 1H), 4.20 (d, *J* = 3.6 Hz, 2H), 3.72 (s, 3H). ¹³C NMR (101 MHz, DMSO-*d*₆) δ: 165.88, 159.82, 149.89, 149.76, 143.24, 139.18, 133.02, 130.10, 126.62, 125.45, 125.00, 123.57, 119.59, 119.13, 113.43, 112.58, 55.52, 50.64, 43.20. MS (ESI) *m/z* = 391 (M+H)⁺. UPLC (mobile phase A): purity 99.0%.

2-Chloro-*N*-((5-chloro-8-hydroxyquinolin-7-yl)(4-methoxyphenyl)methyl)acetamide

(**YUM86, 9**). The same procedure for the synthesis of **YUM70** was followed using 5-chloro-8-hydroxyquinoline (196 mg, 1.04 mmol), 3-methoxybenzaldehyde (393 mg, 2.82 mmol), and 2-chloroacetamide (90 mg, 0.94 mmol) as reactants to yield **YUM86** as an ivory solid (98 mg, 27%). ¹H NMR (400 MHz, DMSO-*d*₆) δ: 10.38 (bs, 1H), 9.12 (d, *J* = 8.4 Hz, 1H), 8.97 (dd, *J* = 4.0, 1.2 Hz, 1H), 8.50 (dd, *J* = 8.4, 1.6 Hz, 1H), 7.73 (dd, *J* = 8.4, 4.0 Hz, 1H), 7.69 (s, 1H), 7.19 (d, *J* = 8.4 Hz, 2H), 6.90 (d, *J* = 8.8 Hz, 2H), 6.60 (d, *J* = 8.4 Hz, 1H), 4.19 (d, *J* = 1.2 Hz, 2H), 3.72 (s, 3H). ¹³C NMR (101 MHz, DMSO-*d*₆) δ: 165.76, 158.85, 149.75, 149.71, 139.16, 133.52, 133.00, 128.62, 126.52, 125.44, 125.37, 123.48, 119.10, 114.35, 55.58, 50.32, 43.21. MS (ESI) *m/z* = 391 (M+H)⁺. UPLC (mobile phase A): purity 96.5%.

***N*-((5-chloro-8-hydroxyquinolin-7-yl)(3-methoxyphenyl)methyl)butyramide (YUM89, 10).**

The same procedure used for the synthesis of **YUM70** was followed using 5-chloro-8-hydroxyquinoline (116 mg, 0.61 mmol), 3-methoxybenzaldehyde (254 mg, 1.83 mmol), and

butyramide (60 mg, 0.67 mmol) as reactants to yield **YUM89** as a white fluffy solid (153 mg, 65%). ¹H NMR (400 MHz, DMSO-*d*₆) δ: 10.32 (s, 1H), 8.96 (dd, *J* = 5.6, 1.6 Hz, 1H), 8.73 (d, *J* = 8.8 Hz, 1H), 8.48 (dd, *J* = 8.4, 1.6 Hz, 1H), 7.72 (dd, *J* = 8.8, 4.4 Hz, 1H), 7.70 (s, 1H), 7.23 (t, *J* = 8.0 Hz, 1H), 6.84-6.80 (m, 3H), 6.70 (d, *J* = 8.8 Hz, 1H), 3.71 (s, 3H), 2.21 (t, *J* = 7.2 Hz, 2H), 1.59 (sextet, *J* = 7.6 Hz, 2H), 0.87 (t, *J* = 7.6 Hz, 3H). ¹³C NMR (101 MHz, DMSO-*d*₆) δ: 171.94, 159.76, 149.69, 149.66, 144.12, 139.16, 132.97, 129.96, 126.73, 125.91, 125.29, 123.42, 119.64, 118.99, 113.42, 112.32, 55.47, 49.79, 37.72, 19.28, 14.08. MS (ESI) *m/z* = 385 (M+H)⁺. UPLC (mobile phase A): purity 99.9%.

***N*-((5-chloro-8-hydroxyquinolin-7-yl)(2-chlorophenyl)methyl)butyramide (YUM91, 11)**. The same procedure for the synthesis of **YUM70** was followed using 5-chloro-8-hydroxyquinoline (116 mg, 0.61 mmol), 2-chlorobenzaldehyde (265 mg, 1.83 mmol), and butyramide (60 mg, 0.67 mmol) as reactants to yield **YUM91** as an off-white solid (45 mg, 19%). ¹H NMR (400 MHz, CDCl₃) δ: 8.83 (dd, *J* = 4.4, 1.6 Hz, 1H), 8.51 (dd, *J* = 8.4, 1.2 Hz, 1H), 7.59 (s, 1H), 7.57 (dd, *J* = 8.4, 4.0 Hz, 1H), 7.50-7.48 (m, 1H), 7.41-7.39 (m, 1H), 7.26-7.23 (m, 2H), 6.87 (d, *J* = 8.0 Hz, 1H), 6.68 (d, *J* = 8.0 Hz, 1H), 2.29 (t, *J* = 7.2 Hz, 2H), 1.74 (sextet, *J* = 7.6 Hz, 2H), 0.99 (t, *J* = 7.2 Hz, 3H). ¹³C NMR (101 MHz, DMSO-*d*₆) δ: 171.72, 150.47, 149.69, 139.50, 139.08, 133.44, 133.00, 130.08, 129.45, 129.20, 127.63, 126.82, 125.50, 124.06, 123.53, 118.60, 48.50, 37.54, 19.28, 14.06. MS (ESI) *m/z* = 389 (M+H)⁺. UPLC (mobile phase A): purity 99.0%.

***N*-((5-chloro-8-hydroxyquinolin-7-yl)(4-chlorophenyl)methyl)butyramide (YUM92, 12)**. The same procedure for the synthesis of **YUM70** was followed using 5-chloro-8-hydroxyquinoline (116 mg, 0.61 mmol), 4-chlorobenzaldehyde (261 mg, 1.83 mmol), and butyramide (60 mg, 0.67 mmol) as reactants to yield **YUM92** as an off-white solid (102 mg, 43%). ¹H NMR (400 MHz, DMSO-*d*₆) δ: 10.4 (bs, 1H), 8.97 (dd, *J* = 4.4, 1.6 Hz, 1H), 8.77 (d, *J* = 8.4 Hz, 1H), 8.49 (dd, *J* =

8.8, 1.6 Hz, 1H), 7.74 (dd, $J = 8.8, 4.4$ Hz, 1H), 7.71 (s, 1H), 7.39 (d, $J = 8.8$ Hz, 2H), 7.27 (d, $J = 8.4$ Hz, 2H), 6.69 (d, $J = 8.8$ Hz, 1H), 2.21 (t, $J = 7.6$ Hz, 2H), 1.56 (sextet, $J = 7.6$ Hz, 2H), 0.87 (t, $J = 7.6$ Hz, 3H). $^{13}\text{C NMR}$ (101 MHz, DMSO- d_6) δ : 170.02, 149.76, 149.73, 141.44, 139.14, 133.00, 132.01, 129.28, 128.84, 126.56, 125.41, 123.50, 119.17, 49.49, 37.69, 19.23, 14.08. **MS** (ESI) $m/z = 389$ (M+H) $^+$. **UPLC** (mobile phase A): purity 97.3%.

***N*-((5-chloro-8-hydroxyquinolin-7-yl)(3-chlorophenyl)methyl)butyramide (YUM94, 13)**. The same procedure for the synthesis of **YUM70** was followed using 5-chloro-8-hydroxyquinoline (173 mg, 0.92 mmol), 3-chlorobenzaldehyde (388 mg, 2.76 mmol), and butyramide (90 mg, 1.01 mmol) as reactants to yield **YUM94** as a white cotton (180 mg, 50%). $^1\text{H NMR}$ (400 MHz, DMSO- d_6) δ : 10.4 (bs, 1H), 8.97 (dd, $J = 4.4, 1.6$ Hz, 1H), 8.80 (d, $J = 8.8$ Hz, 1H), 8.49 (dd, $J = 8.4, 1.6$ Hz, 1H), 7.74 (dd, $J = 8.4, 4.0$ Hz, 1H), 7.72 (s, 1H), 7.38-7.30 (m, 3H), 7.24-7.22 (m, 1H), 6.71 (d, $J = 8.8$ Hz, 1H), 2.22 (t, $J = 7.2$ Hz, 2H), 1.56 (sextet, $J = 7.2$ Hz, 2H), 0.87 (t, $J = 7.2$ Hz, 3H). $^{13}\text{C NMR}$ (101 MHz, DMSO- d_6) δ : 172.08, 149.80, 149.76, 145.00, 139.15, 133.54, 133.01, 130.85, 127.43, 127.01, 126.48, 126.20, 125.46, 125.19, 123.54, 119.22, 49.68, 37.68, 19.22, 14.04. **MS** (ESI) $m/z = 389$ (M+H) $^+$. **UPLC** (mobile phase A): purity 98.9%.

***N*-((5-chloro-8-hydroxyquinolin-7-yl)(3-hydroxyphenyl)methyl)butyramide (YUM166, 14)**. The same procedure for the synthesis of **YUM70** was followed using 5-chloro-8-hydroxyquinoline (250 mg, 1.40 mmol), 3-hydroxybenzaldehyde (512 mg, 4.19 mmol), and butyramide (134 mg, 1.54 mmol) as reactants. The product obtained from recrystallization was further purified by column chromatography (*n*-hexane:EtOAc=1:1) to yield **YUM166** as a beige solid (185 mg, 36%). $^1\text{H NMR}$ (400 MHz, CDCl_3) δ : 8.81 (d, $J = 4.0$ Hz, 1H), 8.49 (d, $J = 8.4$ Hz, 1H), 7.55 (dd, $J = 8.4, 4.0$ Hz, 1H), 7.51 (s, 1H), 7.14 (t, $J = 7.6$ Hz, 1H), 7.09 (d, $J = 8.8$ Hz, 1H), 6.88 – 6.84 (m, 2H), 6.72 (d, $J = 7.6$ Hz, 1H), 6.50 (d, $J = 8.4$ Hz, 1H), 2.28 (t, $J = 7.6$ Hz, 2H), 1.70 (sextet, $J =$

7.6 Hz, 2H), 0.94 (t, $J = 7.6$ Hz, 3H). ^{13}C NMR (101 MHz, DMSO- d_6) δ : 171.99, 157.77, 149.64, 149.61, 143.83, 139.10, 132.96, 129.81, 126.83, 125.99, 125.26, 123.38, 119.00, 118.10, 114.44, 114.32, 49.76, 37.70, 19.28, 14.06. MS (ESI) $m/z = 371$ (M+H) $^+$. UPLC (mobile phase A): purity 95.1%.

2-Chloro-*N*-((5-chloro-8-methoxyquinolin-7-yl)(3-methoxyphenyl)methyl)acetamide

(**YUM227**, **16**). To a stirring solution of **YUM82** (39 mg, 0.10 mmol) in DMF (~4 mL) at room temperature was added potassium carbonate (17 mg, 0.12 mmol) followed by methyl iodide (16 mg, 0.11 mmol) dropwise. The reaction mixture was stirred for 4 hrs, and then concentrated. The resulting residue was diluted with EtOAc, and the organic layer was washed with water (20 mL), sat. NaHCO₃ (aq.) (20 mL), and brine (20 mL), and then concentrated *in vacuo*. The residue was purified by column chromatography (*n*-hexane:EtOAc=3:1) to yield **YUM227** as a white crystal (28 mg, 69%). ^1H NMR (400 MHz, DMSO- d_6) δ : 9.22 (d, $J = 8.4$ Hz, 1H), 9.03 (dd, $J = 4.0, 1.6$ Hz, 1H), 8.53 (dd, $J = 8.8, 1.6$ Hz, 1H), 7.72 (dd, $J = 8.4, 4.0$ Hz, 1H), 7.71 (s, 1H), 7.27 (td, $J = 7.6, 1.6$ Hz, 1H), 6.86 – 6.82 (m, 3H), 6.66 (d, $J = 8.4$ Hz, 1H), 4.24 – 4.16 (m, 2H), 4.03 (s, 3H), 3.72 (s, 3H). ^{13}C NMR (101 MHz, CDCl₃) δ : 165.38, 159.90, 152.99, 150.08, 143.43, 141.98, 133.37, 133.07, 129.80, 127.24, 126.67, 126.22, 122.12, 118.79, 112.93, 112.42, 62.74, 55.29, 53.93, 42.71. MS (ESI) $m/z = 405$ (M+H) $^+$. UPLC (mobile phase A): purity 99.0%.

***N*-((5-chloro-8-methoxyquinolin-7-yl)(3-methoxyphenyl)methyl)butyramide** (**YUM117**, **15**).

The same procedure for the synthesis of **YUM227** was followed using **YUM89** (50 mg, 0.13 mmol), potassium carbonate (22 mg, 0.16 mmol), methyl iodide (21 mg, 0.14 mmol) in DMF (~4 mL). The resulting residue after extraction was purified by column chromatography (*n*-hexane:EtOAc=3:1, EtOAc) to yield **YUM117** as a yellow oil (33 mg, 64%). ^1H NMR (400 MHz, CDCl₃) δ : 8.97 (d, $J = 2.4$ Hz, 1H), 8.56 (dd, $J = 8.8, 1.6$ Hz, 1H), 7.63 (s, 1H), 7.53 (dd, $J = 8.8,$

4.4 Hz, 1H), 7.24 (t, $J = 8.0$ Hz, 1H), 6.86 – 6.74 (m, 4H), 6.59 (d, $J = 8.4$ Hz, 1H), 3.93 (s, 3H), 3.78 (s, 3H), 2.29 (td, $J = 7.6, 2.4$ Hz, 2H), 1.74 (sextet, $J = 7.6$ Hz, 2H), 0.99 (t, $J = 7.2$ Hz, 3H). ^{13}C NMR (101 MHz, CDCl_3) δ : 172.29, 159.81, 152.82, 150.03, 143.48, 142.87, 134.23, 133.36, 129.61, 127.07, 126.84, 126.14, 121.96, 118.97, 112.98, 112.19, 62.54, 55.26, 53.40, 38.77, 19.15, 13.83. MS (ESI) $m/z = 399$ (M+H)⁺. UPLC (mobile phase A): purity 98.6%.

***N*-(Benzo[*d*][1,3]dioxol-5-yl(5-chloro-8-methoxyquinolin-7-yl)methyl)butyramide**

(**YUM245**, **17**). The same procedure for the synthesis of **YUM227** was followed using **YUM70** (33 mg, 0.0827 mmol), potassium carbonate (14 mg, 0.0992 mmol), methyl iodide (13 mg, 0.0910 mmol) in DMF (~4 mL). The resulting residue after extraction was purified by column chromatography (*n*-hexane:EtOAc=3:1, 1:1) to yield **YUM245** as a white solid (24 mg, 70%). ^1H NMR (400 MHz, CDCl_3) δ : 8.95 (dd, $J = 4.4, 1.6$ Hz, 1H), 8.54 (dd, $J = 8.4, 1.2$ Hz, 1H), 7.58 (s, 1H), 7.51 (dd, $J = 8.4, 4.0$ Hz, 1H), 6.75 – 6.69 (m, 3H), 6.64 (d, $J = 8.0$ Hz, 1H), 6.50 (d, $J = 8.0$ Hz, 1H), 5.92 (d, $J = 2.0$ Hz, 2H), 3.97 (s, 3H), 2.26 (td, $J = 7.6, 2.8$ Hz, 2H), 1.71 (sextet, $J = 7.2$ Hz, 2H), 0.96 (t, $J = 7.2$ Hz, 3H). ^{13}C NMR (101 MHz, CDCl_3) δ : 172.26, 152.73, 150.08, 147.94, 146.84, 143.50, 135.14, 134.21, 133.34, 127.04, 126.60, 126.19, 121.98, 119.90, 108.20, 107.42, 101.17, 62.62, 53.25, 38.75, 19.12, 13.83. MS (ESI) $m/z = 413$ (M+H)⁺. UPLC (mobile phase A): purity 98.9%.

***N*-(Benzo[*d*][1,3]dioxol-5-yl(8-hydroxyquinolin-7-yl)methyl)butyramide** (**YUM272**, **20**).

8-Hydroxyquinoline (183 mg, 1.26 mmol), piperonal (518 mg, 3.45 mmol), butyramide (100 mg, 1.15 mmol) and ethyl acetate were placed in a microwave tube, the sealed vessel was heated by microwave to 180 °C for 30 min. After cooling to room temperature, the mixture was triturated with ethyl acetate and hexane. The crude solid was purified by column chromatography (*n*-hexane:EtOAc=3:1) to yield **YUM272** as an ivory solid (60 mg, 14%). ^1H NMR (400 MHz,

DMSO-*d*₆) δ : 9.89 (bs, 1H), 8.85 (dd, $J = 4.4, 1.6$ Hz, 1H), 8.61 (d, $J = 8.8$ Hz, 1H), 8.30 (dd, $J = 8.4, 1.6$ Hz, 1H), 7.55 – 7.52 (m, 2H), 7.41 (d, $J = 8.4$ Hz, 1H), 6.81 (d, $J = 8.0$ Hz, 1H), 6.79 (d, $J = 1.6$ Hz, 1H), 6.70 (dd, $J = 8.0, 1.2$ Hz, 1H), 6.61 (d, $J = 8.4$ Hz, 1H), 5.95 (d, $J = 0.8$ Hz, 2H), 2.18 (td, $J = 7.2, 2.8$ Hz, 2H), 1.53 (sextet, $J = 7.2$ Hz, 2H), 0.85 (t, $J = 7.2$ Hz, 3H). ¹³C NMR (75 MHz, DMSO-*d*₆) δ : 171.76, 149.76, 148.79, 147.63, 146.35, 138.47, 137.02, 136.48, 127.90, 126.64, 125.39, 122.17, 120.57, 117.77, 108.40, 107.89, 101.33, 49.91, 37.68, 19.28, 14.12. MS (ESI) $m/z = 365$ (M+H)⁺, 363 (M-H)⁻. HPLC (mobile phase A): purity 97.1%.

Methyl 2-(3-(butyramido(5-chloro-8-hydroxyquinolin-7-yl)methyl)phenoxy)acetate (YUM347A, 21). YUM166 (130 mg, 0.35 mmol), methyl chloroacetate (0.034 mL, 0.385 mmol), and potassium carbonate (58 mg, 0.42 mmol) were added in anhydrous DMF (2 mL), and the reaction mixture was heated at 80 °C for overnight. After cooling to room temperature, the residue was partitioned between water and ethyl acetate, and the aqueous layer was extracted with EtOAc. The combined organic phase was dried over Na₂SO₄, and concentrated *in vacuo*. The resulting residue was purified using column chromatography (DCM:EtOAc=10:1, 5:1, *n*-Hexane:EtOAc=1:1, EtOAc) to obtain YUM347A as a beige crystal (72 mg, 46%). ¹H NMR (300 MHz, CDCl₃) δ : 8.86 (d, $J = 3.0$ Hz, 1H), 8.52 (d, $J = 8.4$ Hz, 1H), 8.04 (d, $J = 9.0$ Hz, 1H), 7.62 (s, 1H), 7.49 (dd, $J = 8.4, 3.9$ Hz, 1H), 7.05 (t, $J = 7.8$ Hz, 1H), 6.77 (s, 1H), 6.69 – 6.66 (m, 2H), 6.48 (d, $J = 9.0$ Hz, 1H), 5.27 (d, $J = 15.9$ Hz, 1H), 4.53 (d, $J = 15.9$ Hz, 1H), 3.74 (s, 3H), 2.30 (td, $J = 7.5, 3.0$ Hz, 2H), 1.70 (sextet, $J = 7.5$ Hz, 2H), 0.92 (t, $J = 7.5$ Hz, 3H). ¹³C NMR (75 MHz, CDCl₃) δ : 173.46, 170.53, 156.77, 150.63, 149.67, 142.64, 142.30, 133.71, 133.55, 129.49, 127.99, 126.89, 126.30, 122.04, 117.80, 114.70, 113.85, 70.53, 54.36, 52.17, 38.56, 19.18, 13.82. MS (ESI) $m/z = 443$ (M+H)⁺, 441 (M-H)⁻. HPLC: purity 98.6%.

2-(3-(Butyramido(5-chloro-8-hydroxyquinolin-7-yl)methyl)phenoxy)acetic acid (YUM354, 22). To a solution of **YUM347A** (43 mg, 0.097 mmol) in MeOH (2 mL) was added 50% NaOH (40 drops), and the mixture was stirred at room temperature for 1 hr. After neutralization with 3 eq of 1N HCl, the precipitate was filtered, washed with ice-water, and dried to obtain **YUM354** as a beige solid (14 mg, 34%). **¹H NMR** (400.1 MHz, CDCl₃) δ: 8.97 (d, *J* = 2.4 Hz, 1H), 8.56 (dd, *J* = 8.8, 1.6 Hz, 1H), 7.63 (s, 1H), 7.53 (dd, *J* = 8.8, 4.4 Hz, 1H), 7.24 (t, *J* = 8.0 Hz, 1H), 6.86 – 6.74 (m, 4H), 6.59 (d, *J* = 8.4 Hz, 1H), 3.93 (s, 3H), 3.78 (s, 3H), 2.29 (td, *J* = 7.6, 2.4 Hz, 2H), 1.74 (sextet, *J* = 7.6 Hz, 2H), 0.99 (t, *J* = 7.2 Hz, 3H). **¹³C NMR** (100.6 MHz, CDCl₃) δ: 172.29, 159.81, 152.82, 150.03, 143.48, 142.87, 134.23, 133.36, 129.61, 127.07, 126.84, 126.14, 121.96, 118.97, 112.98, 112.19, 62.54, 55.26, 53.40, 38.77, 19.15, 13.83. **MS** (ESI) *m/z* = 429 (M+H)⁺, 427 (M-H)⁻. **UPLC**: purity 98.6%.

3-(Butyramido(5-chloro-8-hydroxyquinolin-7-yl)methyl)benzoic acid (YUM401, 23). The same procedure for the synthesis of **YUM70** was followed using 5-chloro-8-hydroxyquinoline (350 mg, 1.95 mmol), 3-carboxybenzaldehyde (586 mg, 3.9 mmol), and butyramide (186 mg, 2.14 mmol) to obtain **YUM401** as an off-white solid (461 mg, 59%) after washing the crude product with diethyl ether and methanol. **¹H NMR** (300 MHz, DMSO-*d*₆) δ: 12.98 (s, 1H), 10.43 (s, 1H), 8.97 (d, *J* = 3.3 Hz, 1H), 8.85 (d, *J* = 8.8 Hz, 1H), 8.50 (d, *J* = 8.6 Hz, 1H), 7.88 – 7.79 (m, 2H), 7.77 – 7.70 (m, 2H), 7.55 – 7.42 (m, 2H), 6.77 (d, *J* = 8.6 Hz, 1H), 2.22 (t, *J* = 7.2 Hz, 2H), 1.56 (sextet, *J* = 7.2 Hz, 2H), 0.87 (t, *J* = 7.3 Hz, 3H). **¹³C NMR** (75 MHz, DMSO-*d*₆) δ: 172.05, 167.60, 149.77, 142.93, 139.10, 133.02, 132.01, 131.34, 129.24, 128.42, 128.08, 126.54, 125.40, 123.53, 119.13, 49.77, 37.67, 19.25, 14.05. **MS** (ESI) *m/z* = 399 (M+H)⁺, 397 (M-H)⁻. **HPLC** (mobile phase A): purity 97.5%.

***N*-((5-Chloro-8-hydroxyquinolin-7-yl)(3-cyanophenyl)methyl)butyramide (YUM402, 24).**

The same procedure for the synthesis of **YUM70** was followed using 5-chloro-8-hydroxyquinoline (200 mg, 1.11 mmol), 3-cyanobenzaldehyde (292 mg, 2.227 mmol), and butyramide (106 mg, 1.22 mmol) to obtain **YUM402** as an ivory solid (8 mg, 2%) after purification by column chromatography (*n*-Hexane:EtOAc=3:1) followed by recrystallization from ethanol. **¹H NMR** (300 MHz, CDCl₃+2 drops of MeOD) δ: 8.85 (d, *J* = 4.0 Hz, 1H), 8.54 (d, *J* = 8.4 Hz, 1H), 7.64 – 7.57 (m, 3H), 7.56 – 7.51 (m, 2H), 7.41 (t, *J* = 8.0 Hz, 1H), 6.53 (s, 1H), 2.30 (t, *J* = 7.5 Hz, 2H), 1.72 (d, *J* = 7.5 Hz, 2H), 0.97 (t, *J* = 7.4 Hz, 3H). **¹³C NMR** (75 MHz, DMSO-*d*₆) δ: 172.20, 149.90, 149.80, 143.95, 139.14, 133.04, 132.49, 131.37, 130.65, 130.27, 126.37, 125.54, 124.77, 123.62, 119.28, 119.18, 111.83, 49.78, 37.63, 19.18, 14.04. **MS** (ESI) *m/z* = 380 (M+H)⁺. **HPLC** (mobile phase B): purity 95%.

***N*-(Benzo[*d*][1,3]dioxol-5-yl(5-bromo-8-hydroxyquinolin-7-yl)methyl)butyramide**

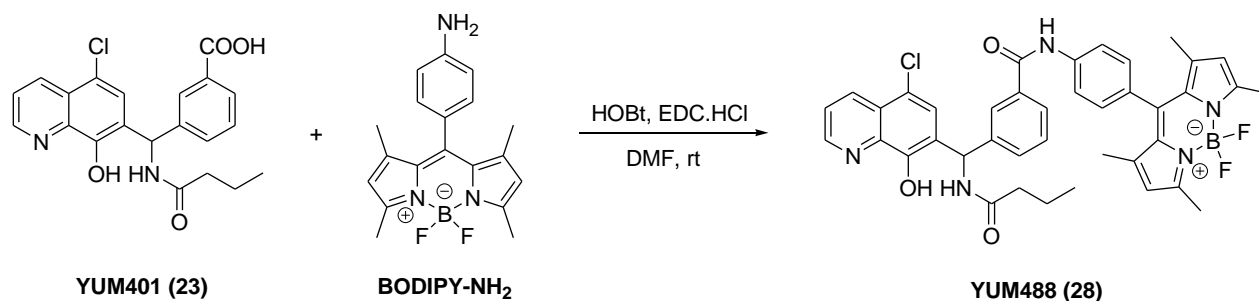
(YUM411, 25). The same procedure for the synthesis of **YUM70** was followed using 5-bromoquinoline-8-ol (300 mg, 1.339 mmol), piperonal (402 mg, 2.678 mmol), and butyramide (128 mg, 1.473 mmol) to obtain **YUM411** as a tan solid (14 mg, 2%). **¹H NMR** (300 MHz, DMSO-*d*₆) δ: 10.39 (bs, 1H), 8.93 (s, 1H), 8.68 (d, *J* = 8.3 Hz, 1H), 8.41 (d, *J* = 7.5 Hz, 1H), 7.87 (s, 1H), 7.71 (d, *J* = 4.0 Hz, 1H), 6.91 – 6.76 (m, 2H), 6.70 (d, *J* = 7.5 Hz, 1H), 6.60 (d, *J* = 7.5 Hz, 1H), 5.96 (s, 2H), 2.19 (t, *J* = 6.6 Hz, 2H), 1.54 (sextet, *J* = 7.2 Hz, 2H), 0.85 (t, *J* = 6.6 Hz, 3H). **¹³C NMR** (75 MHz, DMSO-*d*₆) δ: 171.83, 150.11, 149.66, 147.74, 146.56, 139.35, 136.36, 135.42, 129.96, 126.83, 126.54, 123.73, 120.54, 108.92, 108.51, 107.81, 101.42, 49.64, 37.68, 19.25, 14.07. **MS** (ESI) *m/z* = 444 (M+H)⁺, 442 (M-H)⁻. **HPLC** (mobile phase B): purity 98.8%.

***N*-((5-Chloro-8-(((2*E*,6*E*)-3,7,11-trimethyldodeca-2,6,10-trien-1-yl)oxy)quinolin-7-yl)(3-chlorophenyl)methyl)butyramide (YUM137, 26).** To a dried flask were added **YUM194** (97

mg, 0.25 mmol), triphenylphosphine (72 mg, 0.275 mmol), and trans-farnesol (61 mg, 0.275 mmol) in THF with stirring, and the flask was covered by rubber septum. While stirring, DEAD (40% in toluene, 120 mg, 0.275 mmol) was added dropwise, and the reaction mixture was heated at 60 °C for overnight. After cooling, the resulting residue was concentrated under reduced pressure, and then purified by column chromatography (*n*-Hexane:EtOAc=5:1) to afford **YUM137** as an ivory solid (24 mg, 28%). **¹H NMR** (400 MHz, CDCl₃) δ: 8.96 (dd, *J* = 4.0, 1.6 Hz, 1H), 8.55 (dd, *J* = 8.4, 1.6 Hz, 1H), 7.61 (s, 1H), 7.53 (dd, *J* = 8.4, 4.0 Hz, 1H), 7.27 (s, 1H), 7.23 – 7.21 (m, 2H), 7.15 – 7.12 (m, 1H), 6.99 (d, *J* = 8.8 Hz, 1H), 6.56 (d, *J* = 8.4 Hz, 1H), 5.39 (td, *J* = 6.8, 0.8 Hz, 1H), 5.16 – 5.09 (m, 3H), 4.39 (dd, *J* = 10.8, 6.8 Hz, 1H), 2.28 (td, *J* = 8.0, 4.4 Hz, 2H), 2.11 – 1.97 (m, 8H), 1.78 – 1.71 (m, 2H), 1.70 (s, 3H), 1.62 (s, 9H), 0.98 (t, *J* = 7.2 Hz, 3H). **MS** (ESI) *m/z* = 593 (M+H)⁺, 615 (M+Na)⁺.

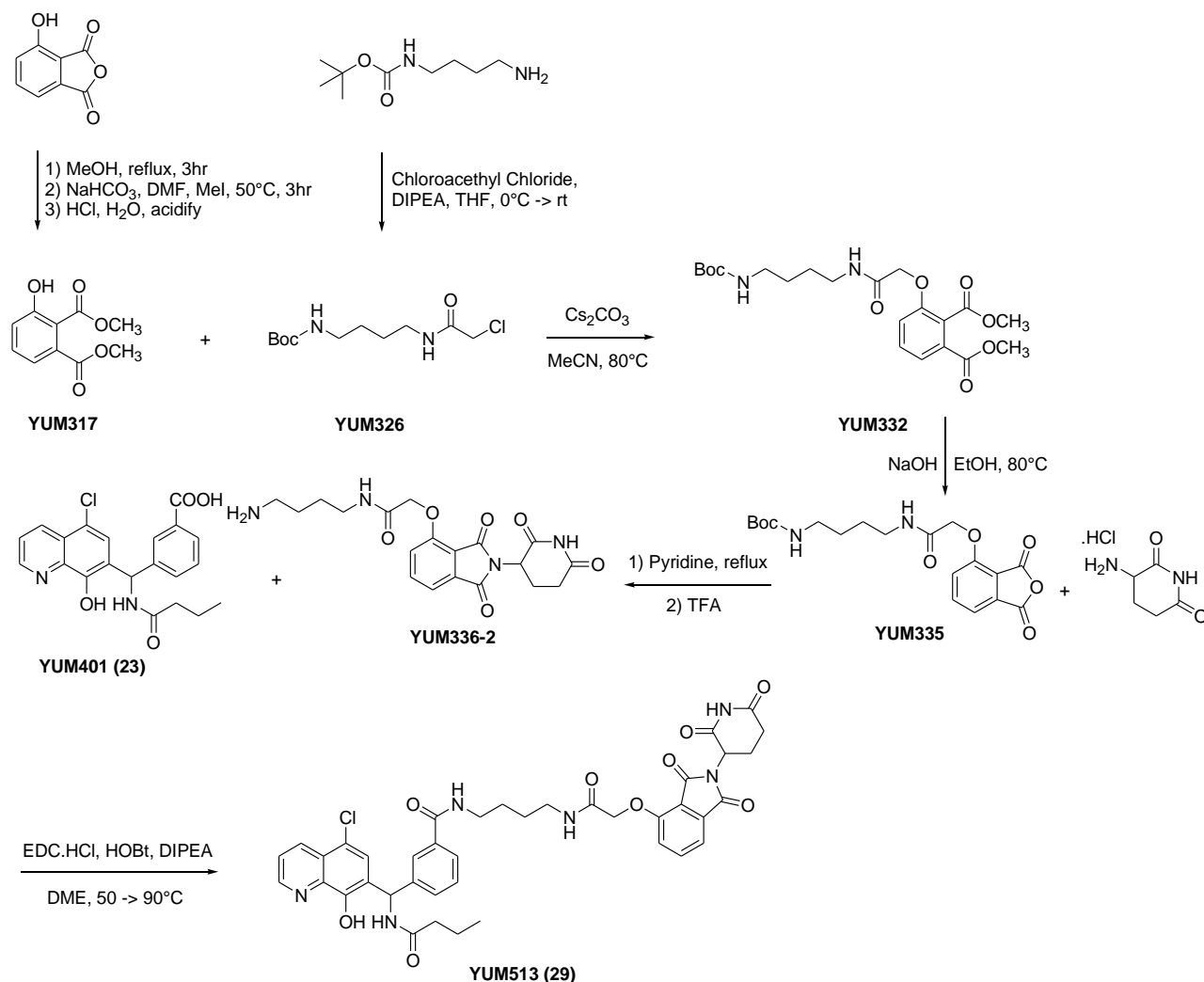
***N*-((5-Chloro-8-hydroxyquinolin-7-yl)(3-(((2*E*,6*E*)-3,7,11-trimethyldodeca-2,6,10-trien-1-yl)oxy)phenyl)methyl)butyramide (YUM168, 27)**. The same procedure for the synthesis of **YUM137** was followed using **YUM166** (100 mg, 0.269 mmol), triphenylphosphine (78 mg, 0.296 mmol), trans-farnesol (66 mg, 0.296 mmol), and DEAD (40% in toluene, 129 mg, 0.296 mmol) to obtain **YUM168** as a yellow solid (55 mg, 36%). **¹H NMR** (400 MHz, CDCl₃) δ: 8.92 (dd, *J* = 4.0, 1.6 Hz, 1H), 8.52 (dd, *J* = 8.4, 1.6 Hz, 1H), 7.56 (s, 1H), 7.49 (dd, *J* = 8.8, 4.4 Hz, 1H), 7.27 (s, 1H), 7.13 (t, *J* = 8.0 Hz, 1H), 6.96 (d, *J* = 8.4 Hz, 1H), 6.77 (d, *J* = 7.6 Hz, 1H), 6.70 – 6.68 (m, 2H), 6.50 (d, *J* = 8.8 Hz, 1H), 5.71 (s, 1H), 5.42 (t, *J* = 6.8 Hz, 1H), 5.11 – 5.02 (m, 3H), 4.42 (dd, *J* = 10.8, 6.8 Hz, 1H), 2.24 (td, *J* = 7.6, 4.4 Hz, 2H), 2.06 – 1.95 (m, 8H), 1.75 – 1.68 (m, 5H), 1.59 (s, 9H), 0.95 (t, *J* = 7.2 Hz, 3H). **MS** (ESI) *m/z* = 575.19 (M+H)⁺, **HPLC** (mobile phase A): purity 96.0%.

Scheme 2. Synthesis of BODIPY conjugated YUM401 (YUM488)



3-(Butyramido(5-chloro-8-hydroxyquinolin-7-yl)methyl)-N-(4-(5,5-difluoro-1,3,7,9-tetramethyl-5H-4λ⁴,5λ⁴-dipyrrolo[1,2-c:2',1'-f][1,3,2]diazaborinin-10-yl)phenyl)benzamide (YUM488, 28). To a stirred solution of **YUM401** (30 mg, 0.075 mmol) in DMF was added HOBT (10 mg, 0.075 mmol) and EDC.HCl (14 mg, 0.075 mmol) at 0 °C. The mixture was stirred for 15 min at 0 °C, and for 1 hr at room temperature. Then, **BODIPY-NH₂** (26 mg, 0.075 mmol) was added and the reaction mixture was stirred for overnight at room temperature. The mixture was diluted with brine and extracted with ethyl acetate, and the organic phase was concentrated under reduced pressure. The resulting residue was triturated with ethyl acetate and dichloromethane to obtain **YUM488** (17 mg, 31%) as an orange solid. ¹H NMR (300 MHz, DMSO-*d*₆) δ: 10.53 (s, 1H), 8.98 (dd, *J* = 4.2, 1.5 Hz, 1H), 8.86 (d, *J* = 8.6 Hz, 1H), 8.50 (dd, *J* = 8.6, 1.6 Hz, 1H), 7.95 (d, *J* = 8.6 Hz, 2H), 7.87 – 7.84 (m, 2H), 7.76 – 7.72 (m, 2H), 7.53 – 7.48 (m, 2H), 7.33 (d, *J* = 8.4 Hz, 2H), 6.81 (d, *J* = 8.6 Hz, 1H), 6.19 (s, 2H), 2.45 (s, 6H), 2.24 (t, *J* = 7.3 Hz, 2H), 1.58 (sextet, *J* = 7.3 Hz, 2H), 1.42 (s, 6H), 0.88 (t, *J* = 7.4 Hz, 3H). MS (ESI) *m/z* = 720 (M+H)⁺, 700 (M-F)⁺, 718 (M-H)⁻. HPLC (mobile phase A): purity 97.6%.

Scheme 3. Synthesis of PROTAC conjugate to YUM401 (YUM513)



Tert-butyl (4-(2-chloroacetamido)butyl)carbamate (YUM326). To a solution of *N*-*tert*-butyl-4-aminobutan-1-amine (1.0 mL, 5.22 mmol) in anhydrous THF was added chloroacetyl chloride (0.57 mL, 5.74 mmol) and DIPEA (0.91 mL, 5.22 mmol) in the ice bath. The resulting solution was allowed to warm at room temperature for 3 hrs. The reaction mixture was then diluted with EtOAc and water. The organic layer was separated, washed with water, dried over Na₂SO₄ and concentrated to obtain **YUM326** as an ivory solid (1.3 g, 97%). ¹H NMR (300 MHz, CDCl₃) δ:

6.66 (bs, 1H), 4.58 (bs, 1H), 4.05 (s, 1H), 3.33 (q, $J = 6.3$ Hz, 2H), 3.14 (q, $J = 6.3$ Hz, 2H), 1.60 – 1.50 (m, 4H), 1.44 (s, 9H).

Dimethyl 3-hydroxyphthalate (YUM317). A mixture of 3-hydroxy phthalic anhydride (250 mg, 1.52 mmol) in MeOH was refluxed for 3 hrs. The mixture was cooled and concentrated, and the resulting residue was suspended in the solution of NaHCO₃ (358 mg, 4.25 mmol) in DMF followed by addition of iodomethane (0.23 mL, 3.64 mmol). The reaction mixture was heated at 50 °C for 3 hrs, and then acidified with 4N HCl and aqueous layer was extracted with EtOAc. The combined organic layer was washed with water and brine, dried over Na₂SO₄, and concentrated. The crude product was purified by column chromatography (*n*-Hexane:EtOAc=1:1) to obtain **YUM317** as a yellow liquid (300 mg, 94%). ¹H NMR (300 MHz, CDCl₃) δ : 10.57 (s, 1H), 7.46 (t, $J = 7.8$ Hz, 1H), 7.08 (dd, $J = 8.7, 1.2$ Hz, 1H), 6.96 (dd, $J = 7.5, 1.2$ Hz, 1H), 3.92 (s, 3H), 3.89 (s, 3H).

Dimethyl 3-(2-((4-((tert-butoxycarbonyl)amino)butyl)amino)-2-oxoethoxy)phthalate (YUM332). A solution of **YUM317** (1.1 g, 5.23 mmol) in MeCN was treated with **YUM326** (1.26 g, 4.76 mmol) and Cs₂CO₃ (4.19 g, 12.8 mmol). The resulting mixture was heated at 80 °C for 12 hrs, and then concentrated under reduced pressure. The residue was then diluted with EtOAc and water, and the combined organic layer was separated, washed with water, dried over Na₂SO₄ and concentrated. The crude product was purified by column chromatography (DCM:MeOH=10:1) to obtain **YUM332** as a yellow liquid (1.63 g, 78%). ¹H NMR (300 MHz, CDCl₃) δ : 7.64 (d, $J = 7.8$ Hz, 1H), 7.48 (t, $J = 8.1$ Hz, 1H), 7.14 (d, $J = 8.4$ Hz, 1H), 7.05 (bs, 1H), 4.60 (s, 3H), 3.95 (s, 3H), 3.91 (s, 3H), 3.32 (q, $J = 6.5$ Hz, 2H), 3.15 – 3.10 (m, 2H), 1.64 – 1.47 (m, 4H), 1.44 (s, 9H).

Tert-butyl (4-(2-((1,3-dioxo-1,3-dihydroisobenzofuran-4-yl)oxy)acetamido)butyl)carbamate (YUM335). To a solution of **YUM332** (1.6 g, 3.65 mmol) in EtOH was added 3N NaOH (3.65 mL, 10.9 mmol), and the resulting mixture was heated at 80 °C for 2 hrs. The reaction mixture was

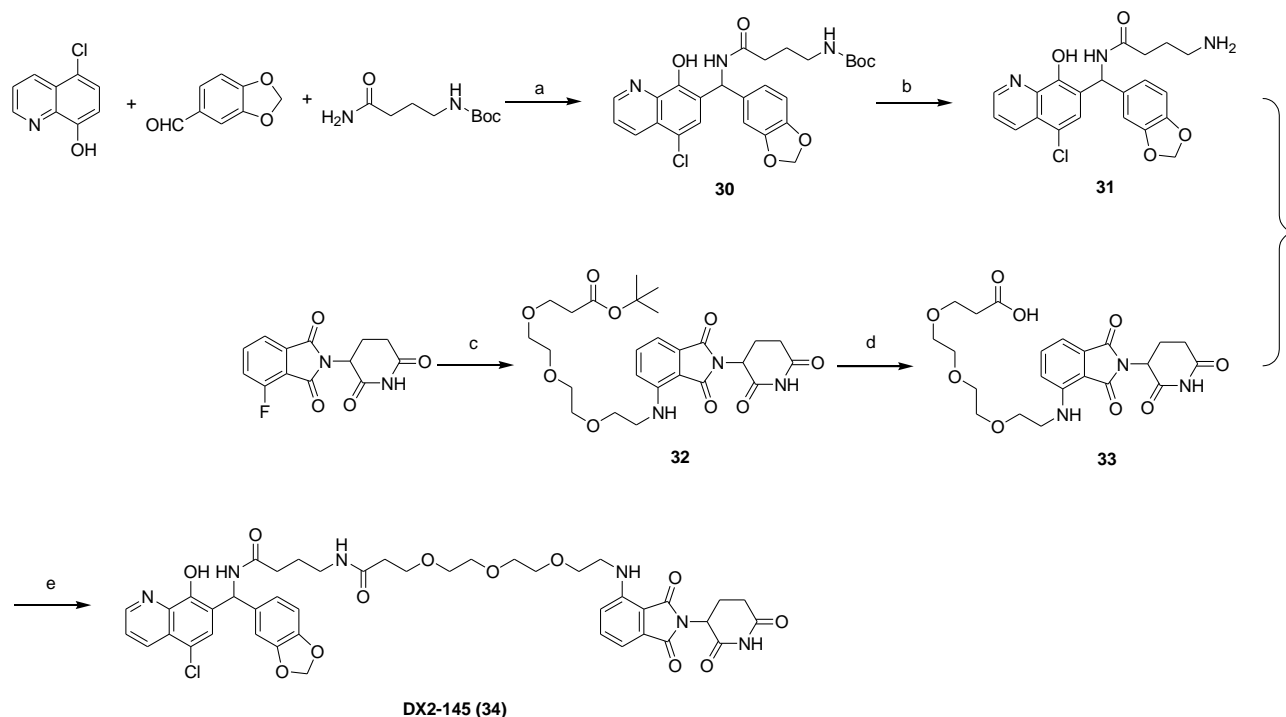
concentrated under reduced pressure, and the crude mixture was dissolved in water and EtOAc, and then acidified using 1N HCl. The combined organic layer was separated, washed with water, dried over Na₂SO₄, and concentrated under reduced pressure to obtain **YUM335** as a yellow solid (540 mg, 38%). ¹H NMR (300 MHz, CDCl₃) δ: 7.64 (d, *J* = 7.2 Hz, 1H), 7.46 (t, *J* = 8.1 Hz, 1H), 7.22 (bs, 1H), 7.14 (d, *J* = 8.4 Hz, 1H), 4.62 (s, 2H), 3.35 (d, *J* = 5.1 Hz, 2H), 3.14 (bs, 2H), 1.57 (bs, 4H), 1.45 (s, 9H).

***N*-(4-Aminobutyl)-2-((2-(2,6-dioxopiperidin-3-yl)-1,3-dioxoisindolin-4-yl)oxy)acetamide (YUM336-2)**. To a solution of **YUM335** (540 mg, 1.37 mmol) in pyridine was added 3-aminopiperidine-2,6-dione HCl (227 mg, 1.37 mmol), and the resulting solution was heated under reflux for 12 hrs. After cooling, the reaction mixture was concentrated under reduced pressure, and the crude Boc-protected intermediate was purified by column chromatography (DCM:MeOH=10:1). The Boc-protected intermediate was dissolved in DCM and treated with TFA, and the reaction mixture was heated at 50 °C for 2 hrs. The crude product was purified by crystallization from EtOAc to obtain **YUM336-2** as an ivory solid (99 mg, 19%). ¹H NMR (300 MHz, MeOD) δ: 8.19 (t, *J* = 7.0 Hz, 1H), 7.82 (t, *J* = 7.8 Hz, 1H), 7.56 (d, *J* = 7.3 Hz, 1H), 7.45 (d, *J* = 8.5 Hz, 1H), 5.14 (dd, *J* = 12.4, 5.4 Hz, 1H), 4.78 (s, 2H), 3.40 – 3.37 (m, 2H), 2.96 (t, *J* = 6.6 Hz, 2H), 2.90 – 2.64 (m, 3H), 2.18 – 2.10 (m, 1H), 1.72 – 1.64 (m, 4H).

3-(Butyramido(5-chloro-8-hydroxyquinolin-7-yl)methyl)-*N*-(4-(2-((2-(2,6-dioxopiperidin-3-yl)-1,3-dioxoisindolin-4-yl)oxy)acetamido)butyl)benzamide (YUM513, 29). To a solution of **YUM401** (15 mg, 0.037 mmol), EDC.HCl (7.2 mg, 0.037 mmol), HOBT (6.1 mg, 0.045 mmol) and DIPEA (14.5 mg, 0.112 mmol) in DMF was added **YUM336-2** (19 mg, 0.037 mmol). The reaction mixture was heated at 50 °C for 16 hrs, and then cooled down to room temperature. The mixture was diluted with EtOAc, washed with water and brine, dried over Na₂SO₄, and

concentrated. The crude product was purified by column chromatography (DCM, DCM:0.5M NH₄ in MeOH=10:1) to obtain **YUM513**. MS (ESI) m/z = 783 (M+H)⁺, 781 (M-H)⁻. HPLC (mobile phase A): purity 94%.

Scheme 4. The synthesis of DX2-145



Reagents and conditions: a) neat, microwave, 140°C, overnight; b) TFA, DCM, rt, 2h; c) *tert*-butyl 3-(2-(2-(2-aminoethoxy)ethoxy)ethoxy)propanoate, DIEA, DMF, 90°C, overnight; d) TFA, DCM, 3h, rt; e) HATU, DIEA, DMF, overnight.

The synthesis of the PROTAC molecule **DX2-145** consists of the generation of both the modified **YUM70** derivative **31** as well as a PEG3-pomalidomide chimera part **33**. The synthesis of **31**, with an additional amino group on the side chain of **YUM70** to facilitate the attachment with the linker part, started with a three-component Betti reaction under a neat condition generating intermediate **30**. A subsequent acidic deprotection with TFA yielded **31**. A S_NAr reaction between 2-(2,6-dioxopiperidin-3-yl)-4-fluoroisindoline-1,3-dione and *tert*-butyl 3-(2-(2-(2-

aminoethoxy)ethoxy)ethoxy)propanoate gave rise to **32**. The *tert*-butyl ester of **32** was then hydrolyzed with TFA in DCM to give the other key intermediate **33**. The coupling reaction between **31** and **33** in the presence of HATU and DIEA in DMF yielded the final product **DX2-145**.

***tert*-Butyl (4-((benzo[*d*][1,3]dioxol-5-yl(5-chloro-8-hydroxyquinolin-7-yl)methyl)amino)-4-oxobutyl)carbamate (30)**. A mixture of 5-chloro-8-hydroxyquinoline (500 mg, 2.78 mmol), benzo[*d*][1,3]dioxole-5-carbaldehyde (1.25 g, 8.33 mmol) and *tert*-butyl (4-amino-4-oxobutyl)carbamate (510 mg, 2.52 mmol) were mixed and heated at 140 °C. The solids melted upon heating to generate a brown mixture that was stirred at the same temperature overnight. The mixture was taken up by EtOAc, filtered and washed with EtOAc to give **30** as a white solid (748 mg, 52%). ¹H NMR (400 MHz, DMSO-*d*₆) δ 10.31 (s, 1H), 8.96 (dd, *J* = 4.2, 1.6 Hz, 1H), 8.69 (d, *J* = 8.7 Hz, 1H), 8.49 (dd, *J* = 8.6, 1.6 Hz, 1H), 7.75 – 7.70 (m, 2H), 6.86 – 6.82 (m, 2H), 6.80 (t, *J* = 5.6 Hz, 1H), 6.74 – 6.70 (m, 1H), 6.61 (d, *J* = 8.7 Hz, 1H), 5.97 (s, 2H), 2.92 (q, *J* = 6.7 Hz, 2H), 2.21 (td, *J* = 7.4, 2.7 Hz, 2H), 1.62 (p, *J* = 7.3 Hz, 2H), 1.37 (s, 9H). LC-MS (ESI) *m/z* 514.2 [M + H]⁺.

4-Amino-N-(benzo[*d*][1,3]dioxol-5-yl(5-chloro-8-hydroxyquinolin-7-yl)methyl)butanamide (31). To a solution of **30** (67 mg, 0.13 mmol) in DCM (2 mL) was added TFA (0.4 mL). The resulting solution was stirred at room temperature for 2h and concentrated to give **31** as a light yellow gel (50 mg, 92%), which was used in the next step without further purification. ¹H NMR (300 MHz, MeOD) δ 8.95 (dd, *J* = 4.4, 1.5 Hz, 1H), 8.68 (dd, *J* = 8.6, 1.5 Hz, 1H), 7.75 (dd, *J* = 8.6, 4.4 Hz, 1H), 7.58 (s, 1H), 6.83 – 6.74 (m, 3H), 6.68 (s, 1H), 5.94 (s, 2H), 2.99 (t, *J* = 7.6 Hz, 2H), 2.51 (td, *J* = 7.1, 2.1 Hz, 2H), 2.05 – 1.86 (m, 2H). LC-MS (ESI) *m/z* 414.1 [M + H]⁺.

tert-Butyl 3-(2-(2-(2-((2-(2,6-dioxopiperidin-3-yl)-1,3-dioxoisindolin-4-yl)amino)ethoxy)ethoxy)ethoxy)propanoate (32). To a solution of 2-(2,6-dioxopiperidin-3-yl)-4-fluoroisindoline-1,3-dione (80 mg, 0.29 mmol) and *tert*-butyl 3-(2-(2-(2-aminoethoxy)ethoxy)ethoxy)propanoate (80 mg, 0.29 mmol) in DMF (4 mL) was added DIEA (75 mg, 0.58 mmol) and the mixture was heated at 90 °C overnight. The mixture was then diluted with EtOAc, washed with water, brine, dried over anhydrous Na₂SO₄, and purified with flash chromatography (50% EtOAc in hexane) to give **32** (57 mg, 37%) as a white solid. ¹H NMR (300 MHz, MeOD) δ 7.53 (dd, *J* = 8.5, 7.2 Hz, 1H), 7.05 (t, *J* = 7.9 Hz, 2H), 5.07 (dd, *J* = 12.3, 5.4 Hz, 1H), 3.77 – 3.55 (m, 12H), 3.49 (t, *J* = 5.3 Hz, 2H), 2.92 – 2.62 (m, 3H), 2.46 (td, *J* = 6.2, 0.9 Hz, 2H), 2.19 – 2.09 (m, 1H), 1.44 (s, 9H). LC-MS (ESI) *m/z* 534.2 [M + H]⁺.

3-(2-(2-(2-((2-(2,6-Dioxopiperidin-3-yl)-1,3-dioxoisindolin-4-yl)amino)ethoxy)ethoxy)ethoxy)propanoic acid (33). To a solution of **32** (57 mg, 0.11 mmol) in DCM (2 mL) was added TFA (0.4 mL). The resulting solution was stirred at room temperature for 3h and concentrated to give **33** as a light yellow gel (51 mg, 98%), which was used in the next step without further purification. LC-MS (ESI) *m/z* 478.1 [M + H]⁺.

***N*-(Benzo[*d*][1,3]dioxol-5-yl(5-chloro-8-hydroxyquinolin-7-yl)methyl)-4-(3-(2-(2-(2-((2-(2,6-dioxopiperidin-3-yl)-1,3-dioxoisindolin-4-yl)amino)ethoxy)ethoxy)ethoxy)propanamido)butanamide (DX2-145).** To a solution of **33** (57 mg, 0.12 mmol) and HATU (68 mg, 0.18 mmol) in DMF (2 mL) was added **31** (49 mg, 0.12 mmol) followed by DIEA (46 mg, 0.16 mmol). The resulting mixture was stirred at room temperature overnight. The mixture was then diluted with EtOAc, washed with water, brine, dried over anhydrous Na₂SO₄, and purified with preparative HPLC (10-95% CH₃CN in H₂O, 0.05% formic acid as additive) to give **DX2-145** (57 mg, 37%) as a white solid. ¹H NMR (400 MHz, MeOD) δ 8.88 (dt, *J* = 4.1, 1.9 Hz, 1H), 8.49 (ddd, *J* = 8.6, 2.7, 1.

5 Hz, 1H), 7.61 (dddd, $J = 8.6, 4.3, 2.3, 0.9$ Hz, 1H), 7.55 (s, 1H), 7.51 (dddd, $J = 8.4, 7.1, 3.6, 1.2$ Hz, 1H), 7.02 (td, $J = 6.9, 2.8$ Hz, 2H), 6.84 – 6.74 (m, 3H), 6.68 – 6.65 (m, 1H), 5.91 (d, $J = 1.2$ Hz, 2H), 5.04 (ddt, $J = 12.4, 5.4, 1.1$ Hz, 1H), 3.72 – 3.64 (m, 4H), 3.64 – 3.54 (m, 8H), 3.44 (td, $J = 5.3, 2.4$ Hz, 2H), 3.24 (t, $J = 6.8$ Hz, 2H), 2.91 – 2.63 (m, 3H), 2.44 – 2.33 (m, 4H), 2.14 – 2.06 (m, 1H), 1.83 (p, $J = 7.2$ Hz, 2H). LC-MS (ESI) m/z 873.3 $[M + H]^+$. Purity 99.6%.

MATERIALS and METHODS

MTT assay

Cytotoxicity was assessed by 3-(4,5-dimethylthiazol-2-yl)-2, 5-diphenyltetrazolium bromide (MTT) assay as previously described (7). Cells were seeded in 96-well plates at 3000-7000 cells/well depending on the cell line. After overnight incubation, cells were treated with indicated compounds for 72 hr. After treatment, MTT (0793, VWR) solution was added to the wells to a final concentration of 0.3 mg/ml and incubated for 4 hr at 37 °C. The supernatant was removed and 100 μ l of DMSO was added to wells. Then the plates were shaken for 15 min at room temperature and absorbance was measured at 570 nm.

Colony formation assay

Cells were plated in 96-well plates at 200 cells/well. After overnight attachment, compounds were added to the wells at sequential dilutions. Cells were kept in culture until visible colonies formed in control wells. Colonies were then fixed, stained with 0.05% crystal violet solution (2% formaldehyde, 40% methanol in distilled water), washed with water to remove excess stain, and imaged with Odyssey Imaging Systems (LI-COR Biosciences, Lincoln, NE).

Human liver microsomal stability study *in vitro*

Microsomal stability of YUM70 (1 μ M) was determined at 37 °C in 0.5 mg/mL human liver microsomes and 1 mM NADPH cofactor in a total volume of 400 μ L of 100 mM potassium

phosphate buffer (pH 7.4 containing 3.3 mM MgCl₂). The reactions were stopped at 0, 5, 10, 15, 30, and 60 min, by adding threefold the volume of CH₃CN. The collected fractions were centrifuged for 5 min at 14000 rpm and the supernatant (5 µl) was collected for LC–MS/MS analyses. The amount of parent compound remaining was determined. The natural logarithm of the amount of parent compound remaining was plotted against time to calculate the rate of disappearance and half-life of the tested compounds.

Short pharmacokinetic study

Plasma concentration of YUM70 was determined in CD-1 mouse following intravenous (IV) and *per os* (PO) administration of YUM70. The drug solution was directly prepared in citrate buffer at 2 mg/mL, and then was diluted with sterile saline (1:1), 1 mg/mL drug solution was obtained for oral gavage (30 mg/Kg) and IV injection (15 mg/kg). At the given time point, blood samples were collected using heparinized calibrated pipettes. Samples were centrifuged at 15000 rpm for 10 min. Subsequently, blood plasma was collected from the upper layer. The plasma was frozen at -80 °C for later analysis.

Protein expression and purification

The His-tagged recombinant proteins were expressed in *E.Coli*. BL21 (DE3) pRARE2 (Rosetta 2 (DE3); Novagen) and purified as described previously (8). Briefly, GRP78 plasmids were transformed into Rosetta 2 cells, which were then grown in TB broth supplemented with 8 g/L glycerol, 50 µg/mL kanamycin or 100 µg/mL ampicillin at 37 °C to an OD₆₀₀ of approximately 1.5-2. The culture was allowed to cool to 18 °C over a period of 1 h and induced with 0.5 mM isopropyl thio-β-D-galactoside for 18 hr. Bacterial cells were harvested by centrifugation at 4000 × g for 20 min at 4 °C and the cell pellet was resuspended in lysis buffer (100 mM HEPES, 500 mM NaCl, 10% glycerol, 10 mM imidazole, 0.5 mM TCEP, pH 8.0

supplemented with EDTA-free protease inhibitor and Benzonase® nuclease (Sigma, 2000 U); 15 mL lysis buffer/g cell pellet). Cells were lysed by sonication and the cleared supernatant was purified using 1 mL Ni-NTA resin washed sequentially with buffer (20 mM HEPES pH 7.5, 500 mM NaCl, 10% glycerol, and 0.5 mM TCEP) containing increasing concentrations of imidazole (10 mM, 25 mM and 500 mM). The recombinant enzyme was purified using PD-10 desalting column (GE Healthcare) with filtration buffer (20 mM HEPES, 300 mM NaCl, 10% glycerol, 0.5 mM TCEP, pH 7.5). Protein purity was assessed by SDS-PAGE.

Partial proteolysis

GRP78 (5 µg for SDS-PAGE analysis) was incubated with 1 mM ATP, 1 mM ADP, 100 µM YUM70, 100 µM YUM70 + 1 mM ATP, 100 µM YUM70 + 1 mM ADP, 100 µM VER, 100 µM VER+1 mM ATP, 100 µM VER + 1mM ADP for 30 min at room temperature. GRP78 was digested by adding 0.1 µg trypsin (Promega, V5280) per 2 µg protein and incubated at 37 °C for 30 min. Samples were quenched by the addition of 5X loading buffer and boiling and separated on a 4-20% pre-made SDS-PAGE gel (Bio-Rad). Gels were visualized by coomassie stain.

Pathway analysis

Bru-seq data sets of MIA PaCa-2 cells treated with YUM70 were filtered using the cut-off values > 10 normalized counts and mean reads per kilobase per million (RPKM) > 0.5 . After filter, a total of 8,949 genes were ranked based on fold change values versus DMSO control. The ranked-order gene list was analyzed using GSEA for pathway identification. GSEA was performed based on the Kolmogorov– Smirnov statistics (9). For each gene set, the ES (enrichment scores) were normalized to account for differences in gene set size. The false discovery rate (FDR) was calculated relative to the normalized enrichment score (NES) values. DAVID (Database for Annotation, Visualization, and Integrated Discovery) functional annotation analysis (10) was

performed on the list of up- and downregulated genes with a fold change ≥ 2 (216 upregulated and 92 downregulated). Only those terms that reported a *p*-value of ≤ 0.05 and count number ≥ 6 genes were selected for analysis.

Connectivity map

Connectivity map (CMap) is a web resource that uses transcriptional expression profiles to identify relationships between other expression profiles, diseases, and therapeutics (<https://clue.io/cmap>). The changes in gene expression from a disease, gene knockdown or overexpression or treatment with a small molecule are compared for similarity to all available signatures in the database. We used the top 150 upregulated and downregulated genes as input to search for compounds and genes showing a similar signature. Compound or genes were selected based on the connectivity score >90.0 .

Competitive binding assay

Competition between PACMA 57 (a PDI-selective probe) and YUM70 was determined as described (11). Briefly, 0.3 μM recombinant PDI protein was incubated with 100, 10, and 1 μM of YUM70 for 1 h at 37 °C followed by 1 h incubation with 500nM of PACMA 57. Solutions were mixed with 5x SDS sample buffer and analyzed by SDS/PAGE. After fluorescence scanning gels were stained with coomassie blue. PACMA 31 is a PDI inhibitor (11) used as a positive control.

Competition between CMFDA (a GSTO1-selective probe) and YUM70 was determined as described (12). Briefly, 1 μM recombinant GSTO1 protein was incubated with 100, 10, and 1 μM of YUM70 for 1 hr at 37 °C followed by 1 hr incubation with 500nM of CMFDA. Solutions were mixed with 5x SDS sample buffer and analyzed by SDS/PAGE, and then gels were scan and stain as stated above. The reported GSTO1 inhibitor, C127 (12) was used as a positive control.

PDI reductase assay

Recombinant PDI protein (0.4 μM) was incubated with indicated compounds at 37°C for 1 hr in sodium phosphate buffer (100 mM sodium phosphate, 2mM EDTA, and 8 μM DTT, pH 7.0). Then the reaction mixture consisting of DTT (500 μM) and bovine insulin (130 μM) was added to the incubated PDI protein. The reduction reaction was catalyzed by PDI at room temperature, and the resulting aggregation of reduced insulin B chains was measured at 620 nm. % PDI activity was calculated from absorbance values at T= 0 to 80 min as described (11).

Molecular docking

YUM70, along with an inactive analog, YUM117 were docked into the substrate binding site as well as the novolactone-binding site of GRP78 (PDB: 5E85) using GOLD (Genetic Optimization for Ligand Docking) software package, version 4.0 (Cambridge Crystallographic Data Centre, Cambridge, U.K.). NR-peptide was removed from the substrate-binding pocket of the protein as a part of the protein preparation procedure for docking. Prior to docking, 10 different conformations were generated for each ligand using OMEGA v3.0.0 (OpenEye Scientific, Santa Fe, NM), a systematic, knowledge-based conformer generator (13). Docking studies were performed using the standard default settings with 100 genetic algorithms (GA) runs on each molecule and allowing side-chain flexibility of important allosteric site residues within their rotamer library.

Isolation of RNA and cDNA preparation

Cells were treated with the compounds at indicated dose and time. Total RNA was isolated from each cell line using the RNeasy Mini Kit (Qiagen, 74104) according to the manufacturer's protocol. The concentrations of the RNA preparations were determined by NanoDropTM (Thermo Fisher Scientific). The total RNA was reversed transcribed into cDNA using 1 μg of total RNA in the presence of random primers, dNTPs, and reverse transcriptase (cDNA Reverse Transcription Kit, 4374966, Applied Biosystem,) following the manufacturer's protocol.

PCR: After first-strand cDNA synthesis, 5 µl of the reaction mixture was used to prepare a 20 µl PCR mix containing Phusion® High-Fidelity DNA polymerase (New England Bio Labs, M0530S) using 2 min at 98 °C, 30 cycles at 98 °C for 20 sec, 56 °C for 30 sec, 72 °C for 20 sec, 1 min at 72 °C, 4 °C forever. PCR reactions were then subjected to electrophoresis on 1 % agarose gel. Actin was used as an internal control. Band intensity was calculated in ImageJ (NIH) software. All primer sequences are presented below.

RT-PCR primer information

The specific primer pair for actin comprised a sense primer 5'TTG CCG ACA GGA TGC AGA A-3' and an anti-sense primer 5'GCC GAT CCA CAC GGA GTA CT-3'. The specific primer pair for GRP78 comprised a sense primer 5'-GCCTGTATTTCTAGACCTGCC-3' and an anti-sense primer 5'-TTCATCTTGCCAGCCAGTTG-3'. The specific primer pair for CHAC-1 comprised of a sense primer 5' CCTGAAGTACCTGAATGTGCGAGA 3' and an anti-sense primer 5' GCAGCAAGTATTCAAGGTTGTGGC 3'. The specific primer pair for DDIT3 comprised of a sense primer 5'TCTTGACCCTGCTTCTCTGG3' and an anti-sense primer 5'GCTGTGCCACTTTCCTTTCA3'.

siRNA

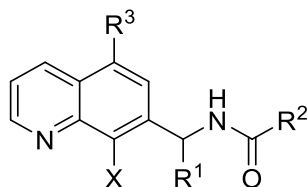
GRP78 siRNAs (Silencer® Select siRNA, Ambion Inc, s6979, s6980) and non specific control siRNA (Silencer® Select siRNA, Ambion Inc, AM4611) were purchased from Thermo Fisher Scientific. siRNA transfection was carried out with Lipofectamine® RNAiMAX transfection reagent (Invitrogen, 13778-075) following the manufacturer's protocol.

References

1. Cardellicchio C, Capozzi MAM, Naso F. The Betti base: the awakening of a sleeping beauty. *Tetrahedron-Asymmetry* **2010**;21:507-17
2. McLean LR, Zhang Y, Li H, Li Z, Lukasczyk U, Choi YM, *et al.* Discovery of covalent inhibitors for MIF tautomerase via cocrystal structures with phantom hits from virtual screening. *Bioorg Med Chem Lett* **2009**;19:6717-20
3. Nesvadba P. Easy large scale syntheses of 2,6-di-t-butyl-7-cyano-, 7-carboxy- and 7-methoxycarbonyl quinone methides. *Synthetic Commun* **2000**;30:2825-32
4. Tramonti.M. Advances in chemistry of Mannich bases. *Synthesis-Stuttgart* **1973**:703-75
5. Gilbert AM, Bursavich, M. G., Lombardi, S., Georgiadis, K. E., Reifenberg, E., Flannery, C. R., and Morris, E. A. . N-((8-hydroxy-5-substituted-quinolin-7-yl)(phenyl)methyl)-2-phenyloxy/amino-aceta mide inhibitors of ADAMTS-5 (Aggrecanase-2). *Bioorg Med Chem Lett* **2008**;18:6454-7
6. Kenyon V, Rai, G., Jadhav, A., Schultz, L., Armstrong, M., Jameson, J. B., 2nd, Perry, S., Joshi, N., Bougie, J. M., Leister, W., Taylor-Fishwick, D. A., Nadler, J. L., Holinstat, M., Simeonov, A., Maloney, D. J., and Holman, T. R. Discovery of potent and selective inhibitors of human platelet-type 12- lipoxygenase. *J Med Chem* **2011**;54:5485-97
7. Carmichael J, DeGraff WG, Gazdar AF, Minna JD, Mitchell JB. Evaluation of a tetrazolium-based semiautomated colorimetric assay: assessment of chemosensitivity testing. *Cancer Res* **1987**;47:936-42
8. Wisniewska M, Karlberg T, Lehtio L, Johansson I, Kotenyova T, Moche M, *et al.* Crystal structures of the ATPase domains of four human Hsp70 isoforms: HSPA1L/Hsp70-hom, HSPA2/Hsp70-2, HSPA6/Hsp70B', and HSPA5/BiP/GRP78. *PLoS One* **2010**;5:e8625

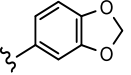
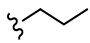
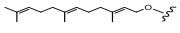
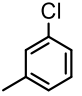
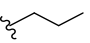
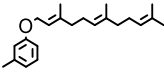
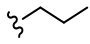
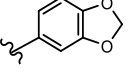
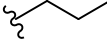
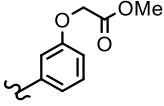
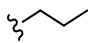
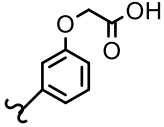
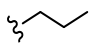
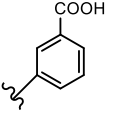
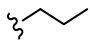
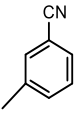
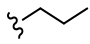
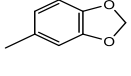
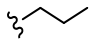
9. Subramanian A, Tamayo P, Mootha VK, Mukherjee S, Ebert BL, Gillette MA, *et al.* Gene set enrichment analysis: a knowledge-based approach for interpreting genome-wide expression profiles. *Proc Natl Acad Sci U S A* **2005**;102:15545-50
10. Huang da W, Sherman BT, Lempicki RA. Systematic and integrative analysis of large gene lists using DAVID bioinformatics resources. *Nat Protoc* **2009**;4:44-57
11. Xu S, Butkevich AN, Yamada R, Zhou Y, Debnath B, Duncan R, *et al.* Discovery of an orally active small-molecule irreversible inhibitor of protein disulfide isomerase for ovarian cancer treatment. *Proc Natl Acad Sci U S A* **2012**;109:16348-53
12. Ramkumar K, Samanta S, Kyani A, Yang S, Tamura S, Ziemke E, *et al.* Mechanistic evaluation and transcriptional signature of a glutathione S-transferase omega 1 inhibitor. *Nat Commun* **2016**;7:13084
13. Hawkins PC, Skillman AG, Warren GL, Ellingson BA, Stahl MT. Conformer generation with OMEGA: algorithm and validation using high quality structures from the Protein Databank and Cambridge Structural Database. *J Chem Inf Model* **2010**;50:572-84

Table S1. Cytotoxicity of YUM70 analogs in pancreatic cancer cell lines



Compds	X	R ¹	R ²	R ³	IC ₅₀ (μM) ^a		
					MIA PaCa-2	PANC-1	BxPC-3
YUM70	OH			Cl	2.8±0.9	4.5±1.1	9.6±0.7
YUM72	OH			Cl	2.8±1.9	4.9±1.2	8.7±1.8
YUM75	OH			Cl	4.2±0.5	3.7±0.2	6.1±1.7
YUM79	OH			Cl	2.5±0.5	3.0±1.6	2.9±0.6
YUM82	OH			Cl	4.2±0.6	6.4±1.7	5.0±2.2
YUM86	OH			Cl	14.4±3.9	18.2±0.3	13.8±0.9
YUM89	OH			Cl	1.7±0.5	13.1±1.9	8.2±0.3
YUM91	OH			Cl	3.7±0.3	5.8±0.2	13.9±2.3
YUM92	OH			Cl	>30.0	>30.0	>30.0
YUM94	OH			Cl	2.3±1.4	8.1±1.8	9.2±1.1
YUM166	OH			Cl	2.8±0.6	3.0±0.6	8.9±4.2
YUM227	OCH ₃			Cl	3.3±0.3	6.5±0.5	10.3±3.3
YUM117	OCH ₃			Cl	>30.0	>30.0	>30.0

Table S1. Continue ...

Compds	X	R ¹	R ²	R ³	IC ₅₀ (μM) ^a		
					MIA PaCa-2	PANC-1	BxPC-3
YUM245	OCH ₃			Cl	>30.0	>30.0	>30.0
YUM137				Cl	>30	>30	>30
YUM168	OH			Cl	>30	>30	>30
YUM272	OH			H	0.8±0.9	1.9±0.4	6.2±2.9
YUM347A	OH			Cl	28.6±1.9	>30	>30
YUM354	OH			Cl	28±2.9	>30	>30
YUM401	OH			Cl	5.8±0.7	13.8±0.5	11.6±3.1
YUM402	OH			Cl	1±0.7	6.7±4.5	21.3±3.2
YUM411	OH			Br	1.3±1.1	4±1.5	13.4±1
VER155008					14.6	>30.0	>30.0

^a IC₅₀ is defined as the compound concentration causing 50% decrease in cell growth and the values expressed as mean ± SD are from three independent experimnts.

Table S2. Top 20 transcriptionally upregulated genes in response to YUM70 treatment in MIA PaCa-2 cells. Nascent RNA Bru-seq was used to assess the effect of YUM70 on genome-wide transcription in two biological replicates of MIA PaCa-2 cells, data of replicate 1 is presented here.

Gene Symbol	Gene Name (Description)	Fold change
FAM129A	Family with sequence similarity 129, member A	23.0
GDF15	Growth differentiation factor 15	23.1
UNC5B	Unc-5 netrin receptor B	23.9
TRIB3	Tribbles homolog 3 (Drosophila)	13.9
SLC1A4	Solute carrier family 1 (glutamate/neutral amino acid transporter), member 4	13.7
ATF3	Activating transcription factor 3	13.8
ASNS	Asparagine synthetase (Glutamine-Hydrolyzing)	11.2
SLFN5	Schlafen family member 5	9.7
CHAC1	ChaC, cation transport regulator homolog 1 (E. coli)	9.0
C6orf226	Chromosome 6 open reading frame 226	8.0
DDIT4	DNA-damage-inducible transcript 4	7.9
AC068580.4	Uncharacterized protein	7.2
SESN2	Sestrin 2	6.9
BBC3	BCL2 binding component 3	6.5
JDP2	Jun dimerization protein 2	6.5
EIF4EBP3	Eukaryotic translation initiation factor 4E binding protein 3	5.9
DDIT3	DNA-damage-inducible transcript 3	5.6
PHGDH	Phosphoglycerate dehydrogenase	5.4
AKNA	AT-hook transcription factor	5.3
UPP1	Uridine phosphorylase 1	5.0

Table S3. Top 20 transcriptionally downregulated genes in response to YUM70 treatment in MIA PaCa-2 cells. Nascent RNA Bru-seq was used to assess the effect of YUM70 on genome-wide transcription in two biological replicates of MIA PaCa-2 cells, data of replicate 1 is presented here.

Gene Symbol	Gene Name (Description)	Fold change
AC120114.5	Uncategorized gene	-8.6
BSCL2	BSCL2 lipid droplet biogenesis associated, seipin	-4.6
BRINP3	BMP/retinoic acid inducible neural specific 3	-4.6
HIST1H3H	Histone cluster 1 H3 family member H	-4.0
TM4SF18	Transmembrane 4 L six family member 18	-3.7
IPO4	Importin 4	-3.7
HIST1H2BO	Histone cluster 1 H2B family member O	-3.7
DPH6	Diphthamine biosynthesis 6	-3.7
TAS2R14	Taste 2 receptor member 14	-3.7
C1orf50	Chromosome 1 open reading frame 50	-3.5
HIST1H2BL	Histone cluster 1 H2B family member L	-3.5
CYB5D1	Cytochrome B5 domain containing 1	-3.2
HIST2H2AB	Histone cluster 2 H2A family member B	-3.2
TCTEX1D2	Tctex1 domain containing 2	-3.2
ATP23	ATP23 metallopeptidase and ATP synthase assembly factor homolog	-3.2
HIST1H2AJ	Histone cluster 1 H2A family member J	-3.2
SHOX2	Short stature homeobox 2	-3.2
HIST1H2BF	Histone cluster 1 H2B fmember F	-3.2
BORCS7	BLOC-1 related complex subunit 7	-3.0
TFAP2A	Transcription factor AP-2 alpha (activating enhancer binding protein 2 alpha)	-2.8

Table S4. Top 24 up-regulated gene set in GSEA of Hallmark pathways. Nascent RNA Bru-seq was used to assess the effect of YUM70 on genome-wide transcription in two biological replicates of MIA PaCa-2 cells, data of replicate 1 is presented here.

Name	SIZE	NES	FDR q-val	NOM p-val
HALLMARK_TNFA_SIGNALING_VIA_NFKB	163	2.9	0.00	0.000
HALLMARK_HYPOXIA	155	2.7	0.00	0.000
HALLMARK_P53_PATHWAY	176	2.6	0.00	0.000
HALLMARK_UNFOLDED_PROTEIN_RESPONSE	106	2.5	0.00	0.000
HALLMARK_INTERFERON_GAMMA_RESPONSE	139	2.2	0.00	0.000
HALLMARK_APOPTOSIS	132	2.2	0.00	0.000
HALLMARK_INFLAMMATORY_RESPONSE	107	2.2	0.00	0.000
HALLMARK_INTERFERON_ALPHA_RESPONSE	76	2.1	0.00	0.000
HALLMARK_IL2_STAT5_SIGNALING	141	2.1	0.00	0.000
HALLMARK_MTORC1_SIGNALING	191	2.1	0.00	0.000
HALLMARK_CHOLESTEROL_HOMEOSTASIS	66	2.0	0.00	0.000
HALLMARK_MYOGENESIS	124	1.9	0.00	0.000
HALLMARK_COAGULATION	74	1.8	0.00	0.000
HALLMARK_EPITHELIAL_MESENCHYMAL_TRANSITION	148	1.8	0.00	0.000
HALLMARK_XENOBIOTIC_METABOLISM	141	1.7	0.00	0.000
HALLMARK_COMPLEMENT	133	1.7	0.01	0.000
HALLMARK_GLYCOLYSIS	178	1.6	0.01	0.002
HALLMARK_PI3K_AKT_MTOR_SIGNALING	91	1.6	0.01	0.002
HALLMARK_ESTROGEN_RESPONSE_EARLY	164	1.6	0.01	0.000
HALLMARK_TGF_BETA_SIGNALING	50	1.5	0.01	0.009
HALLMARK_IL6_JAK_STAT3_SIGNALING	52	1.5	0.02	0.025
HALLMARK_ALLOGRAFT_REJECTION	100	1.5	0.03	0.010
HALLMARK_KRAS_SIGNALING_UP	117	1.4	0.03	0.014
HALLMARK_ESTROGEN_RESPONSE_LATE	155	1.4	0.04	0.009

Table S5. Top 24 up-regulated gene set in GSEA of Gene Ontology. Nascent RNA Bru-seq was used to assess the effect of YUM70 on genome-wide transcription in two biological replicates of MIA PaCa-2 cells, data of replicate 1 is presented here.

Name	SIZE	NES	FDR q-val	NOM p-val
GO_INTRINSIC_APOPTOTIC_SIGNALING_PATHWAY_IN_RESPONSE_TO_ENDOPLASMIC_RETICULUM_STRESS	29	2.6	0.00	0.000
GO_CELLULAR_RESPONSE_TO_TOPOLOGICALLY_INCORRECT_PROTEIN	102	2.5	0.00	0.000
GO_RESPONSE_TO_ENDOPLASMIC_RETICULUM_STRESS	203	2.5	0.00	0.000
GO_POSITIVE_REGULATION_OF_TRANSCRIPTION_FROM_RNA_POLYMERASE_II_PROMOTER_IN_RESPONSE_TO_STRESS	20	2.4	0.00	0.000
GO_REGULATION_OF_DNA_TEMPLATED_TRANSCRIPTION_IN_RESPONSE_TO_STRESS	58	2.4	0.00	0.000
GO_L_AMINO_ACID_TRANSMEMBRANE_TRANSPORTER_ACTIVITY	34	2.3	0.00	0.000
GO_CELLULAR_RESPONSE_TO_GLUCOSE_STARVATION	29	2.3	0.00	0.000
GO_NEUTRAL_AMINO_ACID_TRANSPORT	20	2.3	0.00	0.000
GO_L_AMINO_ACID_TRANSPORT	38	2.3	0.00	0.000
GO_REGULATION_OF_ENDOPLASMIC_RETICULUM_STRESS_INDUCED_INTRINSIC_APOPTOTIC_SIGNALING_PATHWAY	25	2.3	0.00	0.000
GO_RESPONSE_TO_STARVATION	117	2.3	0.00	0.000
GO_INTRINSIC_APOPTOTIC_SIGNALING_PATHWAY	133	2.3	0.00	0.000
GO_RESPONSE_TO_TOPOLOGICALLY_INCORRECT_PROTEIN	136	2.2	0.00	0.000
GO_CELLULAR_RESPONSE_TO_STARVATION	94	2.2	0.00	0.000
GO_RESPONSE_TO_TYPE_I_INTERFERON	46	2.2	0.00	0.001
GO_ER_NUCLEUS_SIGNALING_PATHWAY	30	2.2	0.00	0.001
GO_CELLULAR_RESPONSE_TO_EXTRACELLULAR_STIMULUS	141	2.2	0.00	0.001
GO_AUTOPHAGOSOME_MEMBRANE	22	2.2	0.00	0.001
GO_IRE1_MEDIATED_UNFOLDED_PROTEIN_RESPONSE	52	2.2	0.00	0.002
GO_SERINE_FAMILY_AMINO_ACID_METABOLIC_PROCESS	31	2.1	0.00	0.002
GO_CELLULAR_RESPONSE_TO_EXTERNAL_STIMULUS	190	2.1	0.00	0.002
GO_CELLULAR_RESPONSE_TO_OXYGEN_LEVELS	107	2.1	0.00	0.002
GO_INTERFERON_GAMMA_MEDIATED_SIGNALING_PATHWAY	41	2.1	0.00	0.002
GO_CELLULAR_RESPONSE_TO_INTERFERON_GAMMA	57	2.1	0.00	0.003

Table S6. Top 24 upregulated transcription factors in response to YUM70 treatment in MIA PaCa-2 cells. Nascent RNA Bru-seq was used to assess the effect of YUM70 on genome-wide transcription in two biological replicates of MIA PaCa-2 cells, data of replicate 1 is presented here.

Name	SIZE	NES	FDR q-val	NOM p-val
ATF3_Q6	176	2.1	0.00	0.000
CHOP_01	171	2.0	0.00	0.002
CREB_Q2	210	1.9	0.00	0.004
TGASTMAGC_NFE2_01	135	1.8	0.00	0.011
BACH2_01	200	1.8	0.00	0.009
TGAYRTCA_ATF3_Q6	357	1.8	0.00	0.020
ATF1_Q6	160	1.8	0.00	0.020
AP2ALPHA_01	185	1.7	0.00	0.020
CREBP1_01	136	1.7	0.00	0.019
ATF_01	194	1.7	0.00	0.019
CREB_Q4	213	1.7	0.00	0.020
NFE2_01	188	1.7	0.00	0.020
HEB_Q6	180	1.7	0.00	0.021
SRF_01	34	1.7	0.01	0.022
CREBP1_Q2	191	1.7	0.00	0.023
GGGNNTTCC_NFKB_Q6_01	95	1.7	0.00	0.023
CREB_Q4_01	168	1.7	0.00	0.021
AP1_Q4_01	190	1.7	0.00	0.021
AP2GAMMA_01	190	1.7	0.00	0.021
BACH1_01	192	1.7	0.00	0.021
HNF3B_01	125	1.6	0.00	0.024
AP4_01	184	1.6	0.00	0.027
ATF6_01	91	1.6	0.00	0.027
TCANNTGAY_SREBP1_01	362	1.6	0.00	0.026

Table S7. Top 24 up-regulated micro RNAs in response to YUM70 treatment in MIA PaCa-2 cells. Nascent RNA Bru-seq was used to assess the effect of YUM70 on genome-wide transcription in two biological replicates of MIA PaCa-2 cells, data of replicate 1 is presented here.

Symbol	Related pathways/ disease associated with	Fold change
MIR3191	Activation of BH3-only proteins and Apoptosis Modulation and Signaling.	31.2
MIR24-2	Hepatocellular Carcinoma and Thyroid Cancer, Nonmedullary, 1.	25.9
MIR6734	alpha-linolenic acid (ALA) metabolism and Regulation of lipid metabolism by Peroxisome proliferator-activated receptor alpha (PPARalpha).	6.2
MIR589	miRNA targets in ECM and membrane receptors.	5.2
MIR621	Hyperornithinemia-Hyperammonemia-Homocitrullinuria Syndrome.	4.5
MIR643	Unknown	4.1
MIR4263	Unknown	3
MIR944	Unknown	2.9
MIR193A	Oral Squamous Cell Carcinoma and Melanoma.	2.9
MIR1236	Formation of HIV-1 elongation complex containing HIV-1 Tat and Gene Expression.	2.8
MIR6739	Unknown	2.6
MIR6850	Viral mRNA Translation and Influenza Viral RNA Transcription and Replication.	2.6
MIR4258	Unknown	2.4
MIR570	Unknown	2.4
MIR616	Unknown	2.4
MIR6515	Unknown	2.3
MIR1273C	Unknown	2.2
MIR1289-1	Unknown	2
MIR6783	Unknown	1.9
MIR7111	Unknown	1.8
MIR423	Mesothelioma, Malignant and Muscular Dystrophy, Duchenne Type. Among its related pathways are MicroRNAs in cancer.	1.7
MIR3609	Unknown	1.5
MIR6797	Diamond-Blackfan Anemia 1 and Diamond-Blackfan Anemia.	1.4
MIR5047	mRNA Splicing - Major Pathway	1.2

Table S8. Top 24 down-regulated micro RNAs in response to YUM70 treatment in MIA PaCa-2 cells. Nascent RNA Bru-seq was used to assess the effect of YUM70 on genome-wide transcription in two biological replicates of MIA PaCa-2 cells, data of replicate 1 is presented here.

Symbol	Related pathways/ disease associated with	Log 2Fold change
MIR30A	MicroRNAs in cancer and Parkinsons Disease Pathway/ Leiomyoma, Uterine and Nonalcoholic Fatty Liver Disease.	-7.0
MIR3942	Unknown	-5.3
MIR3657	Unknown	-3.2
MIR576	Unknown	-3.1
MIR3192	Unknown	-2.1
MIR15B	cardiomyocyte hypertrophy and miRNAs involved in DNA damage response/ Glioma and Gastric Cancer	-1.9
MIR6874	Unknown	-1.9
MIR378J	Unknown	-1.8
MIR641	Unknown	-1.8
MIR4755	Unknown	-1.5
MIR454	Colorectal Cancer.	-1.4
MIR3137	Unknown	-1.4
MIR4753	Unknown	-1.3
MIR6728	Unknown	-0.9
MIRLET7D	miRNAs involved in DNA damage response and Metastatic brain tumor/ Acute Promyelocytic Leukemia and Ovarian Cancer.	-0.9
MIRLET7F1	miRNAs involved in DNA damage response and Metastatic brain tumor/ Pituitary Adenoma and Pancreatic Cancer.	-0.9
MIR6832	Unknown	-0.9
MIR6807	Familial Colorectal Cancer.	-0.7
MIR640	Unknown	-0.7
MIR25	miRNAs involved in DNA damage response and MicroRNAs in cancer/ Gastric Cancer and Brain Cancer.	-0.7
MIR590	Unknown	-0.6
MIR1304	Activated PKN1 stimulates transcription of AR (androgen receptor) regulated genes KLK2 and KLK3 and Gene Expression.	-0.5
MIR3153	Unknown	-0.4
MIR3064	mRNA Splicing - Major Pathway and Circadian rythm related genes.	-0.4

Table S9. Top 24 up-regulated LINC RNAs in response to YUM70 treatment in MIA PaCa-2 cells. Nascent RNA Bru-seq was used to assess the effect of YUM70 on genome-wide transcription in two biological replicates of MIA PaCa-2 cells, data of replicate 1 is presented here.

Symbol	Related pathways/ disease associated with	Fold change
LINC01629	Unknown	7.6
C20orf203	Unknown	7
AL138895.1	Unknown	5.7
AC006504.1	Unknown	3
AC112721.2	Unknown	2.9
AC112721.1	Unknown	2.9
AL357153.2	Unknown	2.5
AL160408.1	Unknown	2.4
LINC00662	Unknown	2.3
LUCAT1	Clear Cell Renal Cell Carcinoma and Squamous Cell Carcinoma, Head And Neck.	2.3
CASC21	Unknown	2.1
AL034417.2	Unknown	2
SRP14-AS1	Unknown	2
LINC01089	Gemistocytic Astrocytoma and Astrocytoma.	2
AC016831.5	Unknown	1.8
LINC01006	Unknown	1.8
LINC00941	Lung Cancer Susceptibility 3 and Gastric Cancer	1.8
AL359710.1	Unknown	1.8
AC087762.1	Unknown	1.8
LINC02100	Unknown	1.8
LINC01301	Unknown	1.8
AC016831.1	Unknown	1.7
GMDS-AS1	Unknown	1.7
MIR22HG	Unknown	1.7

Table S10. Top 24 down-regulated LINC RNAs in response to YUM70 treatment in MIA PaCa-2 cells. Nascent RNA Bru-seq was used to assess the effect of YUM70 on genome-wide transcription in two biological replicates of MIA PaCa-2 cells, data of replicate 1 is presented here.

Symbol	Related pathways/ disease associated with	Log 2 Fold change
AL139383.1		-1.7
LINC02101		-1.6
AC003984.1		-1.5
DPH6-AS1		-1.4
AC124657.1		-1.4
AL136164.2		-1.4
AC067956.1		-1.3
AC021231.1		-1.2
AC012625.1		-1.1
LINC00473	Mucoepidermoid Carcinoma and Wilms Tumor 1.	-1.1
AC010983.1		-1.1
AL031599.1		-1
AC103746.1		-1
LINC00376		-0.9
AL356124.1		-0.9
AC073529.1		-0.8
AL161716.1		-0.8
AC104823.1		-0.8
MIR137HG		-0.8
AC087477.2		-0.8
AL359313.1		-0.7
AP005230.1		-0.7
AC010235.1		-0.7
AC048341.2		-0.6

Table S11. Top 29 enriched functions from the upregulated genes in response to YUM70 treatment in MIA PaCa-2 using STRING protein-protein interaction network. Nascent RNA Bru-seq was used to assess the effect of YUM70 on genome-wide transcription in two biological replicates of MIA PaCa-2 cells, data of replicate 1 is presented here.

GO term	Description	Genes mapped	Enrichment Scores	FDR q-val
GO:0034436	glycoprotein transport	3	3.44	0.006
GO:1901329	regulation of odontoblast differentiation	3	3.39	0.007
GO:0036499	PERK-mediated unfolded protein response	10	2.51	0.000
GO:1990440	positive regulation of transcription from RNA polymerase II promoter in response to endoplasmic reticulum stress	12	2.51	0.000
GO:0006564	L-serine biosynthetic process	7	2.34	0.001
GO:0015825	L-serine transport	7	2.11	0.002
GO:0036500	ATF6-mediated unfolded protein response	9	1.96	0.000
GO:0032329	serine transport	8	1.90	0.002
GO:0036003	positive regulation of transcription from RNA polymerase II promoter in response to stress	24	1.88	0.001
GO:0009070	serine family amino acid biosynthetic process	15	1.76	0.000
GO:0006563	L-serine metabolic process	10	1.70	0.001
GO:0070059	intrinsic apoptotic signaling pathway in response to endoplasmic reticulum stress	30	1.53	0.001
GO:0015804	neutral amino acid transport	24	1.48	0.000
GO:1902236	negative regulation of endoplasmic reticulum stress-induced intrinsic apoptotic signaling pathway	16	1.36	0.000
GO:1902235	regulation of endoplasmic reticulum stress-induced intrinsic apoptotic signaling pathway	29	1.30	0.001
GO:0031065	positive regulation of histone deacetylation	17	1.04	0.004
GO:1905898	positive regulation of response to endoplasmic reticulum stress	35	0.92	0.009
GO:1902475	L-alpha-amino acid transmembrane transport	41	0.90	0.001
GO:0015807	L-amino acid transport	41	0.90	0.001
GO:0035794	positive regulation of mitochondrial membrane permeability	20	0.89	0.008
GO:1905710	positive regulation of membrane permeability	20	0.89	0.008
GO:0031063	regulation of histone deacetylation	25	0.86	0.006
GO:0002931	response to ischemia	27	0.79	0.005
GO:1905897	regulation of response to endoplasmic reticulum stress	74	0.78	0.000
GO:0034620	cellular response to unfolded protein	103	0.77	0.001
GO:0060333	interferon-gamma-mediated signaling pathway	41	0.77	0.002
GO:0030968	endoplasmic reticulum unfolded protein response	91	0.77	0.002
GO:0036498	IRE1-mediated unfolded protein response	49	0.75	0.010
GO:0042772	DNA damage response, signal transduction resulting in transcription	17	0.72	0.008

Table S12. Top 14 enriched cellular component from the up-regulated genes upon YUM70 treatment in MIA PaCa-2 using STRING protein-protein interaction network. Nascent RNA Bru-seq was used to assess the effect of YUM70 on genome-wide transcription in two biological replicates of MIA PaCa-2 cells, data of replicate 1 is presented here.

GO term	Description	Genes mapped	Enrichment Scores	FDR q-val
GO:0035976	transcription factor AP-1 complex	5	2.19	0.004
GO:0097413	Lewy body	7	1.85	0.003
GO:0034663	endoplasmic reticulum chaperone complex	9	1.50	0.005
GO:0098553	luminal side of endoplasmic reticulum membrane	14	0.76	0.010
GO:0071556	integral component of luminal side of endoplasmic reticulum membrane	14	0.76	0.010
GO:0005884	actin filament	53	0.49	0.000
GO:0031225	anchored component of membrane	64	0.35	0.009
GO:0030670	phagocytic vesicle membrane	62	0.35	0.004
GO:0031902	late endosome membrane	109	0.31	0.000
GO:0043202	lysosomal lumen	65	0.29	0.000
GO:0005770	late endosome	199	0.26	0.004
GO:0005775	vacuolar lumen	117	0.25	0.000
GO:0031012	extracellular matrix	163	0.21	0.003
GO:0030667	secretory granule membrane	200	0.20	0.008

Table S13. Top 21 enriched reactome pathways from the up-regulated genes upon YUM70 treatment in MIA PaCa-2 using STRING protein-protein interaction network. Nascent RNA Bru-seq was used to assess the effect of YUM70 on genome-wide transcription in two biological replicates of MIA PaCa-2 cells, data of replicate 1 is presented here.

Pathways	Description	Genes mapped	Enrichment Scores	FDR q-val
HSA-977347	Serine biosynthesis	8	2.04	0.000
HSA-381183	ATF6 (ATF6-alpha) activates chaperone genes	9	1.41	0.001
HSA-381033	ATF6 (ATF6-alpha) activates chaperones	11	0.99	0.008
HSA-381042	PERK regulates gene expression	26	0.97	0.001
HSA-352230	Amino acid transport across the plasma membrane	22	0.94	0.002
HSA-380994	ATF4 activates genes	23	0.93	0.002
HSA-379716	Cytosolic tRNA aminoacylation	24	0.83	0.004
HSA-4755510	SUMOylation of immune response proteins	10	0.82	0.005
HSA-381070	IRE1alpha activates chaperones	53	0.67	0.001
HSA-381119	Unfolded Protein Response (UPR)	88	0.65	0.001
HSA-909733	Interferon alpha/beta signaling	45	0.62	0.001
HSA-877300	Interferon gamma signaling	52	0.61	0.001
HSA-381038	XBP1(S) activates chaperone genes	51	0.57	0.002
HSA-425393	Transport of inorganic cations/anions and amino acids/oligopeptides	66	0.52	0.005
HSA-2024096	HS-GAG degradation	20	0.46	0.003
HSA-6785807	Interleukin-4 and Interleukin-13 signaling	59	0.43	0.003
HSA-198933	Immunoregulatory interactions between a Lymphoid and a non-Lymphoid cell	38	0.40	0.004
HSA-6794361	Neurexins and neuroligins	44	0.35	0.009
HSA-400253	Circadian Clock	63	0.30	0.004
HSA-1474244	Extracellular matrix organization	186	0.25	0.000
HSA-1638091	Heparan sulfate/heparin (HS-GAG) metabolism	41	0.25	0.002

Table S14. Top 4 enriched INTERPRO Protein Domains and Features from the up-regulated genes in response to YUM70 treatment in MIA PaCa-2 using STRING protein-protein interaction network. Nascent RNA Bru-seq was used to assess the effect of YUM70 on genome-wide transcription in two biological replicates of MIA PaCa-2 cells, data of replicate 1 is presented here.

Domain	Description	Genes mapped	Enrichment Scores	FDR q-val
IPR000837	AP-1 transcription factor	8	2.22	0.003
IPR004827	Basic-leucine zipper domain	48	1.30	0.000
IPR020846	Major facilitator superfamily domain	67	0.38	0.009
IPR007110	Immunoglobulin-like domain	198	0.13	0.007

Table S15. Connectivity map analysis of YUM70. Top bioactive compound or compound perturbagens (CP), Gene knock-down perturbagens (KD) with positive connectivity score are listed.

Type	Name	Description	CS
CP	Tunicamycin	GLCNAC phosphotransferase inhibitor	99.93
CP	Thapsigargin	ATPase inhibitor	99.82
CP	MG-132	Proteasome inhibitor	99.26
CP	Irinotecan	Topoisomerase inhibitor	99.40
CP	SCH-79797	Proteasome inhibitor	99.29
CP	MLN-2238	Proteasome inhibitor	98.41
CP	z-leu3-VS	Proteasome inhibitor	98.32
CP	JNJ-26854165	HDAC inhibitor	98.27
CP	THM-I-94	HDAC inhibitor	97.60
CP	Panobinostat	HDAC inhibitor	97.53
CP	Topotecan	Topoisomerase inhibitor	93.34
CP	Vorinostat	HDAC inhibitor	92.23
KD	VCP	ATPases / AAA-type	99.95
KD	HSPA5	Heat shock proteins / HSP70	99.53

CS is the connectivity score (from -100 to 100). A positive higher score means more positive connection between the bioactive compound and YUM70.

Table S16. Top 9 down-regulated gene set in GSEA of Hallmark pathways. Nascent RNA Bru-seq was used to assess the effect of YUM70 on genome-wide transcription in two biological replicates of MIA PaCa-2 cells, data of replicate 1 is presented here.

Name	SIZE	NES	FDR q-val	NOM p-val
HALLMARK_E2F_TARGETS	195	-2.9	0.00	0.000
HALLMARK_G2M_CHECKPOINT	193	-2.9	0.00	0.000
HALLMARK_MYC_TARGETS_V1	196	-2.7	0.00	0.000
HALLMARK_MITOTIC_SPINDLE	195	-2.1	0.00	0.000
HALLMARK_SPERMATOGENESIS	78	-2.0	0.00	0.000
HALLMARK_MYC_TARGETS_V2	58	-1.9	0.00	0.000
HALLMARK_OXIDATIVE_PHOSPHORYLATION	193	-1.7	0.00	0.003
HALLMARK_PEROXISOME	86	-1.4	0.05	0.066
HALLMARK_FATTY_ACID_METABOLISM	127	-1.3	0.06	0.120

Table S17. Top 24 down-regulated gene set in GSEA of gene ontology (GO). Nascent RNA Br-
seq was used to assess the effect of YUM70 on genome-wide transcription in two biological
replicates of MIA PaCa-2 cells, data of replicate 1 is presented here.

Name	SIZE	NES	FDR q-val	NOM p-val
GO_SISTER_CHROMATID_SEGREGATION	154	-2.8	0.00	0.000
GO_NUCLEAR_CHROMOSOME_SEGREGATION	186	-2.7	0.00	0.000
GO_CHROMOSOME_SEGREGATION	228	-2.7	0.00	0.000
GO_MITOTIC_SISTER_CHROMATID_SEGREGATION	83	-2.6	0.00	0.000
GO_MITOTIC_NUCLEAR_DIVISION	319	-2.6	0.00	0.000
GO_CONDENSED_CHROMOSOME	162	-2.6	0.00	0.000
GO_CHROMOSOMAL_REGION	284	-2.6	0.00	0.000
GO_CHROMOSOME_CENTROMERIC_REGION	154	-2.6	0.00	0.000
GO_SISTER_CHROMATID_COHESION	95	-2.6	0.00	0.000
GO_CONDENSED_CHROMOSOME_CENTROMERIC_REGION	85	-2.6	0.00	0.000
GO_SPINDLE	256	-2.5	0.00	0.000
GO_MITOTIC_SPINDLE_ORGANIZATION	58	-2.5	0.00	0.000
GO_ORGANELLE_FISSION	403	-2.5	0.00	0.000
GO_KINETOCHORE	105	-2.5	0.00	0.000
GO_SPINDLE_POLE	108	-2.5	0.00	0.000
GO_DNA_PACKAGING	141	-2.5	0.00	0.000
GO_CENTROMERE_COMPLEX_ASSEMBLY	38	-2.4	0.00	0.000
GO_CONDENSED_NUCLEAR_CHROMOSOME	65	-2.4	0.00	0.000
GO_REGULATION_OF_MICROTUBULE_POLYMERIZATION_OR_DEPOLYMERIZATION	147	-2.4	0.00	0.000
GO_REGULATION_OF_CHROMOSOME_SEGREGATION	74	-2.4	0.00	0.000
GO_RNA_SPLICING_VIA_TRANSESTERIFICATION_REACTIONS	248	-2.4	0.00	0.000
GO_RIBONUCLEOPROTEIN_COMPLEX_LOCALIZATION	105	-2.3	0.00	0.000
GO_NEGATIVE_REGULATION_OF_PROTEIN_COMPLEX_DISASSEMBLY	135	-2.3	0.00	0.000
GO_DNA_CONFORMATION_CHANGE	217	-2.3	0.00	0.000

Table S18. Top 24 down-regulated transcription factors upon YUM70 treatment in MIA PaCa-2 cells. Nascent RNA Bru-seq was used to assess the effect of YUM70 on genome-wide transcription in two biological replicates of MIA PaCa-2 cells, data of replicate 1 is presented here.

Name	SIZE	NES	FDR q-val	NOM p- val
E2F1_Q6	205	-2.4	0.00	0.000
E2F4DP2_01	202	-2.3	0.00	0.000
E2F_Q6	205	-2.3	0.00	0.000
E2F_02	203	-2.3	0.00	0.000
E2F1_Q3	207	-2.3	0.00	0.000
E2F1_Q6_01	206	-2.3	0.00	0.000
E2F1DP2_01	202	-2.3	0.00	0.000
E2F4DP1_01	206	-2.3	0.00	0.000
E2F1DP1_01	202	-2.3	0.00	0.000
E2F_Q4	206	-2.3	0.00	0.000
E2F1DP1RB_01	196	-2.2	0.00	0.000
E2F_Q3	191	-2.2	0.00	0.000
E2F1_Q4_01	194	-2.2	0.00	0.000
SGCGSSAAA_E2F1DP2_01	149	-2.2	0.00	0.000
E2F_Q3_01	199	-2.2	0.00	0.000
E2F_01	58	-2.0	0.00	0.000
E2F_Q4_01	197	-2.0	0.00	0.000
NFMUE1_Q6	216	-2.0	0.00	0.000
GCCATNTTG_YY1_Q6	388	-1.9	0.00	0.000
E2F_Q6_01	196	-1.9	0.00	0.000
TCCCRNNRTGC_UNKNOWN	179	-1.9	0.00	0.000
GCGSCMNTTT_UNKNOWN	66	-1.9	0.00	0.000
KRCTCNNNNMANAGC_UNKNOWN	54	-1.9	0.00	0.000
TMTCGCGANR_UNKNOWN	152	-1.8	0.00	0.001

Table S19. Top 29 enriched function term from the down-regulated genes in response to YUM70 treatment in MIA PaCa-2 using STRING protein-protein interaction network. Nascent RNA Bru-seq was used to assess the effect of YUM70 on genome-wide transcription in two biological replicates of MIA PaCa-2 cells, data of replicate 1 is presented here.

GO term	Description	Genes mapped	Enrichment Scores	FDR q-val
GO:0010032	meiotic chromosome condensation	5	3.18	0.002
GO:0070601	centromeric sister chromatid cohesion	7	2.78	0.001
GO:0051988	regulation of attachment of spindle microtubules to kinetochore	12	2.42	0.000
GO:0090267	positive regulation of mitotic cell cycle spindle assembly checkpoint	7	2.24	0.009
GO:0090232	positive regulation of spindle checkpoint	7	2.24	0.009
GO:1904851	positive regulation of establishment of protein localization to telomere	10	2.19	0.000
GO:0070203	regulation of establishment of protein localization to telomere	11	2.13	0.000
GO:0030261	chromosome condensation	24	2.10	0.001
GO:2000816	negative regulation of mitotic sister chromatid separation	23	2.08	0.000
GO:1905819	negative regulation of chromosome separation	23	2.08	0.000
GO:0051383	kinetochore organization	17	2.08	0.000
GO:0007076	mitotic chromosome condensation	14	2.06	0.000
GO:0031577	spindle checkpoint	23	2.05	0.000
GO:1902100	negative regulation of metaphase/anaphase transition of cell cycle	22	2.03	0.000
GO:0045841	negative regulation of mitotic metaphase/anaphase transition	22	2.03	0.000
GO:0070202	regulation of establishment of protein localization to chromosome	12	2.03	0.000
GO:0071174	mitotic spindle checkpoint	21	2.00	0.000
GO:0071173	spindle assembly checkpoint	21	2.00	0.000
GO:0007094	mitotic spindle assembly checkpoint	21	2.00	0.000
GO:0007077	mitotic nuclear envelope disassembly	12	1.99	0.001
GO:0051985	negative regulation of chromosome segregation	28	1.97	0.000
GO:0033046	negative regulation of sister chromatid segregation	28	1.97	0.000
GO:0051292	nuclear pore complex assembly	10	1.92	0.000
GO:0033048	negative regulation of mitotic sister chromatid segregation	26	1.92	0.000
GO:0006999	nuclear pore organization	15	1.84	0.000
GO:0071459	protein localization to chromosome, centromeric region	18	1.80	0.000
GO:0010965	regulation of mitotic sister chromatid separation	51	1.76	0.000
GO:0018206	peptidyl-methionine modification	10	1.72	0.008
GO:1905818	regulation of chromosome separation	54	1.71	0.000

Table S20. Top 25 enriched cellular component from the down-regulated genes in response to YUM70 treatment in MIA PaCa-2 using STRING protein-protein interaction network. Nascent RNA Bru-seq was used to assess the effect of YUM70 on genome-wide transcription in two biological replicates of MIA PaCa-2 cells, data of replicate 1 is presented here.

GO term	Description	Genes mapped	Enrichment Scores	FDR q-val
GO:0097149	centralspindlin complex	3	4.80	0.000
GO:0000942	condensed nuclear chromosome outer kinetochore	4	4.10	0.000
GO:0000796	condensin complex	7	3.34	0.000
GO:0000940	condensed chromosome outer kinetochore	11	3.22	0.000
GO:0070937	CRD-mediated mRNA stability complex	5	2.37	0.009
GO:0000778	condensed nuclear chromosome kinetochore	13	2.30	0.000
GO:0002199	zona pellucida receptor complex	7	2.01	0.002
GO:0042382	paraspeckles	6	1.90	0.005
GO:0097431	mitotic spindle pole	23	1.90	0.001
GO:0005726	perichromatin fibrils	5	1.87	0.007
GO:0031618	nuclear pericentric heterochromatin	8	1.85	0.004
GO:0000777	condensed chromosome kinetochore	101	1.58	0.000
GO:0000779	condensed chromosome, centromeric region	114	1.54	0.000
GO:0005876	spindle microtubule	44	1.45	0.000
GO:0000776	kinetochore	127	1.44	0.000
GO:0072686	mitotic spindle	81	1.43	0.000
GO:0005832	chaperonin-containing T-complex	10	1.42	0.007
GO:0000775	chromosome, centromeric region	182	1.35	0.000
GO:0101031	chaperone complex	18	1.28	0.005
GO:0000922	spindle pole	141	1.24	0.000
GO:0044815	DNA packaging complex	80	1.21	0.000
GO:0005721	pericentric heterochromatin	18	1.20	0.009
GO:0030894	replisome	15	1.20	0.002
GO:0034719	SMN-Sm protein complex	17	1.18	0.001
GO:0000793	condensed chromosome	196	1.17	0.000

Table S21. Top 25 enriched reactome pathways from the down-regulated genes in response to YUM70 treatment in MIA PaCa-2 using STRING protein-protein interaction network. Nascent RNA Bru-seq was used to assess the effect of YUM70 on genome-wide transcription in two biological replicates of MIA PaCa-2 cells, data of replicate 1 is presented here.

Pathways	Description	Genes mapped	Enrichment Scores	FDR q-val
HSA-176417	Phosphorylation of Emi1	6	3.15	0.000
HSA-2514853	Condensation of Prometaphase Chromosomes	11	2.97	0.000
HSA-2980767	Activation of NIMA Kinases NEK9, NEK6, NEK7	7	2.53	0.001
HSA-113507	E2F-enabled inhibition of pre-replication complex formation	9	2.28	0.000
HSA-68884	Mitotic Telophase/Cytokinesis	14	2.21	0.000
HSA-75035	Chk1/Chk2(Cds1) mediated inactivation of Cyclin B:Cdk1 complex	13	1.95	0.000
HSA-156711	Polo-like kinase mediated events	16	1.84	0.000
HSA-390450	Folding of actin by CCT/TriC	10	1.84	0.000
HSA-2468052	Establishment of Sister Chromatid Cohesion	11	1.70	0.002
HSA-2299718	Condensation of Prophase Chromosomes	34	1.66	0.000
HSA-69273	Cyclin A/B1/B2 associated events during G2/M transition	23	1.65	0.003
HSA-2470946	Cohesin Loading onto Chromatin	10	1.63	0.005
HSA-141444	Amplification of signal from unattached kinetochores via a MAD2 inhibitory signal	89	1.57	0.000
HSA-141424	Amplification of signal from the kinetochores	89	1.57	0.000
HSA-774815	Nucleosome assembly	46	1.49	0.000
HSA-606279	Deposition of new CENPA-containing nucleosomes at the centromere	46	1.49	0.000
HSA-3301854	Nuclear Pore Complex (NPC) Disassembly	32	1.47	0.000
HSA-2500257	Resolution of Sister Chromatid Cohesion	112	1.47	0.000
HSA-69618	Mitotic Spindle Checkpoint	104	1.45	0.000
HSA-68877	Mitotic Prometaphase	184	1.39	0.000
HSA-141405	Inhibition of the proteolytic activity of APC/C required for the onset of anaphase by mitotic spindle checkpoint components	19	1.37	0.001
HSA-141430	Inactivation of APC/C via direct inhibition of the APC/C complex	19	1.37	0.001
HSA-4615885	SUMOylation of DNA replication proteins	40	1.34	0.000
HSA-176412	Phosphorylation of the APC/C	18	1.34	0.002
HSA-180746	Nuclear import of Rev protein	30	1.32	0.000

Table S22. Top 7 enriched INTERPRO Protein Domains and Features from the down-regulated genes in response to YUM70 treatment in MIA PaCa-2 using STRING protein-protein interaction network. Nascent RNA Bru-seq was used to assess the effect of YUM70 on genome-wide transcription in two biological replicates of MIA PaCa-2 cells, data of replicate 1 is presented here.

Domain	Description	Genes mapped	Enrichment Scores	FDR q-val
IPR001494	Importin-beta, N-terminal domain	17	1.24	0.009
IPR003034	SAP domain	20	1.02	0.006
IPR007125	Histone H2A/H2B/H3	31	0.97	0.006
IPR000504	RNA recognition motif domain	178	0.72	0.000
IPR001650	Helicase, C-terminal	103	0.51	0.006
IPR014001	Helicase superfamily 1/2, ATP-binding domain	105	0.50	0.006
IPR011989	Armadillo-like helical	172	0.50	0.003

Table S23. Combination index (CI) values for drug combinations calculated in CompuSyn software.

YUM70 (μM)	Topo (μM)	Effect	CI	YUM70 (μM)	SAHA (μM)	Effect	CI
1.0	0.01	0.77	0.59	1.0	0.3	0.79	0.29
0.3	0.01	0.38	0.93	0.3	0.3	0.47	0.56
0.3	0.03	0.95	0.78	1.0	0.1	0.37	0.70

CI < 1 is defined as synergism

Supplementary figure legends

Figure S1. Cytotoxicity of YUM70 in a panel of cancer cell lines. **A.** YUM 70 dose-dependently decreased PANC-1 and UM59 cell proliferation in 3D-culture systems. The diameters of the spheroids ($n = 6$) generated from PANC-1 and UM59 cells were calculated using ImageJ software package (NIH). Data are presented as mean \pm SD of three or more spheroids from three independent experiments. $*p < 0.01$, $** p < 0.001$, $***p < 0.0001$. **B.** IC_{50} values were determined in a panel of 11 cell lines using MTT assay in 2D culture system. Data are presented as mean \pm SD of three independent experiments performed in duplicate. **C.** YUM70 dose-dependently decreased OVCAR-8 cell proliferation in 3D-culture systems. The cell viability of 3D spheroids was determined with CellTiter-Glo® 3D cell viability assay. Diameters were quantified as described in A.

Figure S2. Microsomal stability and pharmacokinetic properties of YUM70. **A.** Metabolic stability was assessed in human liver microsomes in the presence of NADPH. **B.** PK parameters were estimated using non-compartmentalized analysis using Phoenix/WINONLIN. YUM70 concentrations (ng/mL) in mouse plasma were determined at various time points. For IV (intravenous) route, YUM70 was administered at 15 mg/kg and for PO (per os) route, YUM70 was administered at 30 mg/kg. **C.** PK parameters of YUM70 in plasma following IV and PO administration are as follows: C_0 = Initial concentration, $AUC(0-t_{ldc})$ = Area under the concentration-time curve from time zero to time of last detectable concentration, $AUC(0-inf)$ = Area under the concentration-time curve from time zero to infinity, CL = Systemic clearance, V_{ss} : Volume of distribution at steady state, $Bioavailability = (AUC_T \times Dose_{iv}) / (AUC_{iv} \times Dose_T) \times 100\%$, Terminal elimination half-life ($t_{1/2}$) was calculated based on data points ($n = 3$) in the terminal phase.

Figure S3. DAVID functional annotation analysis was performed on nascent RNA Bru-seq data sets to generate signaling pathways upregulated (A) and downregulated (B) in response to YUM70 treatment. The analysis (10)(9)(12)(11)(10) was performed on the list of up- and downregulated genes with a fold change ≥ 2 of replicate 1. Of note .Genome-wide transcription was assessed in two biological replicates of MIA PaCa-2 cells treated with YUM70 (see Figure S5).

Figure S4. ER stress related proteins and mRNA levels in pancreatic cancer cells in response to YUM70. A. Lysates of MIA PaCa-2, PANC-1, and BxPC-3 cells treated with YUM70 at indicated doses were immunoblotted. Relative expression (fold change) of GRP78 and CHOP normalized to actin expression were calculated from the intensity of bands and are presented. A representative experiment out of three is shown in Figure 2. The band intensity was quantified in Image Studio Ver 3.1 software (LI-COR) from three independent experiments and presented as mean fold change \pm SD. The *p*-values were calculated using Student's *t*-test, **p* < 0.05, ***p* < 0.01, ****p* < 0.001. B-C. mRNA levels of GRP78, CHOP, and CHAC1 in MIA PaCA-2 and PANC-1 cells treated with YUM70. The fold change of normalized mRNA levels were calculated by measuring band intensity. The band intensity quantified in ImageJ software from three independent experiments and presented as mean fold change \pm SD at the indicated time (hr) and dose (μ M). The *p*-value was calculated using Student's *t*-test, **p* < 0.05, ***p* < 0.01, ****p* < 0.001. D. Loading control for CHAC1 Western blot used in Figure 2C.

Figure S5. GSEA analysis of transcription after YUM70 treatment reveals increased transcription of ER stress-related genes, UPR, and apoptosis signaling pathways; and decreased transcription of E2F and targets, MYC and targets, and G2M checkpoint. Nascent RNA Bru-seq was used to assess the effect of YUM70 on genome-wide transcription in two biological replicates of MIA PaCa-2 cells. A. common up and down-regulated genes are shown for

two experiments. GSEA of Hallmark pathways and GO biological process using log₂-fold rank-ordered upregulated genes in MIA PaCa-2 cells for Experiment 1 (**Ai and Aii**) and Experiment 2 (**Bi and Bii**), respectively. GSEA of Hallmark pathways and GO biological processes using log₂-fold rank-ordered downregulated genes in MIA PaCa-2 cells for Experiment 1 (**Aiii and Aiv**) and Experiment 2 (**Biii and Biv**) cells, respectively.

Figure S6. YUM70 treatment did not show significant effects on cell cycle progression. A. GSEA plot for G2M checkpoint pathway. **B.** Cell-cycle analysis by flow cytometry of MIA PaCa-2 cells treated with YUM70 at indicated doses and time. **C.** Quantification from three independent experiments of cell-cycle analysis of MIA PaCa-2 cells at indicated doses and time.

Figure S7. YUM70 upregulates proteins involved in the apoptotic pathway. A. Top panel. Lysates of BxPC-3 cells treated with YUM70 at indicated doses and times were immunoblotted with indicated antibodies. Normalized relative densities computed using ImageJ (NIH) are shown above. Bottom panel. Effect of YUM70 on BxPC-3 cells assessed by the Annexin V-FITC apoptosis assay. YUM70 treated cells were stained with Annexin V-FITC and propidium iodide (PI) and analyzed by flow cytometry. Left, cells in the bottom left quadrant of each panel (Annexin V-negative, PI-negative) are viable, whereas cells in the bottom right quadrant (Annexin V-positive, PI-negative) are in the early apoptotic stage, and cells in the top right quadrant (Annexin V-positive, PI-positive) are in the late apoptotic/necrotic stage. Right, percentage of apoptotic cells is shown in a histogram. Data are representative of two independent experiments. **B-D.** Uncut blots for caspase 3 and PARP are shown for MIA PaCa-2, PANC-1, and BxPC-3 cell lines.

Figure S8. YUM70 specifically targets GRP78. YUM70 stabilized GRP78 full-length protein. Unfolding curves of GRP78 full-length protein at various concentrations of **A.** YUM70 **B.** VER and **C.** YUM117, in thermal shift assays. 1%DMSO was used as control. **D.** VER destabilized

GRP78 in PANC-1 cell lysate. Melt curves of GRP78 in a PANC-1 cell lysate treated with VER (100 μ M). 1% DMSO was used as control. Data presented as mean \pm SD are from 3 independent experiments. **E-F.** YUM70 showed increased cytotoxicity in GRP78 siRNA knocked down cells. MIA PaCa-2 cells were transfected with siRNA against GRP78 siRNAs or non-specific siRNA for the indicated time. Western blot was performed on collected cell lysate at the indicated time (hr) (**E**). 24 hr post-transfection, cells were treated with YUM70 or DMSO for 72hr. Cytotoxicity was measured using MTT assay. IC₅₀ values were calculated and presented as mean \pm SD from three independent experiments performed in duplicate (**F**). YUM70 does not bind to other ER proteins PDI and GSTO-1. **G.** Inhibition of PDI determined in PDI reductase assay at compound concentration of 40 μ M. Competition between PACMA57 (probe for PDI) and YUM70 on PDI; 0.3 μ M recombinant PDI protein and 500 nM of PACMA57 were used in the presence/absence of indicated doses of YUM70 and YUM79. Fluorescence scanning (upper), and coomassie blue stain (lower). PACMA 31 is a PDI inhibitor used as a positive control and YUM79 is an analog of YUM70. **H.** Competition between CMFDA (probe for GSTO1) and YUM70 for GSTO1; 1 μ M recombinant GSTO1 protein and 500 nM of CMFDA was used in the presence or absence of compounds. Fluorescence scanning (upper), and coomassie blue stain (lower). C127 is a GSTO1 inhibitor used as a positive control. **I.** YUM70 does not bind to HSP70. CETSA melt curves for HSP70 in PANC-1 cell lysate treated with YUM70 (100 μ M). A representative image from two independent experiments is shown.

Figure S9. GRP78 degradation by YUM-PROTAC. **A.** Chemical structure of DX2-145 (YUM70-PROTAC). **B.** Lysates of MIA PaCa-2 cells were immunoblotted with indicated antibodies. A representative experiment is shown. **C.** Degradation of GRP78 was quantified and presented as mean \pm SD from three independent experiments. **D.** Lysates of MIA PaCa-2 cells

treated with DX2-145 in the presence or absence of MG132 (1 μ M) pre-treatment (2 hr) were immunoblotted with indicated antibodies. **E.** Chemical structure of YUM513 (YUM401-PROTAC). **F.** Lysates of MIA PaCa-2 cells were immunoblotted with indicated antibodies. A representative experiment out of three independent experiments is shown. **G.** Degradation of GRP78 is quantified and presented as mean \pm SD of three independent experiments. The *p*-value was calculated against control using Student's *t*-test, **p* < 0.05, ***p* < 0.01, ****p* < 0.001, **H.** MIA PaCa-2 cells were treated with YUM513 for the indicated times and lysate analyzed by SDS-PAGE-Coomassie staining. Two bands indicated by the red box were submitted separately to the UM Proteomics Core facility for proteomics analysis. **I.** One of the two proteins identified by mass spectrometry that showed over 2 fold degradation was confirmed as GRP78.

Figure S10. Effect of YUM-PROTAC (DX2-145) in presence of parent compounds. A.

Lysates of MIA PaCa-2 cells treated with DX2-145 (10 μ M) in the presence or absence of YUM70 and/or pomalidomide (1, 5, and 10 μ M) pre-treatment (2 hr) were immunoblotted with indicated antibodies. **B.** Normalized GRP78 expression was calculated and presented as mean \pm SD of three independent experiments. **C.** Degradation of GRP78 is quantified at selected doses and presented as mean \pm SD of three independent experiments. **D.** Lysates of MIA PaCa-2 cells treated with DX2-145 (10 μ M) in the presence or absence of YUM401 and/or YUM117 (1, 5, and 10 μ M) pre-treatment (2 hr) were immunoblotted with indicated antibodies. **E.** Normalized GRP78 expression was calculated and presented as mean \pm SD of three independent experiments. **F.** Degradation of GRP78 is quantified at selected doses and presented as mean \pm SD of three independent experiments. The *p*-value was calculated against no treatment (NT) using Student's *t*-test, **p* < 0.05, ***p* < 0.01, ****p* < 0.001.

Figure S11. Effect of cycloheximide (CHX) and actinomycin D (ACD) on the expression of GRP78 following YUM70 treatment. MIA PaCa-2 and PANC-1 cells were treated with CHX (2.5 μ M) 2 hr prior to YUM70 treatment. Cells were treated with YUM70 for 24 hr at indicated doses. GRP78 expression was assessed by Western blot analysis. Similarly, MIA PaCa-2 and PANC-1 cells were treated with ACD (10 nM for MIA PaCa-2 cells and 20 nM for PANC-1 cell) 2 hr prior to YUM70 treatment. Cells were treated with YUM70 for 24 hr at indicated doses. Intensity of bands were measured using Image Studio software and normalized against GRP78 expression and plotted in GraphPad prism. Data represent mean \pm SD from three independent experiments. The *p*-value was calculated using Student's *t*-test, **p* < 0.05, ***p* < 0.01, ****p* < 0.001.

Figure S12. YUM70 does not bind to the truncated protein GRP78ATPase. Protein unfolding melt curves of GRP78 ATPase protein at various concentrations of **A.** YUM70 **B.** VER and **C.** YUM117, 1%DMSO was used as control. **D-F.** Apparent melting temperature T_m derived from thermal shift assays was determined at various concentrations. Data are presented as mean \pm SD. **G.** YUM70 does not inhibit the ATPase activity of truncated protein GRP78 contains ATPase domain. VER 155008 (VER), an HSP70/GRP78 inhibitor, significantly inhibits the ATPase activity of truncated protein GRP78 ATPase in the presence of 2 μ M ATP and 200 nM purified protein using ADP Glo assay kit (Promega). YUM70 does not inhibit the ATPase activity of the GRP78ATPase protein in the presence of 2 μ M ATP and 200 nM purified protein. Experiments were performed in triplicate.

Figure S13: Molecular docking of YUM70 into the peptide-binding site of GRP78 substrate-binding domain. **A.** YUM70 docked into GRP78 substrate-binding domain. **B.** Zoomed image of

the docking conformation of YUM70 in the peptide-binding site shows YUM70 interacting with indicated residues. **C.** YUM70 (pink) is superimposed onto the NR peptide (yellow). **D.** 2D docking interactions plot of YUM70 and GRP78 substrate-binding domain. **E** and **F.** 3D and 2D docking interactions between inactive analog YUM117 and GRP78 substrate-binding domain, respectively. **G.** YUM70 protects full-length GRP78 protein in partial proteolysis by trypsin. Partial protein digestion pattern of GRP78 in the presence or absence of YUM70, ATP and ADP. SDS-PAGE and Coomassie stain showing results of digestion patterns of GRP78 \pm YUM70 and ATP or ADP.

Figure S14. Expression of select ER stress markers induced by YUM70 after knockdown of GRP78 in pancreatic cancer cell lines. MIA PaCa-2, PANC-1, BxPC-3 cells were transfected with non-specific siRNA or GRP78 siRNA-1 (**A**) and GRP78 siRNA-2 (**B**) for 24 hr. Western blot was performed on collected cell lysate. Normalized relative densities computed in Image studio Ver 3.1 software (LI-COR), relative fold change (FC) are shown above. Data are representative of two independent experiments. A colon cancer cell line HT29 has wild-type KRAS was used to determine the GRP78 knockdown efficiency of the siRNAs other than pancreatic cells.

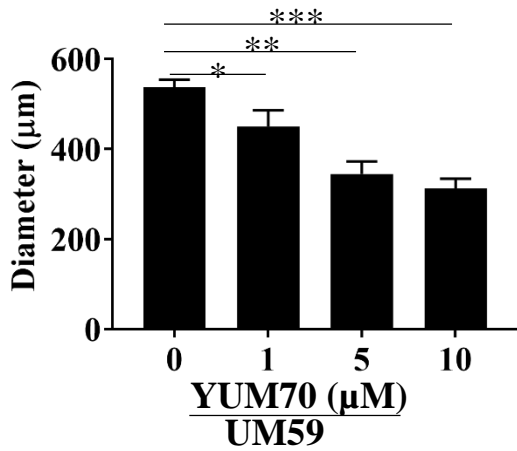
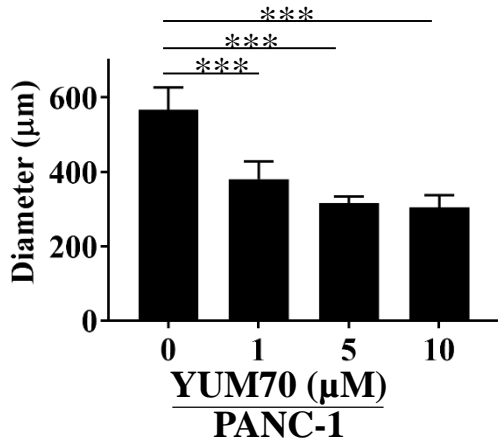
Figure S15. GRP78 and cleaved caspase 3 levels in treated tumor tissue collected from MIA PaCa-2 pancreatic cancer xenograft. **A.** Cleaved caspase 3 immunohistochemistry staining in control and treated tumor sections. The percent of cleaved caspase 3 positive cells was calculated as a number of cleaved caspase 3 positive cells in the total number of cells in each field. ($n = 10$, 5 fields of view from 2 tumors per group). Graphical data is presented as Mean \pm SD, the p -value was calculated using Student's t -test, $*p < 0.05$. **B.** GRP78 immunohistochemistry staining in

control and treated tumor sections. **C.** GRP78 mRNA levels in tumor tissues. Normalized relative densities computed in ImageJ are shown above.

Figure S16. YUM70 showed cytotoxic synergistic effect with MG132 and additive effect with 5 FU, tosedostat, or DFO. A. Cytotoxicity of the standard-of-care drugs in pancreatic cancer cell lines. Colony formation assay of YUM70 in combination with **B-C.** MG132. **D-I.** 5FU, Tosedostat, and DFO in MIA PaCa-2 cells. Cells were treated with YUM70 with/without compounds at indicated concentration and colonies were stained and imaged. Left panel, a representative image of each combination is shown. Right panel, the number of colonies was quantified using Image Studio ver3.1 software from three independent experiments. The red box indicates wells with additive effects from combination treatment. Graphical data is presented as Mean \pm SD, the *p*-value was calculated using Student's *t*-test, **p* < 0.05, ***p* < 0.01.

Figure S1.

A.



B.

Cell lines	Cytotoxicity (IC ₅₀ , μM)
	YUM70
HCT116 p53+/+	4.6±0.2
HCT116 p53-/-	3.4±0.1
H1299	4.3±1.3
A549	15.7±3.5
MCF-7	15.3±5.4
OVCAR-8	3.5±0.7
OVCAR-3	6.7±2.4
Skov-3	21.5±0.1
SHEP-1	10.9±3.9
SHSY-5Y	4.4±0.4
WM115	2.8±0.3

C.

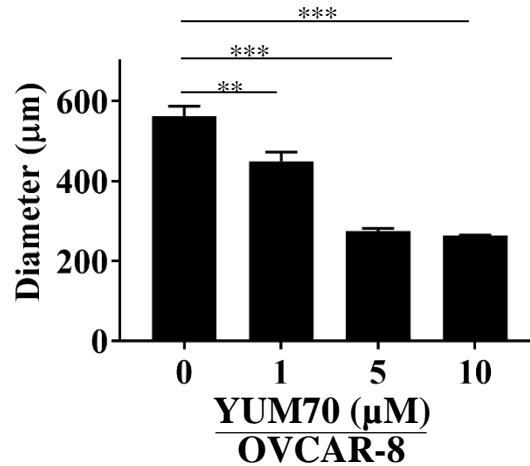
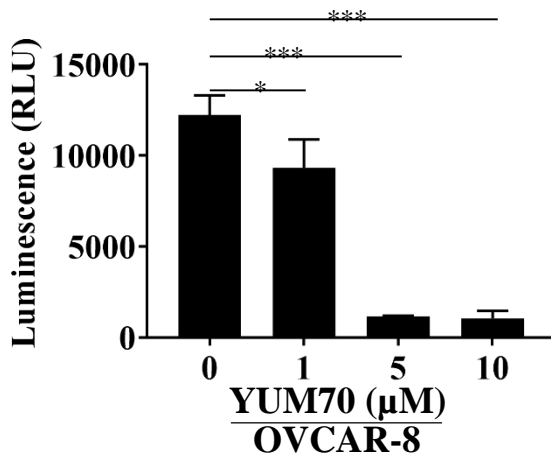
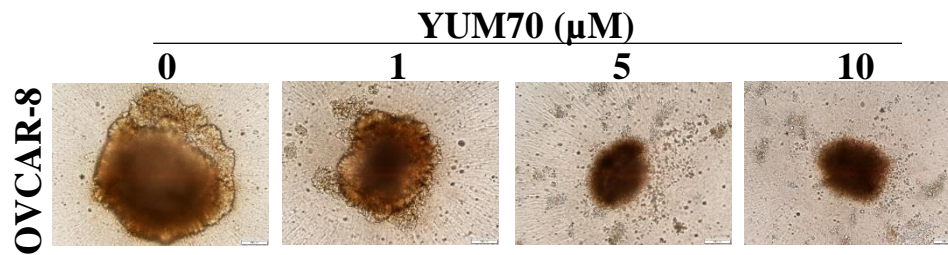


Figure S3.

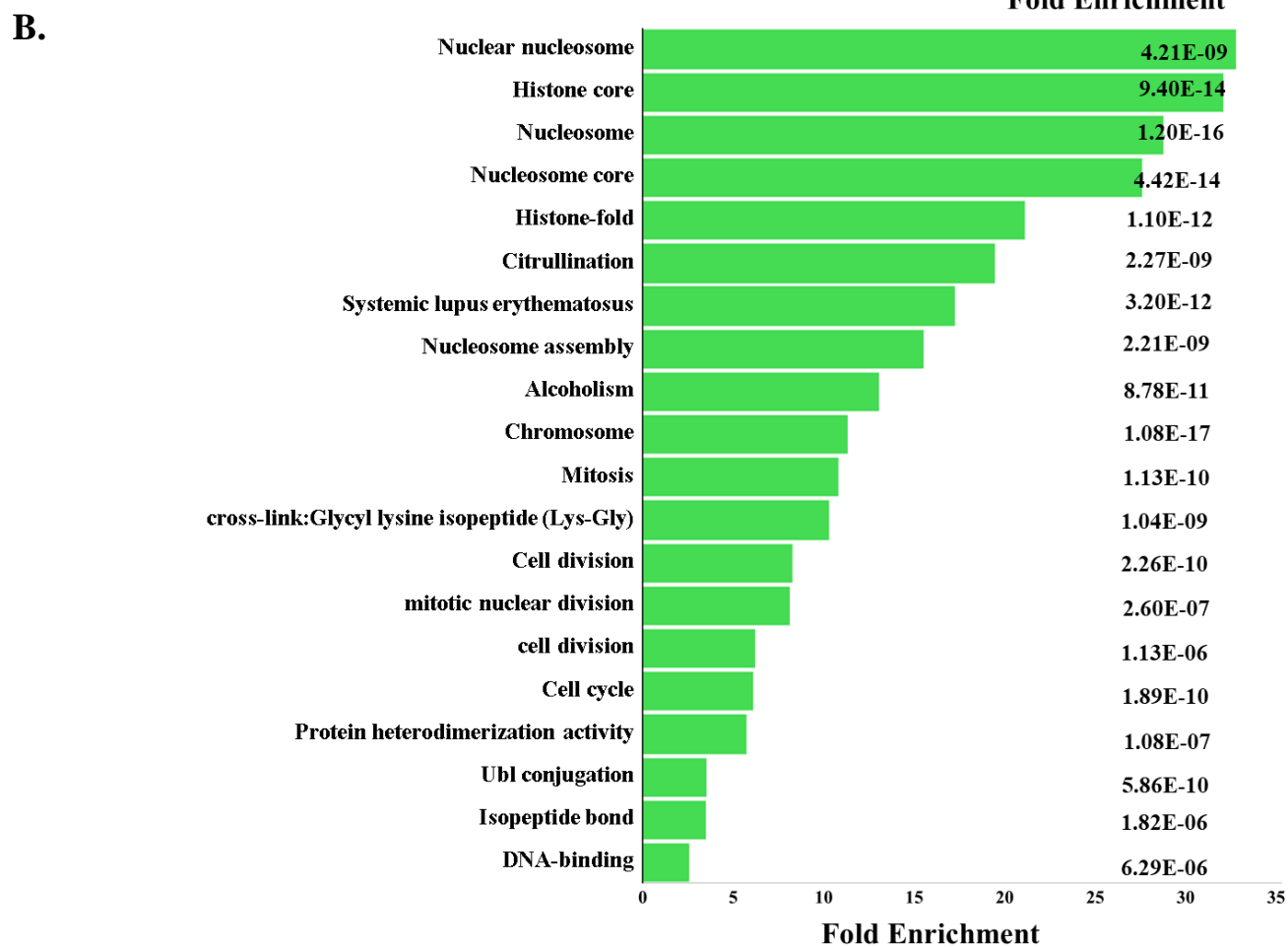
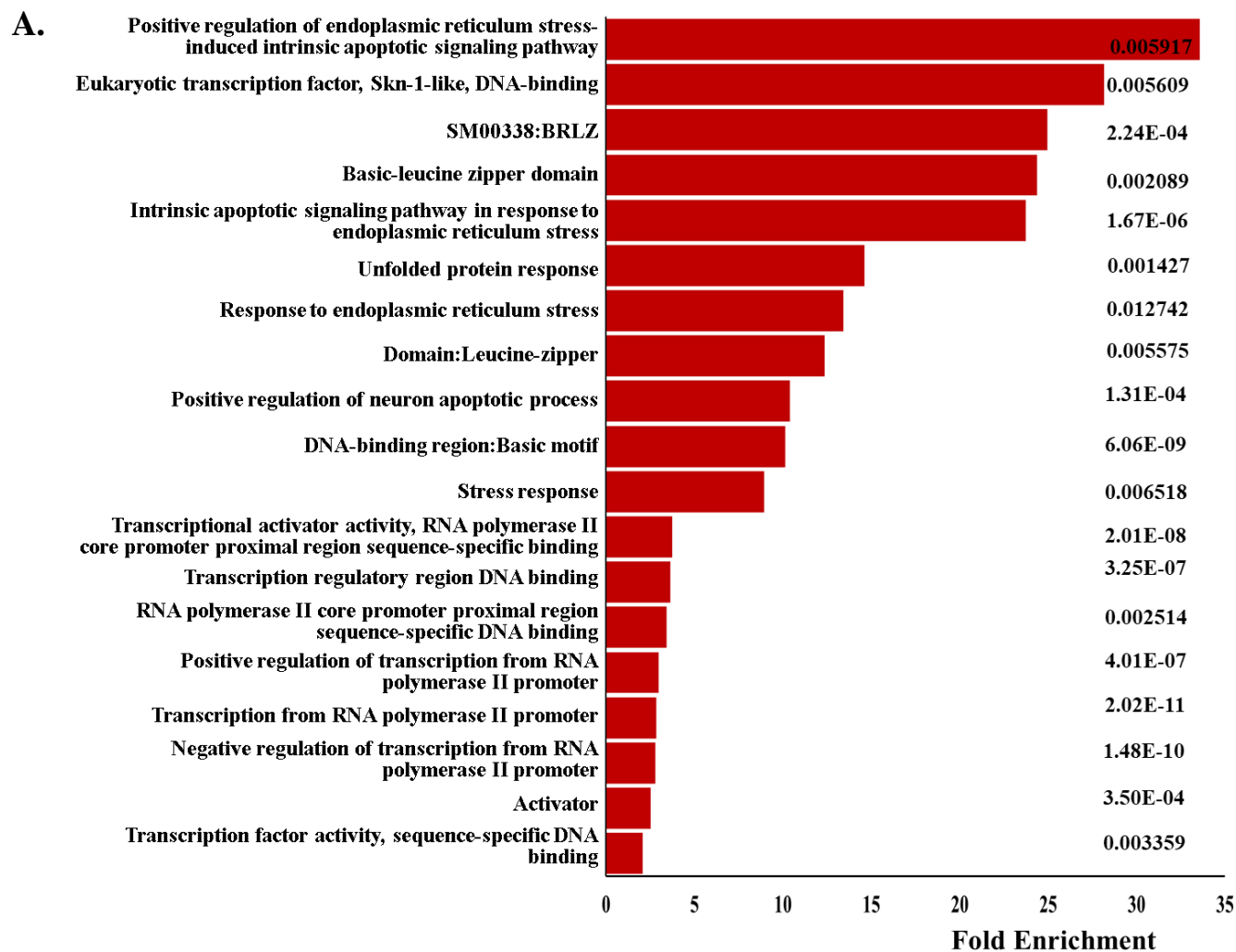


Figure S4

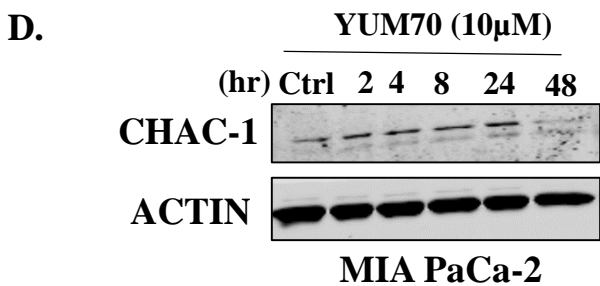
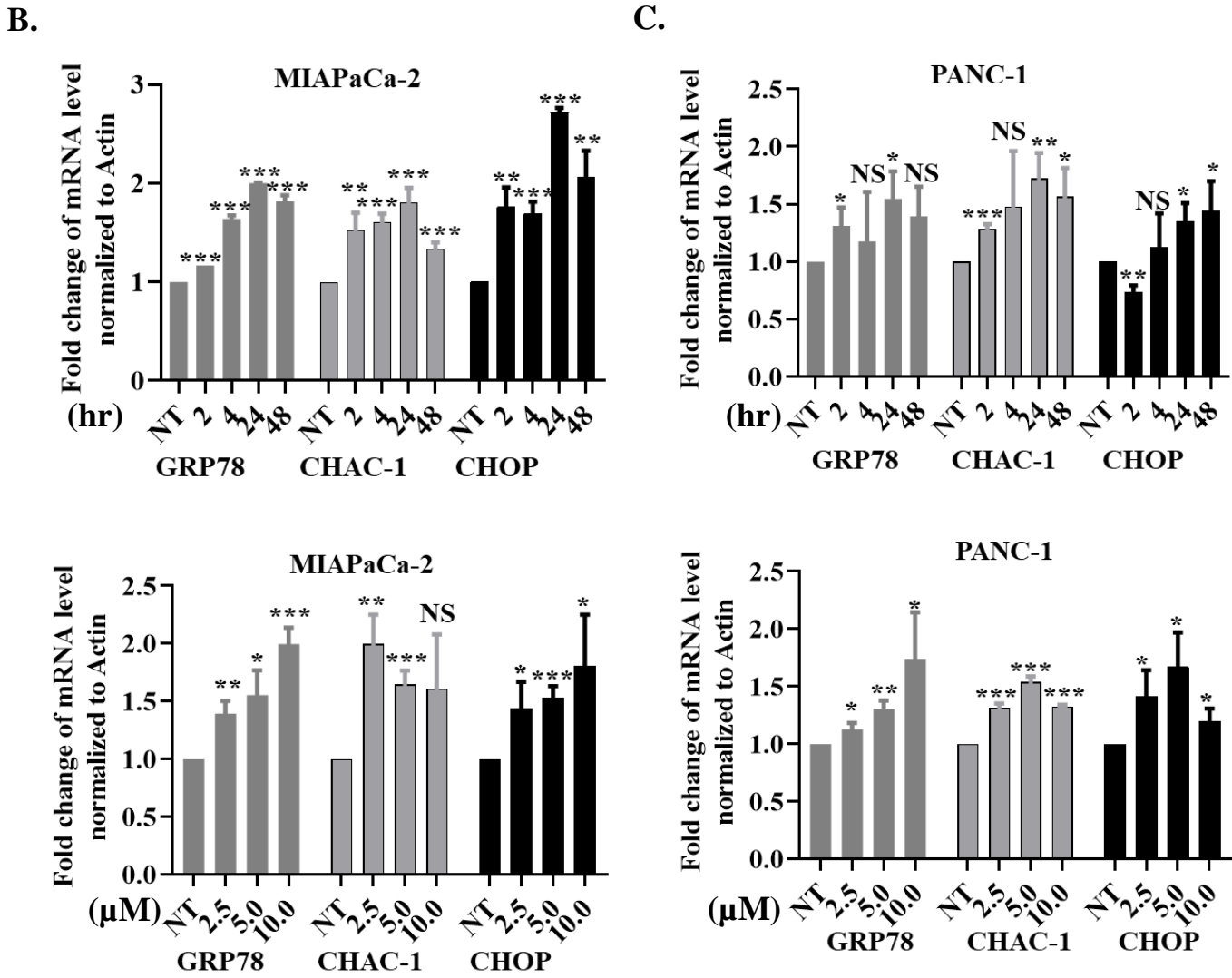
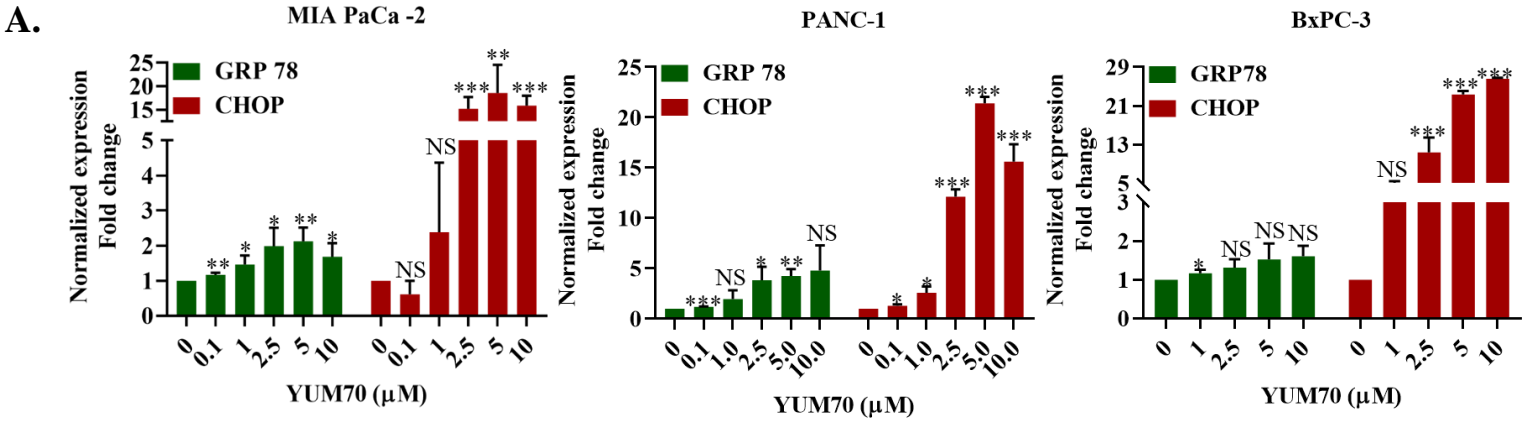
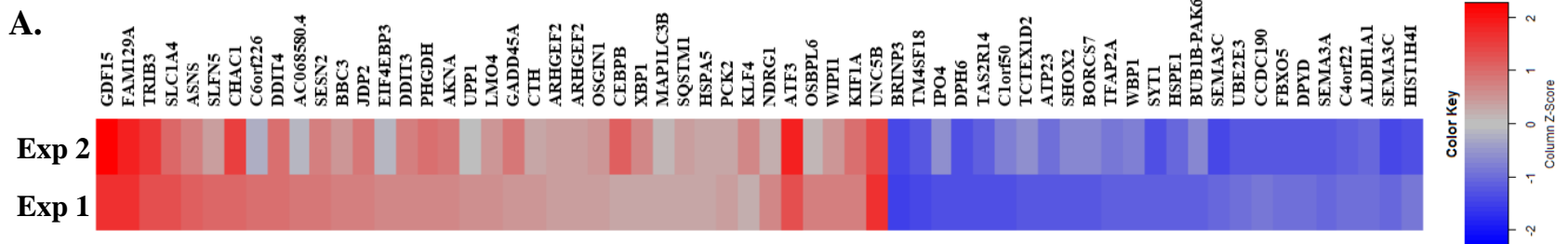
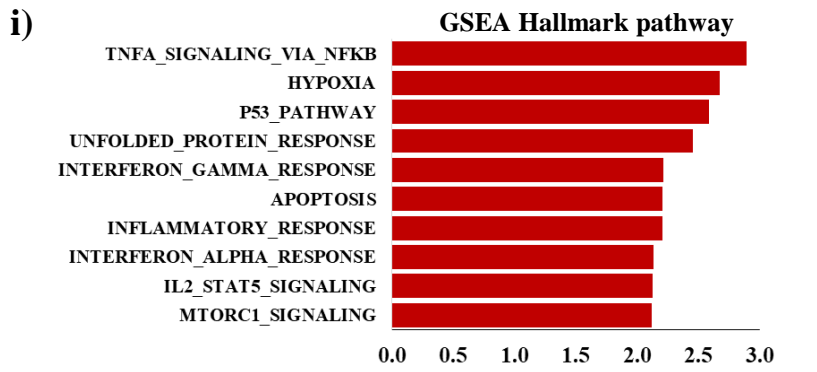


Figure S5



B. Experiment 1



C. Experiment 2

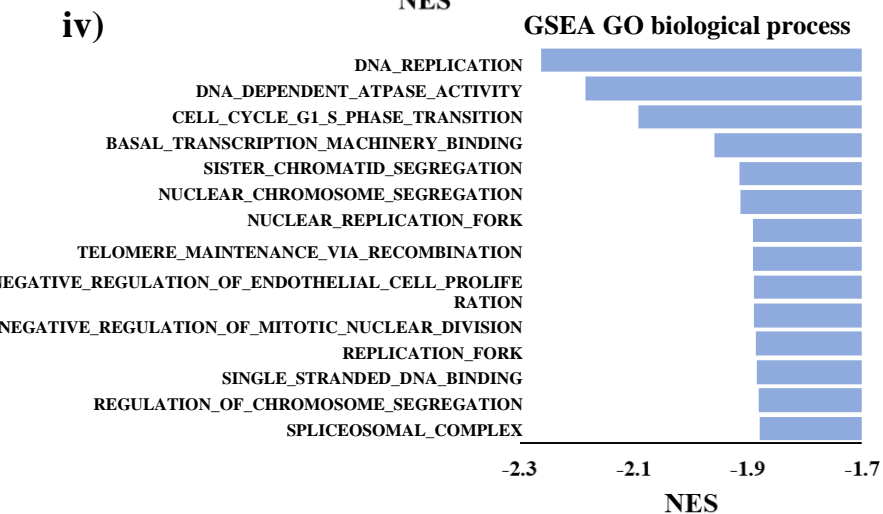
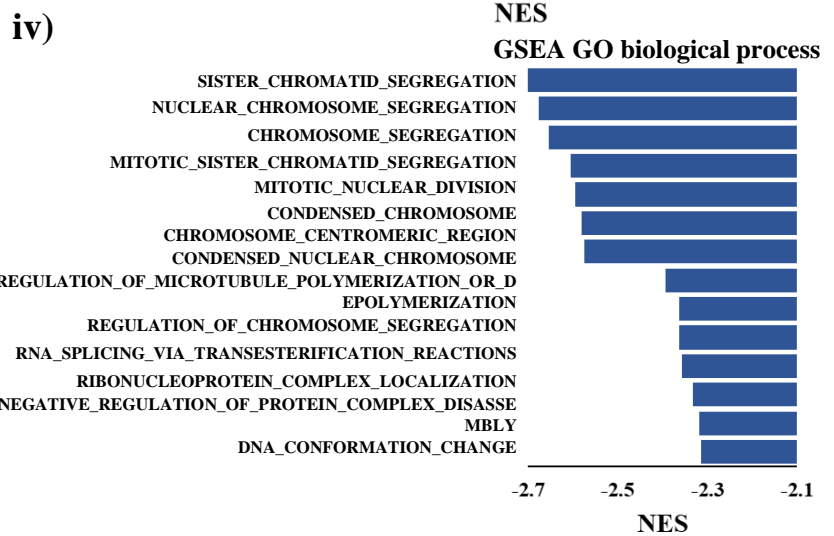
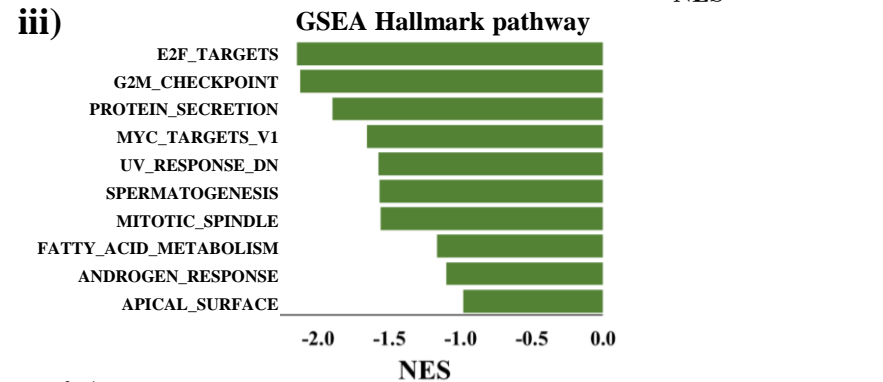
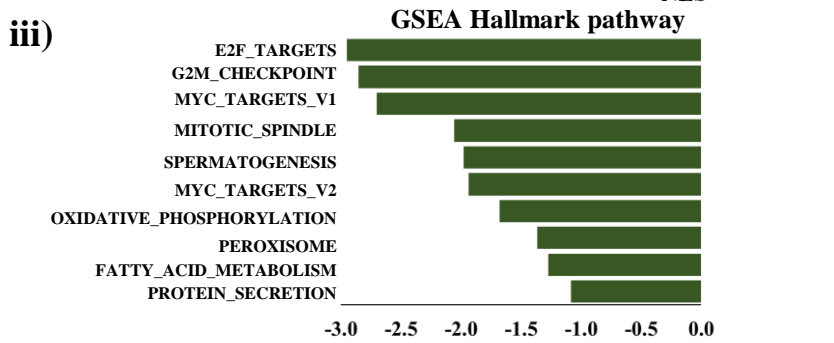
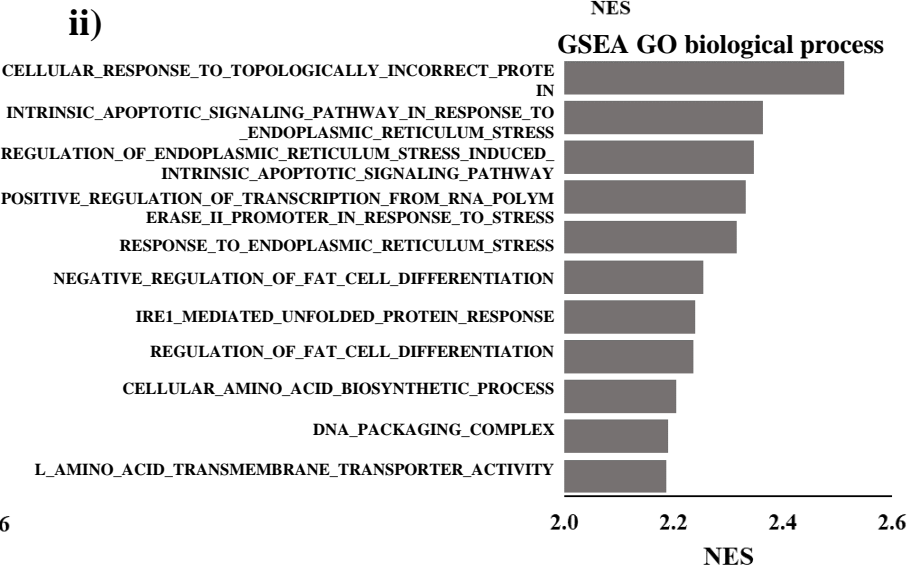
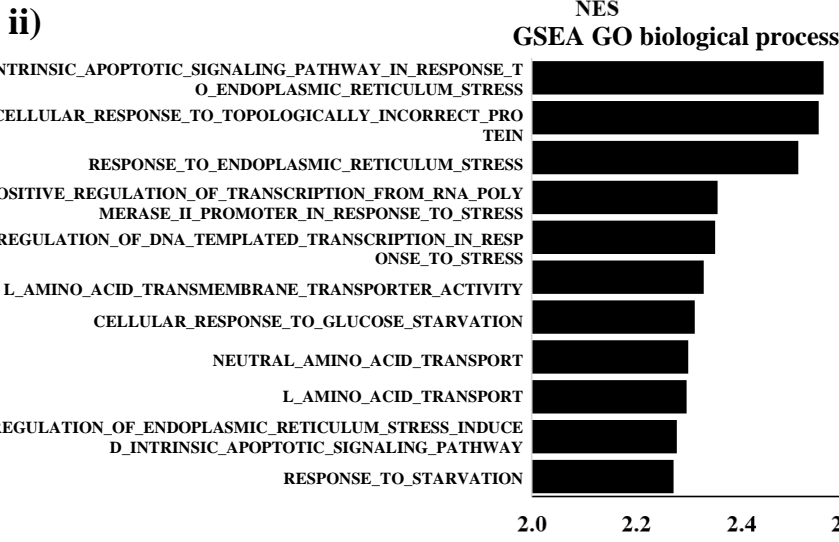
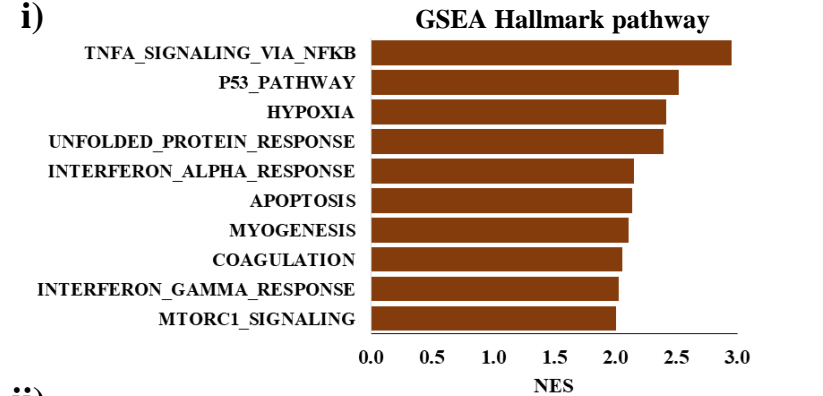
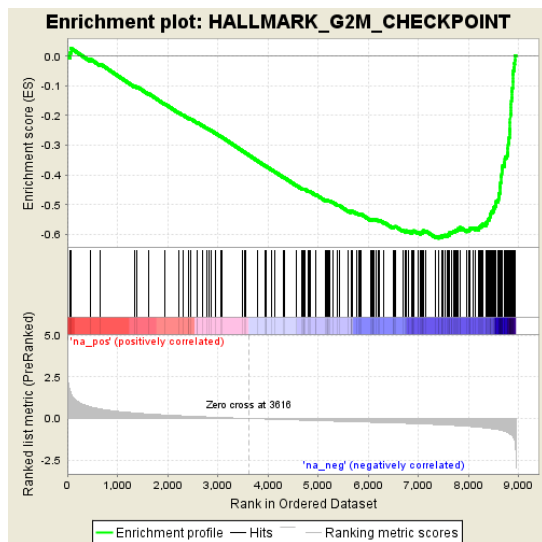


Figure S6

A.



C.

YUM70 (μ M)	24hr		
	G1	S	G2
0	57.3	29.7	12.9
5	50.3	31.3	18.4
10	51.1	30.5	18.4
15	42.5	53.5	4.0

YUM70 (μ M)	48hr		
	G1	S	G2
0	69.0	19.5	11.6
5	52.0	33.0	15.0
10	43.4	42.0	14.6
15	33.7	65.4	0.9

B.

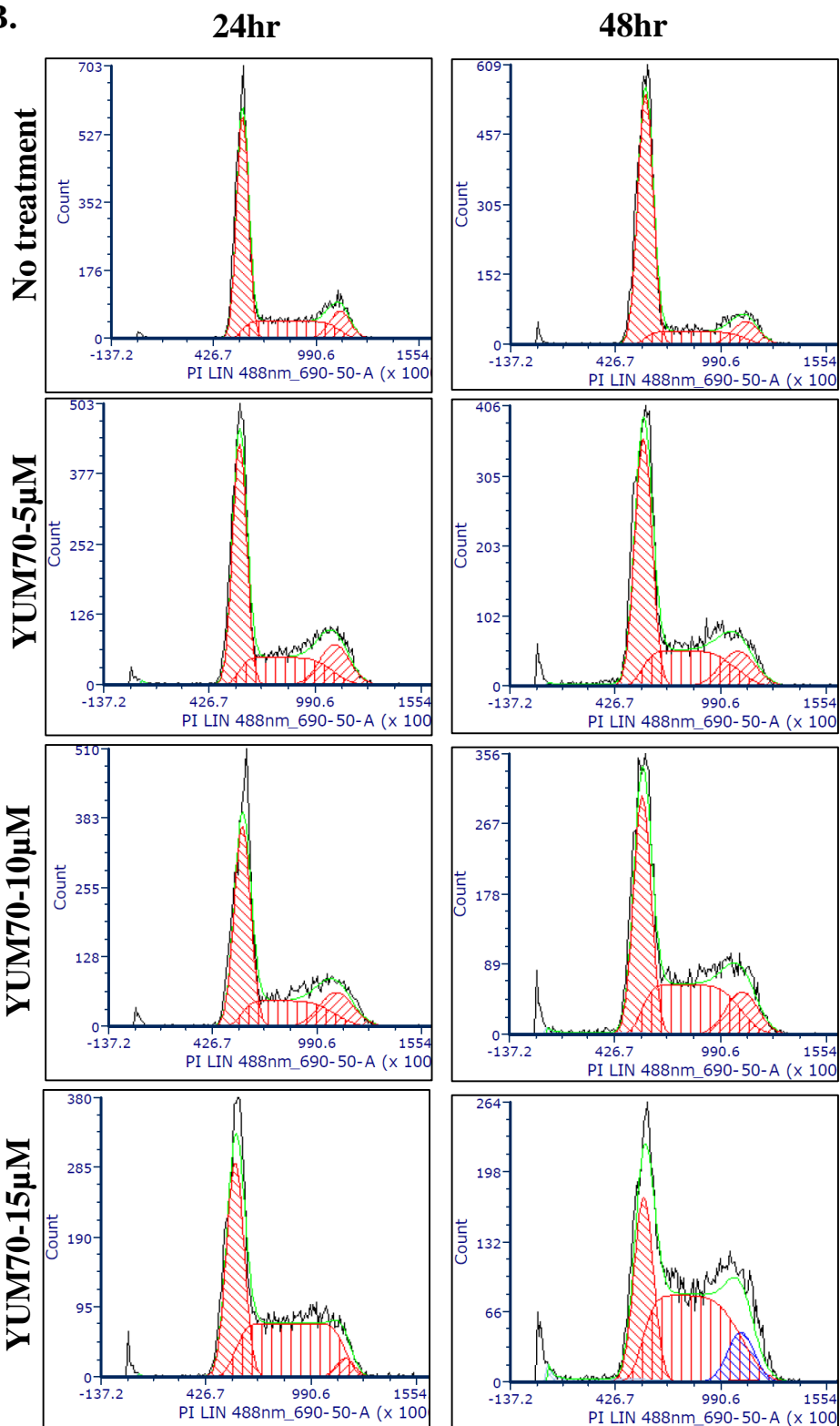
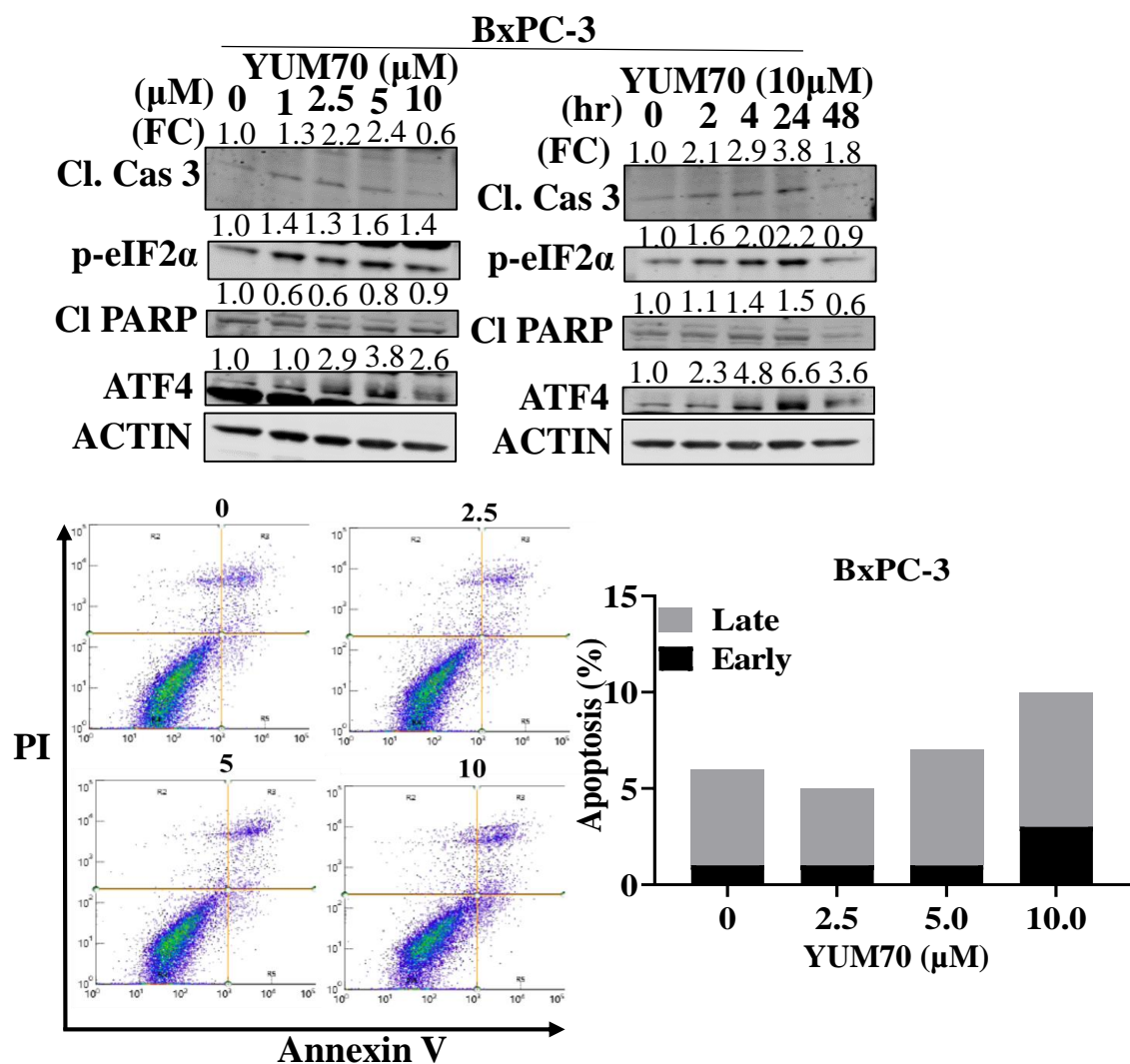
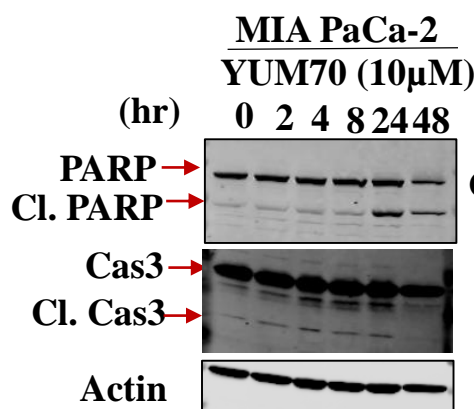


Figure S7

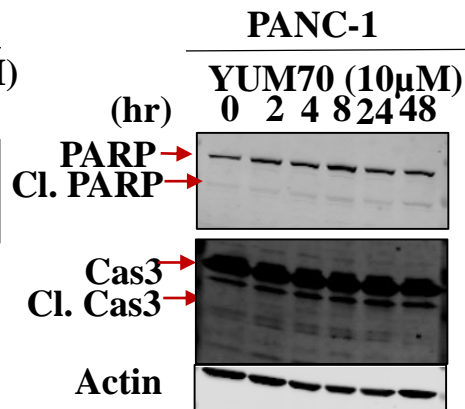
A.



B.



C.



D.

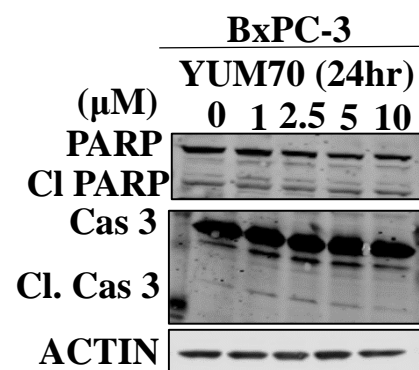
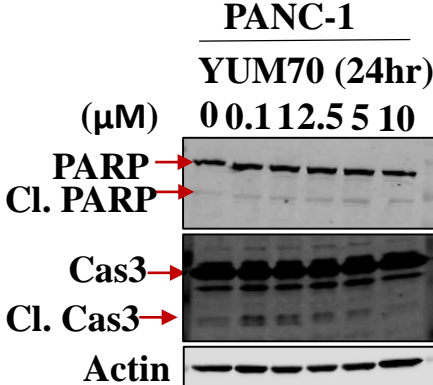
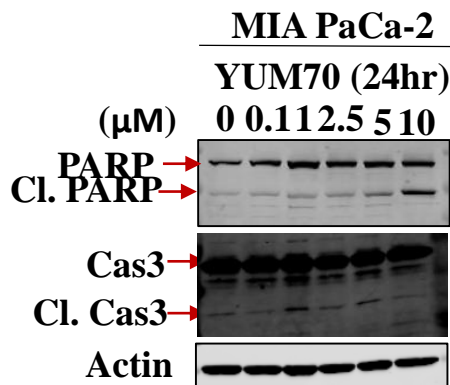
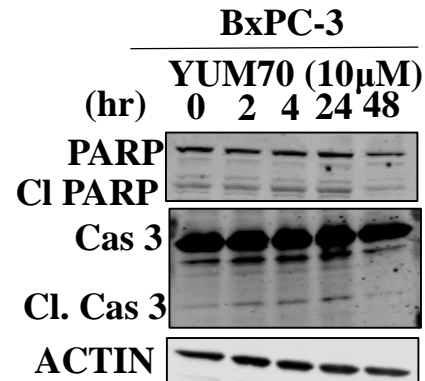


Figure S8.

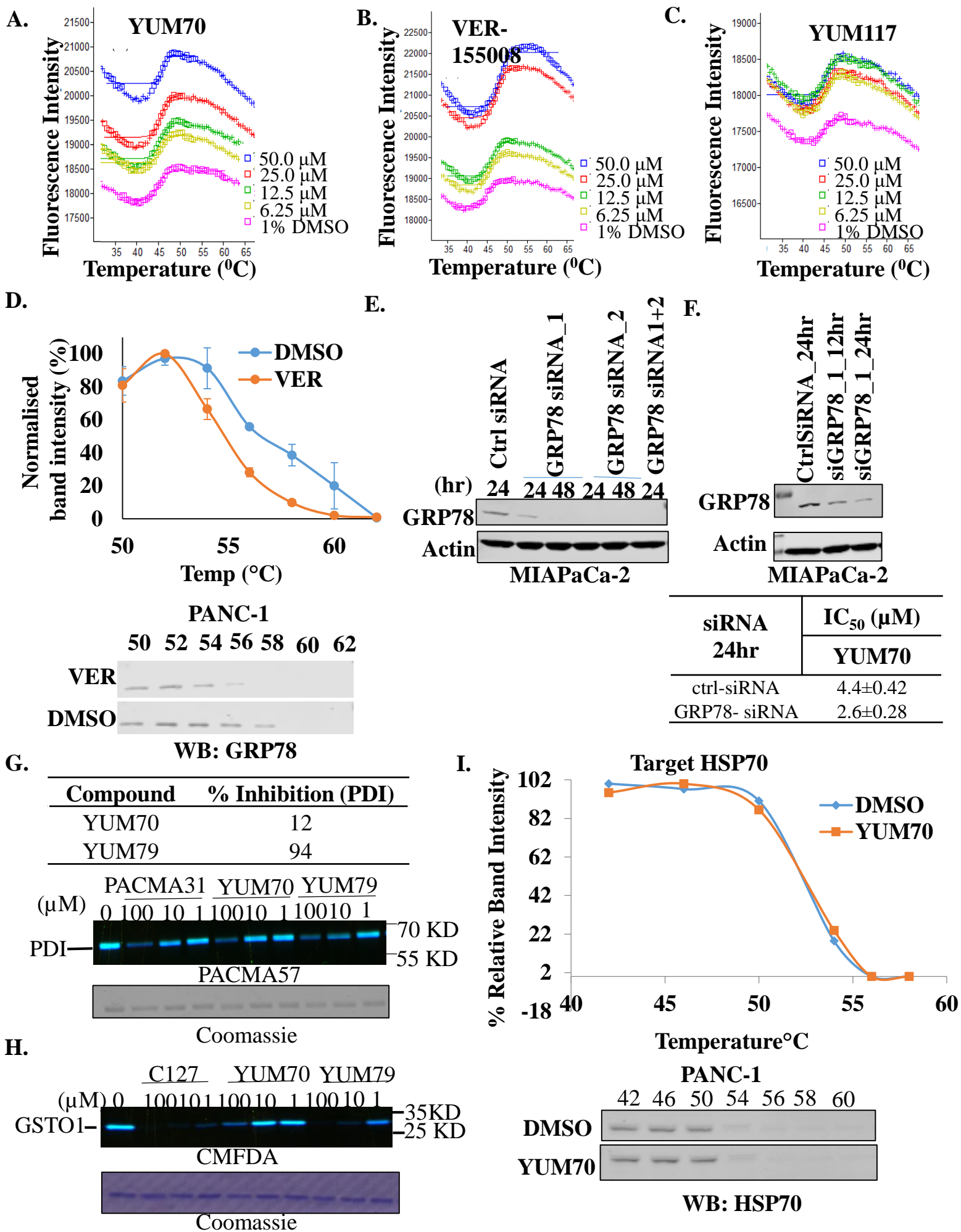


Figure S9.

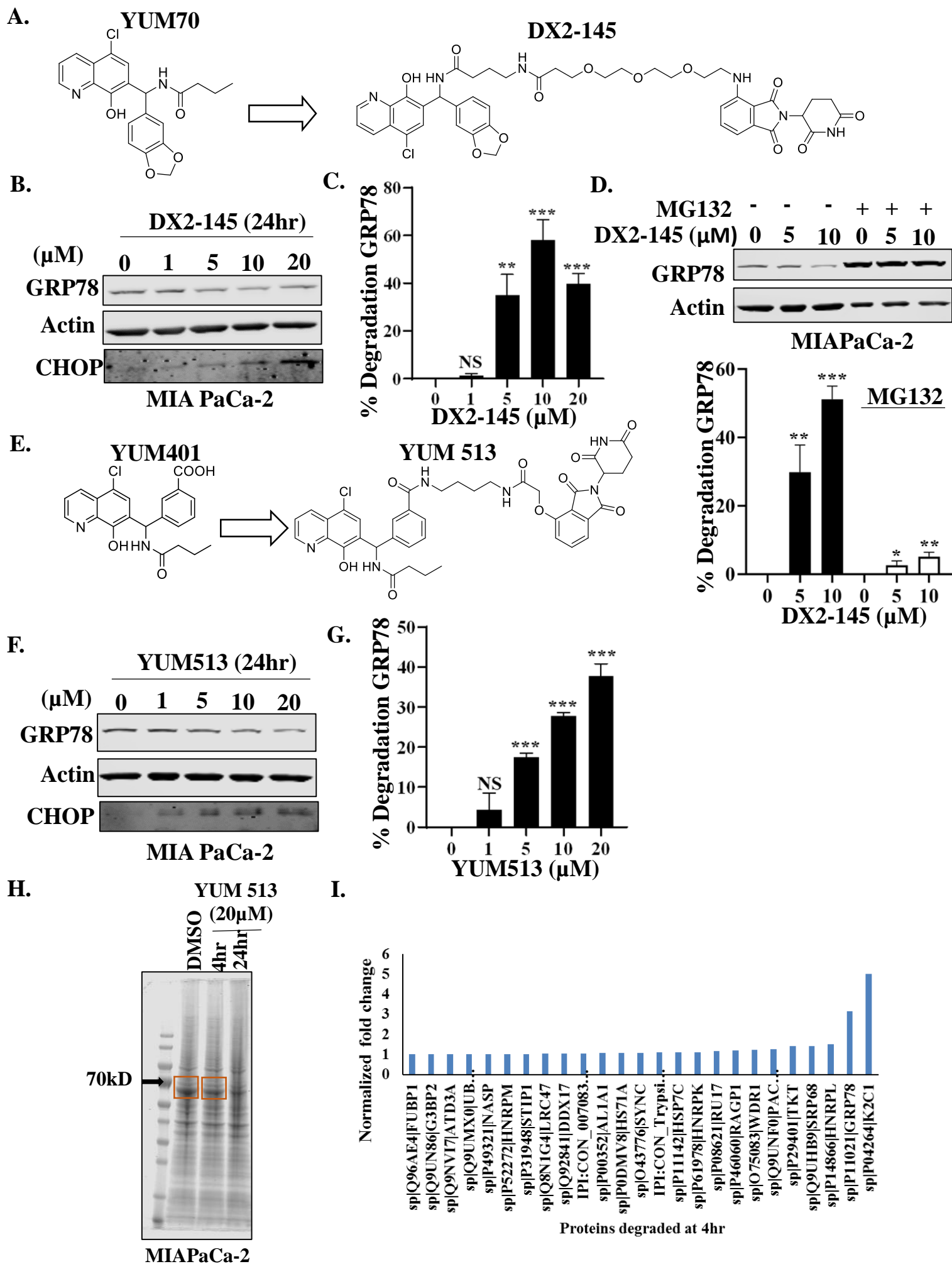


Figure S10.

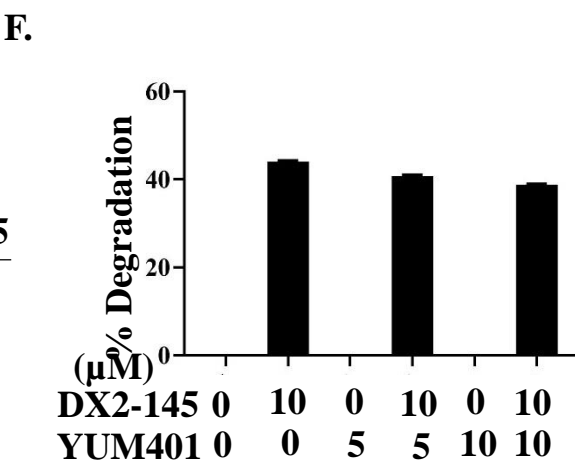
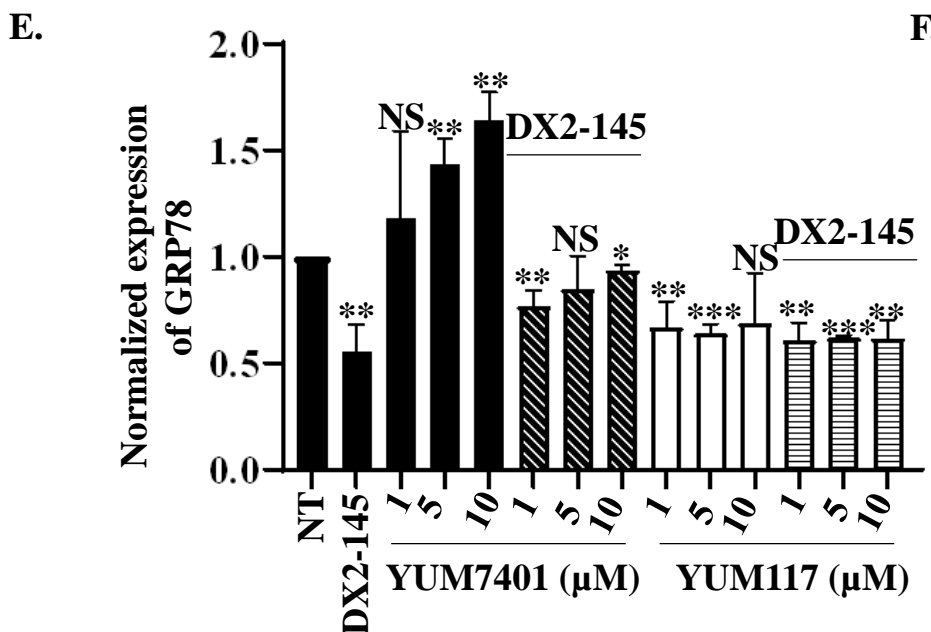
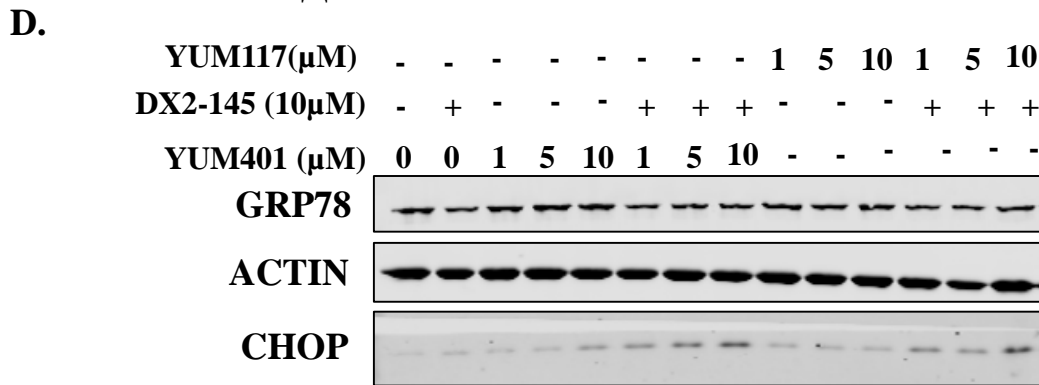
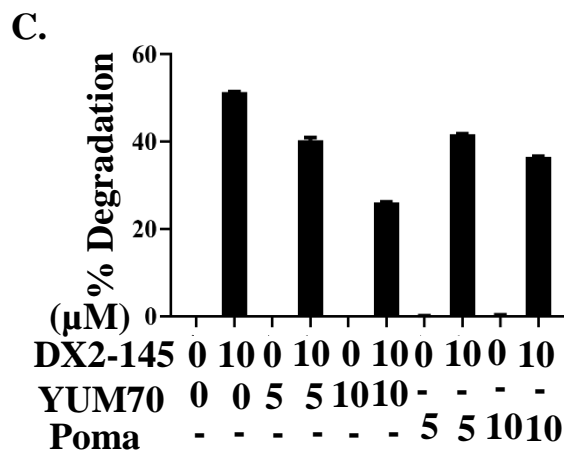
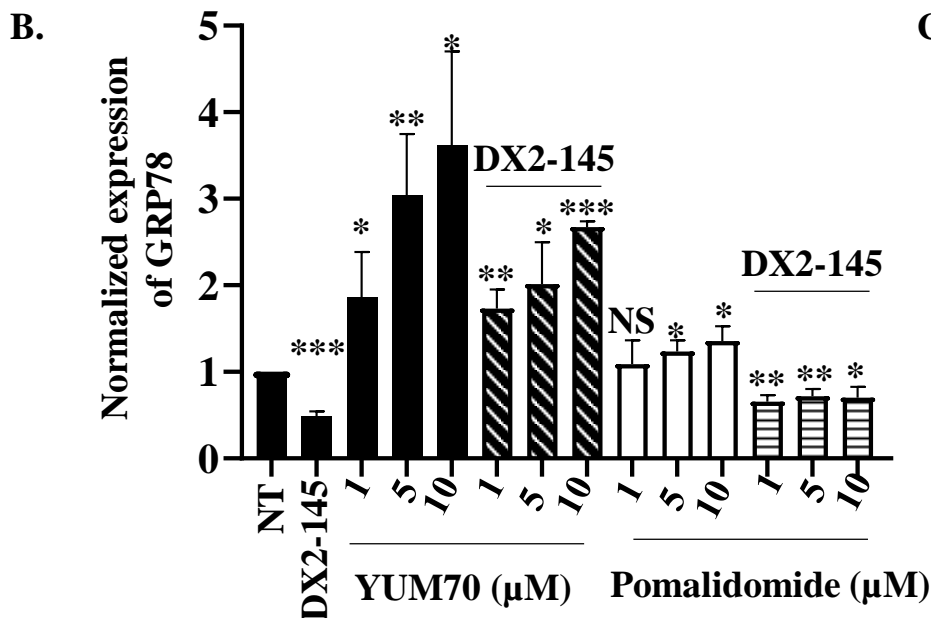
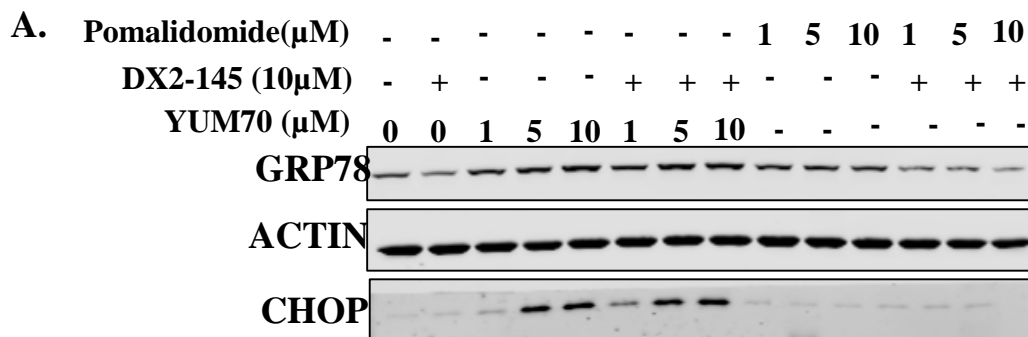
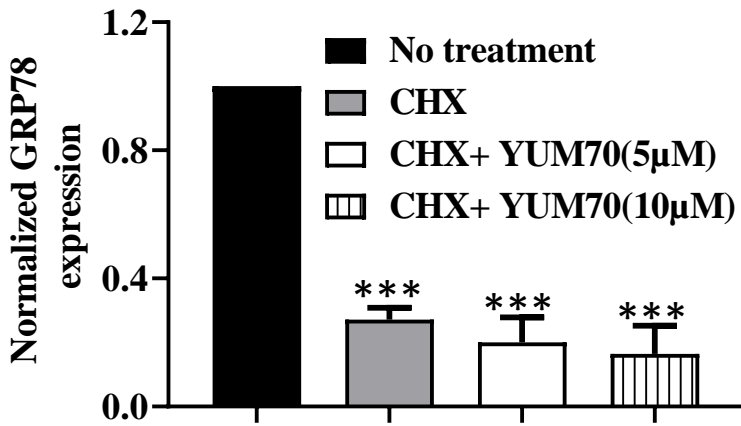
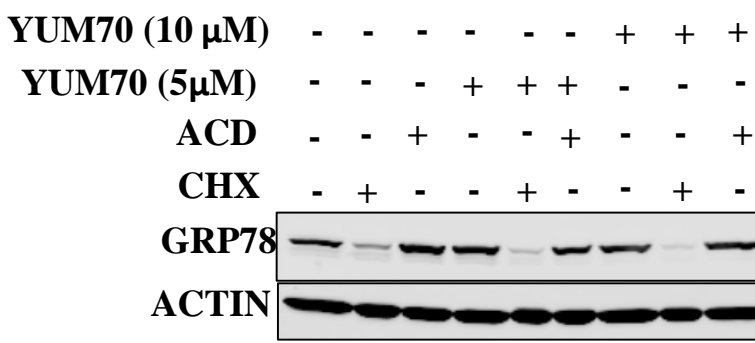


Figure S11.

A.

MIAPaCa-2



B.

PANC-1

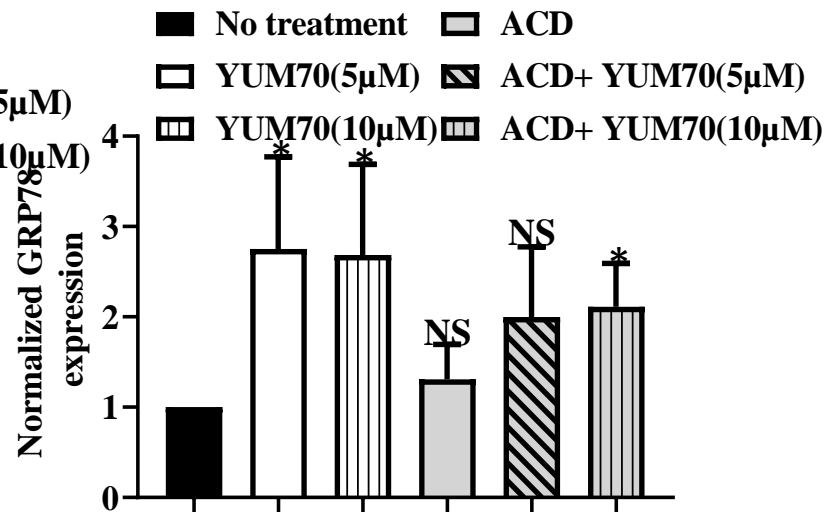
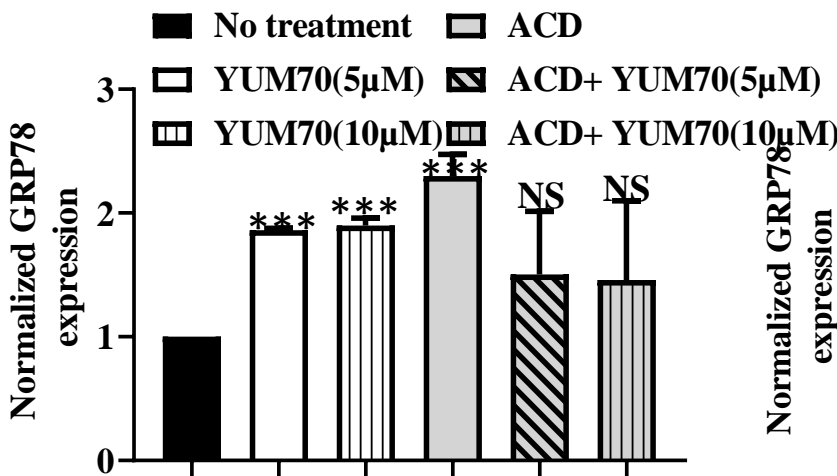
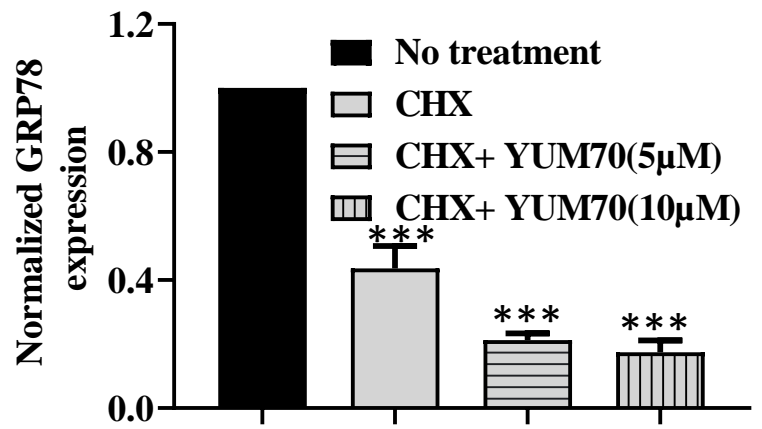
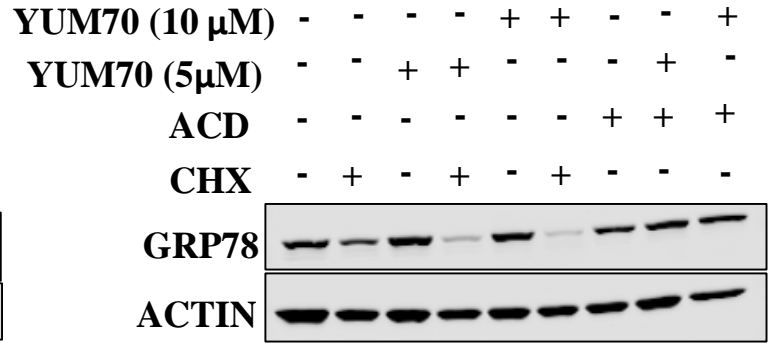
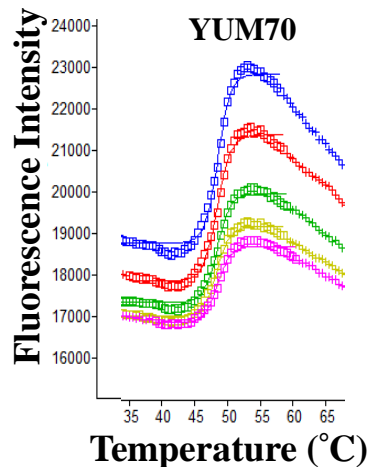
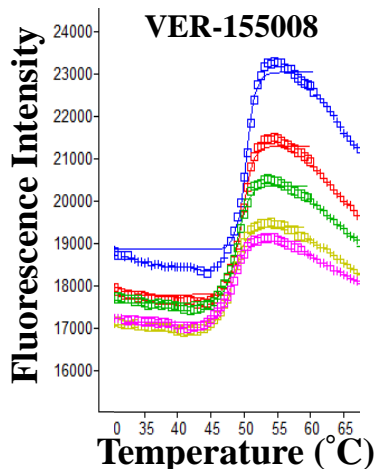


Figure S12.

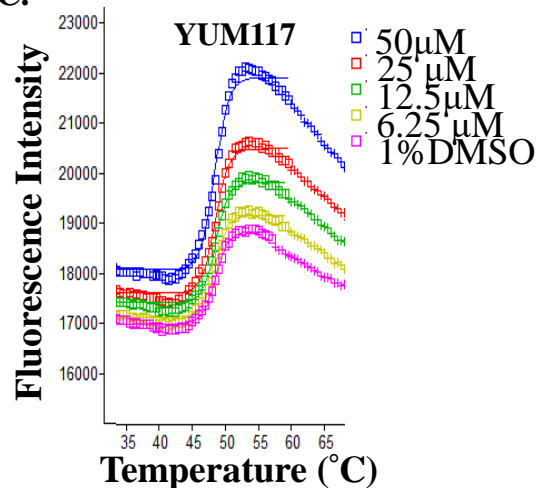
A.



B.



C.



D.

YUM70 (μM)	T _m (Av, °C)	T _m shift
50.00	48.41±0.11	0.01
25.00	48.40±0.00	0.00
12.50	48.30±0.13	-0.10
6.25	48.27±0.10	-0.13
0.00	48.40±0.09	

E.

VER (μM)	T _m (Av, °C)	T _m shift
50.00	50.36±0.09	2.02
25.00	49.59±0.01	1.25
12.50	48.92±0.01	0.58
6.25	48.58±0.07	0.24
0.00	48.34±0.06	

F.

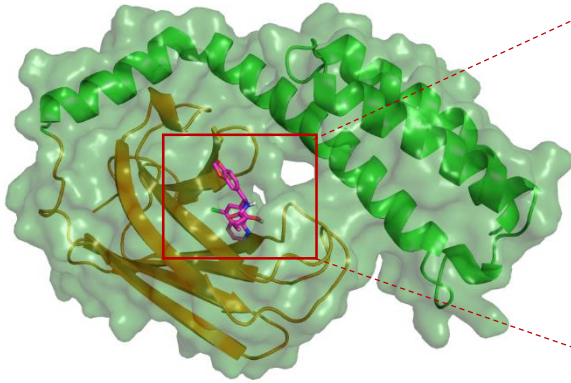
YUM117 (μM)	T _m (Av, °C)	T _m shift
50.00	48.44±0.03	-0.10
25.00	48.53±0.05	-0.01
12.50	48.49±0.06	-0.05
6.25	48.52±0.03	-0.02
0.00	48.54±0.01	

G.

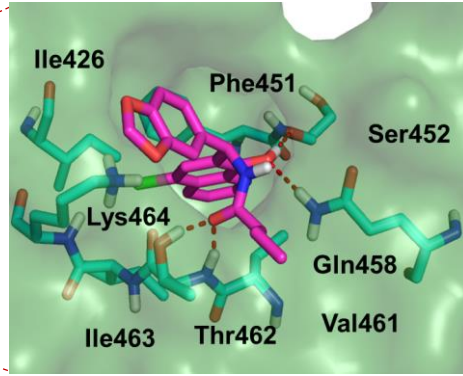
Cpds	IC ₅₀ (μM)
VER	1.0±0.67
YUM70	>50.00

Figure S13

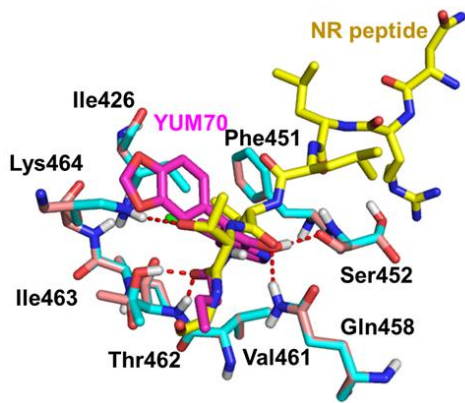
A.



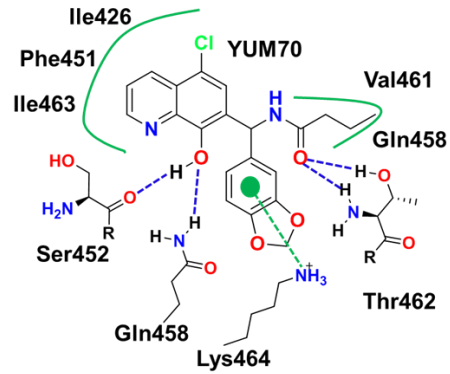
B.



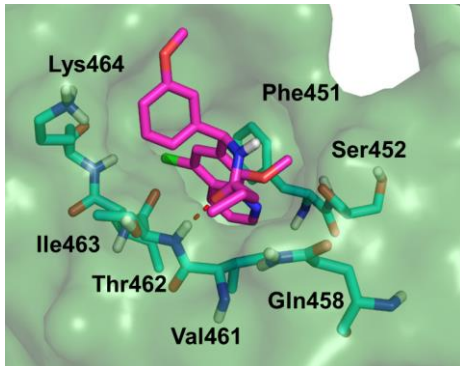
C.



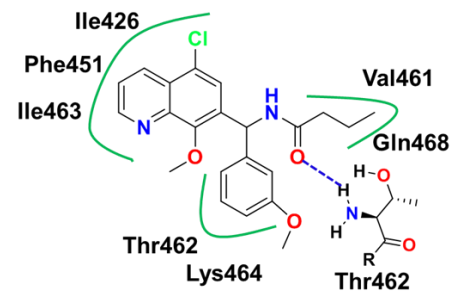
D.



E.



F.



G.

ADP (1mM)	-	-	-	+	-	-	+
ATP (1mM)	-	-	+	-	-	+	-
YUM70 (100µM)	-	-	-	-	+	+	+
Trypsin	-	+	+	+	+	+	+
GRP78	+	+	+	+	+	+	+

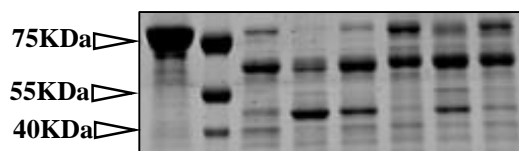
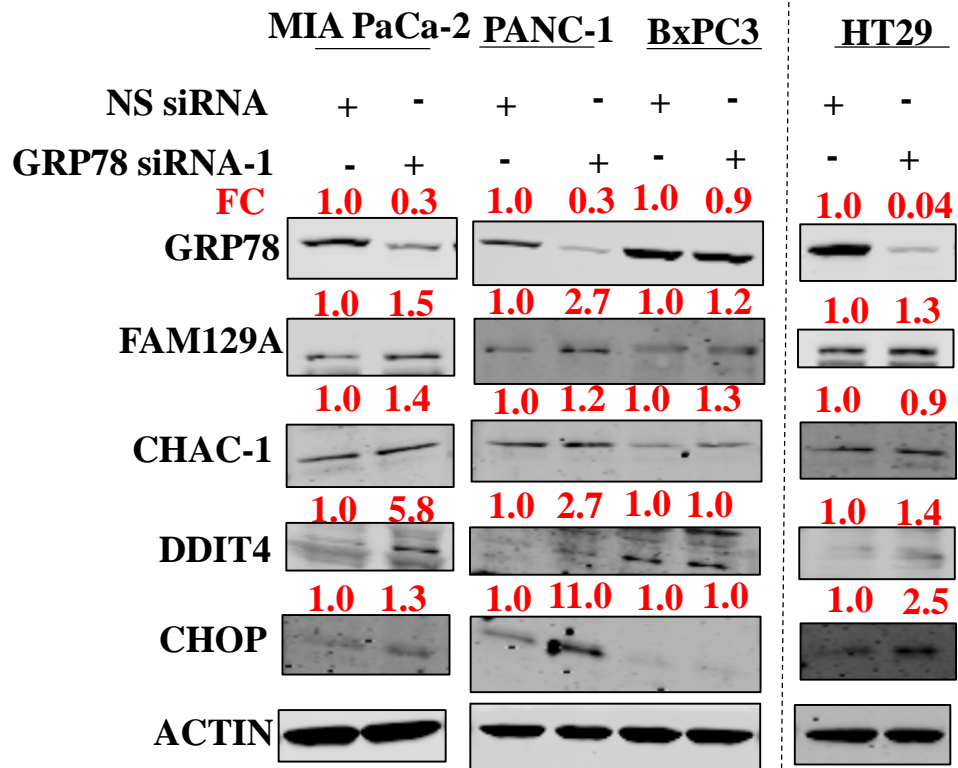


Figure S14

A.



B.

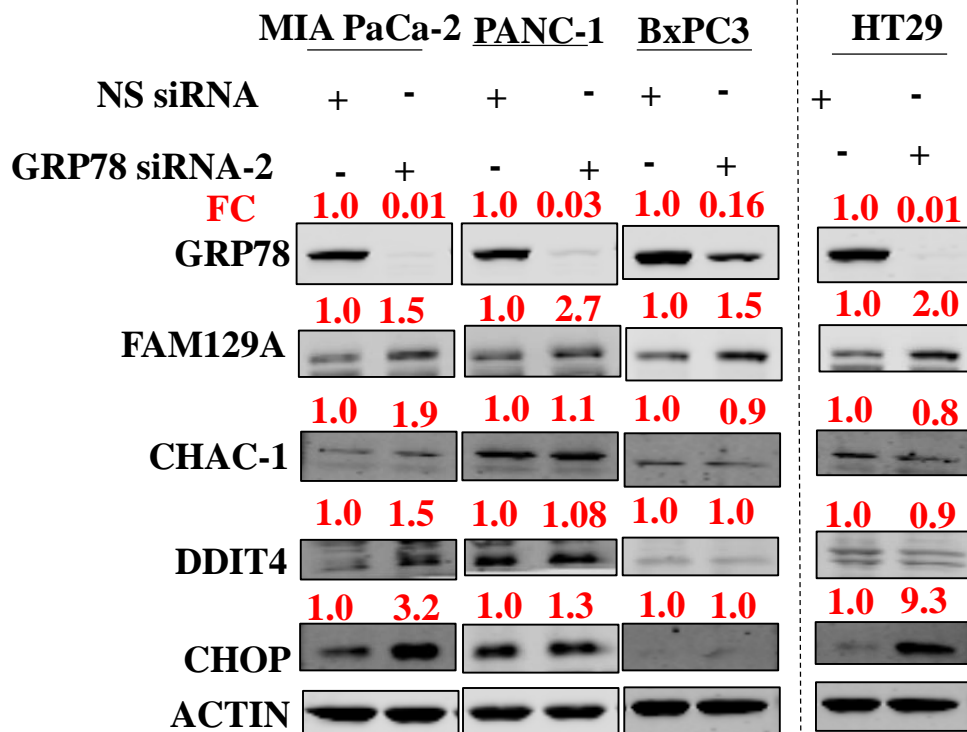


Figure S15

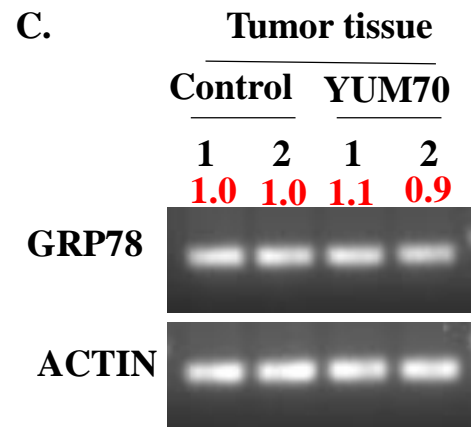
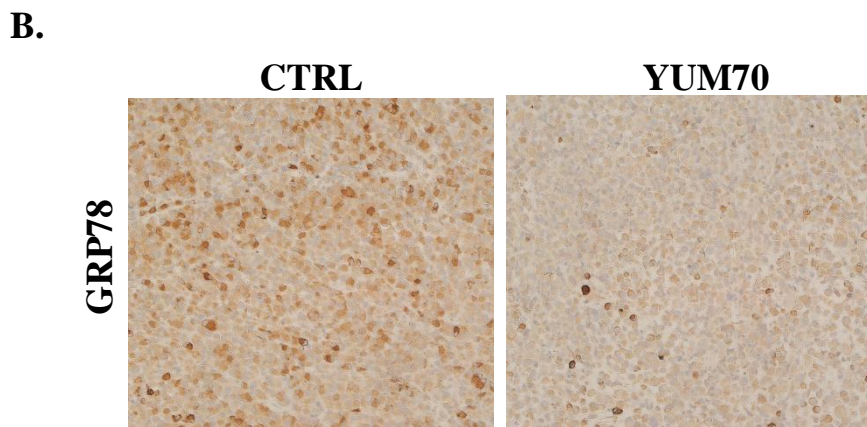
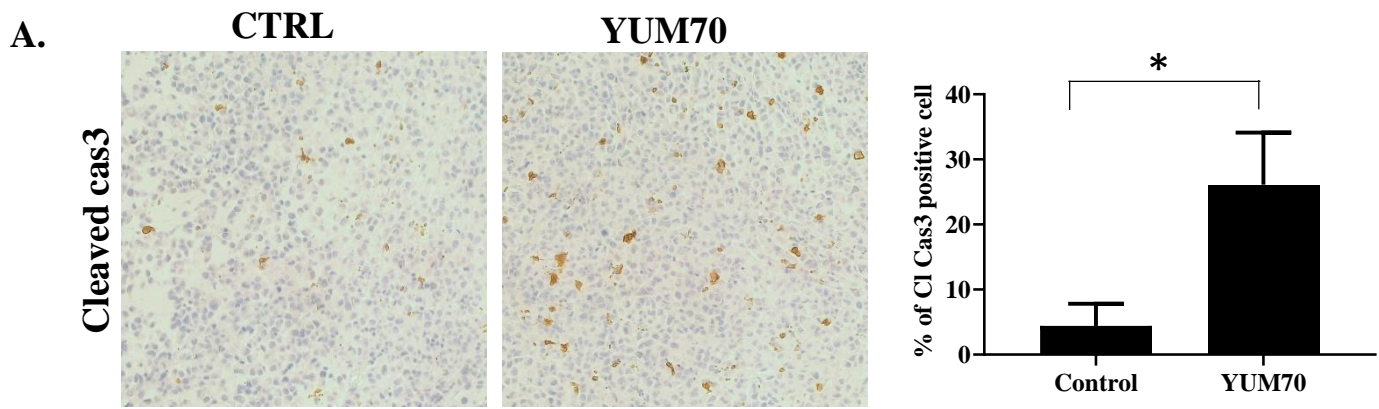


Figure S16.

A.

	IC ₅₀ (μM)		
	MIA PaCa-2	PANC-1	BxPC-3
5FU	11.47±2.03	>30	14.15±3.46
Paclitaxel	0.04±0.00	0.06±0.05	0.01±0.00
Gemcitabine	0.22±0.00	>0.3	0.01±2.09

